NASA Technical Paper 3370

December 1993

Studies of Shuttle Orbiter Arrestment System

Pamela A. Davis
and Sandy M. Stubbs

NASA

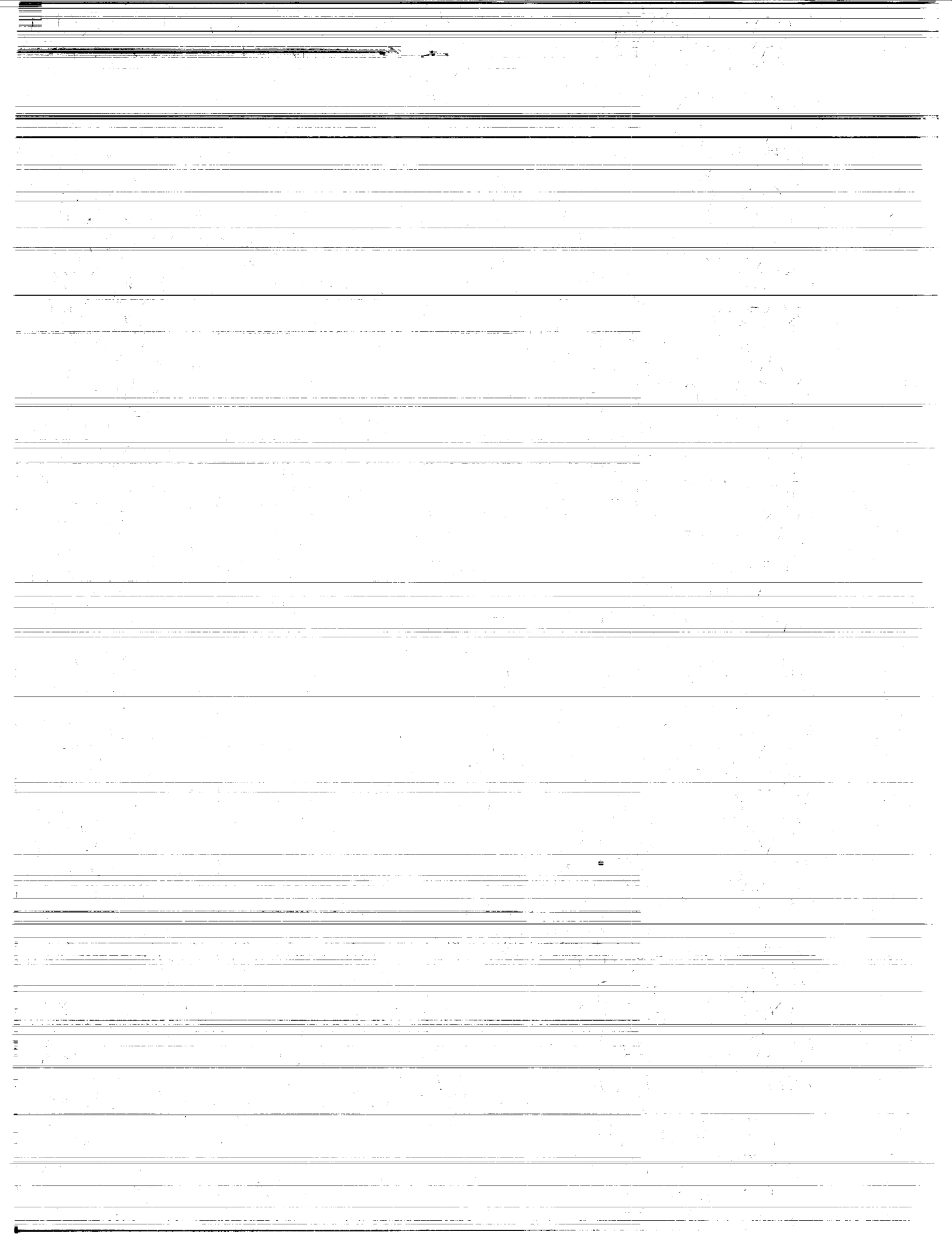

NASA Technical Paper 3370

1993

Studies of Shuttle Orbiter Arrestment System

Pamela A. Davis
and Sandy M. Stubbs
Langley Research Center
Hampton, Virginia

National Aeronautics and Space Administration
Office of Management
Scientific and Technical Information Program

Contents

Abbreviations

AAE	All American Engineering Company
f.s.	full scale
horiz.	horizontal
LMG	left main gear
MLG	main landing gear
m.s.	model scale
NLG	nose landing gear
RMG	right main gear
vert.	vertical

Abstract

Scale model studies of the Shuttle orbiter arrestment system (SOAS) were completed with a 1/27.5-scale model at the NASA Langley Research Center. The purpose of these studies was to determine the proper configuration for a net arrestment system to bring the orbiter to a safe stop with minimal damage in the event of a runway overrun. Tests were conducted for runway on-centerline and off-centerline engagements at simulated speeds up to ≈100 knots (full scale). The results of these tests defined the interaction of the net and the orbiter, the dynamics of off-centerline engagements, and the maximum number of vertical net straps that may become entangled with the nose gear. In addition to these tests, a test program with a 1/8-scale model was conducted by the arrestment system contractor, and the results are presented in the appendix.

Introduction

A number of abort landing sites (such as Benguerir, Morocco; Banjul, The Gambia; and Morón and Zaragoza, Spain) are designated for use by the Space Shuttle orbiter. However, landing abnormalities during aborts could lead to hazardous overrun incidents on these runways. An orbiter overrun has the potential of significantly damaging the vehicle and resulting in crew injuries or fatalities. Because of this potential, a net arrestment system was suggested as a means of bringing the orbiter to a safe stop with a minimum amount of damage in the event of a runway overrun. Runway arrestment systems are currently used on many military runways to safely stop aircraft experiencing mechanical failures. Some of these systems are described in references 1 to 3. To develop an effective net arrestment system for the orbiter, tests were conducted with a 1/27.5-scale model at the NASA Langley Research Center.

This paper presents data from these tests and analyzes these data with respect to the interaction of the net and the orbiter. These tests were conducted at simulated speeds up to ≈100 knots (full scale) with five nets of different geometries. The objectives of the tests were (1) to determine the effect of various net geometries on the net engagement of the nose gear and main gear, (2) to determine whether or not the top horizontal net bundle contacts the crew cabin window, (3) to determine where the top horizontal net bundle comes to rest on the payload bay doors, (4) to evaluate underwing engagements, and (5) to define the dynamics of off-centerline engagements. The 1/27.5-scale tests were developmental in nature. As the tests proceeded, changes were made to improve arrestment characteristics; thus, tests of the different net geometries are not always directly comparable.

In addition to the Langley tests with a 1/27.5-scale model, a follow-on test program with a 1/8-scale model was conducted by All American Engineering Company (now Engineered Systems, a Division of Daytron Incorporated) under NASA contract NAS9-17774 for Johnson Space Center. The purpose of the 1/8-scale tests was to solve some potential problems remaining after the 1/27.5-scale tests and to verify the system design at a larger scale. The results of these tests are discussed in the appendix.

Apparatus and Test Procedures

Model

Figure 1 shows the 1/27.5-scale model of the Space Shuttle orbiter that was used in the Langley tests. The model was geometrically scaled from an early version of the orbiter. It was constructed originally for wind tunnel tests and was slightly overweight for normal Froude scaling (ref. 4). The mass, inertia, and force parameters were scaled by the factors shown in table I so that the slightly overweight model could be used for accurate dynamic testing. Some model geometric and weight parameters are given in table II along with their full scale and orbiter values.

The model was made of fiberglass, and the landing gear struts and drag braces were made of steel. Figures 2(a) and 2(b) are photographs of the landing gear. The nose and main gear tires used for the model were solid-rubber hobby-model tires that were sized to the proper scale to represent the orbiter tires.

To simulate the strut failure load in the drag direction, the gears were hinged in the fore and aft plane, and they were held by soft wire selected to stretch at the properly scaled force to simulate the failure load for the gear. The copper drag wire for the main gear was set to fail at 7.9 lb (model scale), and the nickel drag wire for the nose gear was set to fail at 4.6 lb (model scale). With a drag force applied to the main or nose gear strut at the wheel axle, these values corresponded to gear failure loads of 100 000 lb for the main gear and 58 000 lb for the nose gear. A failure indication system for the nose gear was used to determine if and when the nose gear failed during arrestments. The system consisted of a switch inside the model that was connected to the nose gear by a thread (fig. 2(a)). The thread was used to trigger a flash bulb mounted on the tail of the model so that the time of the nose gear failure could be determined from film coverage. The nose gear was designed to be either free castoring or fixed to simulate when the nose gear steering was disengaged or engaged. Black tape was used to mark the payload bay doors and the crew cabin windows to determine where the top net bundle came to rest and whether it contacted the pilot's windscreen.

A teflon guide was attached to the model behind the nose gear (fig. 2(a)) to guide the model on a launch rail, which is shown in figure 3. Deflectors were used on the nose gear and between the teflon guide and pulley (fig. 2(a)) to prevent strands of the net elements from catching on these launch devices instead of sliding rearward over the fuselage to envelop the wing. These deflectors were test artifacts and were not considered to have an adverse affect on full-scale orbiter net envelopment.

Launch Mechanism

Figure 4 is a plan view of the general arrangement of the 1/27.5-scale test setup, and figure 5 is a sketch of the launch mechanism for the tests, launch rails were fastened to a plywood runway surface. A cross section of this rail system is also shown in figure 5. Two sheaves were mounted at the exit end of the rails, behind the model in the prelaunch position, as well as ≈30 ft above the floor. A single sheave or pulley was mounted under the model fuselage behind the nose gear. A mass was attached to the ends of a single cable that was routed through the sheave system and around the model pulley. (See fig. 5.) The model was held by a trigger pin. Upon release of the trigger pin, the mass would fall accelerating the model along the rail to the desired speed that was measured by a speed trap, which is shown in figure 3. Speed was varied by adjusting the mass and the mass drop height.

Arrestment System

An early version of the arrestment system is shown in figures 6 and 7. The system consisted of a net to ensnare the vehicle, net supports and stanchions to hold the net up, breakaways to release the net from its supports, and energy absorbers to bring the vehicle to rest. As the vehicle moved from right to left along the runway, the nose penetrated the net (fig. 6). The objective was to get the nose of the orbiter through the net so that the net enveloped the wing of the vehicle before the breakaways allowed the net to fall from its supports. The ends of the upper and lower horizontal bundles on each side of the runway were fastened to heavy chains. As the vehicle pulled the net along the runway, the chain links accelerated, one at a time, to the speed of the vehicle and thus produced a semicontrolled deceleration force time history.

Net

A multiple-element net consisting of individual elements with upper and lower horizontal members connected by vertical members was used for the tests (fig. 8). Groups of elements were bundled together to form the entire net assembly with each element acting independently to apply force on the arrested vehicle and at the same time minimizing damage to the vehicle by minimizing localized loading.

A 30-element net was used for the first three net configurations tested. Nylon cording with a diameter of 0.04 in. was used to construct each net. (See fig. 7.) This nylon cord was overstrength compared with one needed for the full-scale orbiter; thus, scale-strength vertical members were used in a 6-in-center portion of the net to determine whether vertical net members would fail or whether they would cause the nose gear to fail. For nets 1 to 3, the scale-strength vertical members were made of cotton thread that broke at ≈1.5 lb, which was actually three times the force desired for correct scale strength. The cotton thread, however, did not stretch significantly before it broke at 1.5 lb, whereas the actual orbiter net is made of nylon that stretches ≈25 percent before it breaks. The cotton, therefore, was considered to break at approximately the same time as scale-strength nylon would in a dynamic arrestment. Cotton thread was not the best net material to be used for the scale-strength vertical elements. However, not stretching significantly and breaking at a higher force were considered to be off-setting characteristics. Thus, the overall net dynamics were considered to be adequate.

The horizontal members were ≈12 ft long. Figure 9 shows the net window geometry for the first three nets tested. Length and horizontal spacing of the vertical members varied for the three different net configurations. The vertical members were double knotted to the horizontal members and then sealed with superglue. The six groups of five elements in the 30-element net were painted yellow, red, orange, green, blue, and black to better distinguish the various net elements. Nets 1 to 3 were supported with stanchions (fig. 6) and the upper horizontal bundle was attached to breakaways (fig. 7) with a breaking force of 0.5 lb (model scale). The nets were installed on the runway in an L-shaped configuration (fig. 10) with a portion of the vertical member lying on the runway to allow the nose gear to clear the lower horizontal bundle before vertical members catching on the orbiter nose pulled the lower horizontal bundle up. Figure 11 illustrates the L-shaped configuration in the net. The photograph shows the Space Shuttle *Enterprise* and a full-size section of nylon net. The *Enterprise* was used for a full-size pull-through test to determine whether the net window opening was satisfactory and to determine, at least statically, how the lower horizontal bundle would behave when vertical net members caught on the orbiter nose or nose gear.

The three different vertical strap lengths for nets 1 to 3 were used to determine the reasonable offset distance for the bottom horizontal bundle to prevent it from catching the nose gear. The theory was that up to three vertical members could catch on the nose gear during arrestment and that they would not generate enough force to break the nose gear. If, however, the center of the nose contacted a vertical member, the nose could lift a number of the lower horizontal members up above the nose gear tire, and the resulting force would cause the nose gear to fail for other than slow speed arrestments. Figure 10 gives the offset distance for the bottom bundle and other geometric data for nets 1 to 3. Figure 10 also shows the lower horizontal bundle in front of the nose gear tires for net 3 when a vertical net member is caught on the stagnation point of the orbiter nose. This configuration was tested to determine if in a dynamic roll into the net, the lower bundle would actually be lifted up in front of the nose gear tire. For these tests, the elevation of the top horizontal bundle was ≈10.9 in. model scale (25 ft full scale). (See fig. 10.)

Nets 4 and 5 were constructed with the net geometry proposed by All American Engineering Company (AAE) and shown in figure 12. These nets had a total of 36 elements divided into six different groups of elements (A to F) with six elements in each group. There were two different net window widths (W and W_1) for the elements in each group. The window widths were the same for groups A and F, B and E, and C and D; however, the location of the first vertical member from the end of each element was offset so that no two vertical members were in the same lateral position when all elements were assembled together to form a single net. Net 4, shown in figure 13, was constructed of nylon parachute cord and net 5, shown in figure 14, was constructed of scale-strength nylon thread that had a breaking strength of 0.5 lb model scale (6000 lb full scale). The same construction technique for the previous nets was used and the groups of elements were also painted. Nets 4 and 5 were supported in a similar manner as the previous nets; that is, stanchions were used for upper bundle supports with breakaways. For some runs, net 4 was supported by attaching the upper horizontal bundle to delayed tearaways, shown in figure 15, in an attempt to keep the upper horizontal bundle from falling before the net enveloped the wing of the vehicle. The delayed tearaway consisted of a short length of nylon parachute cord passed over an eye and behind a block of wood with just enough pressure on the cord to allow it to be pulled through the block with the proper amount of tension. When all the short nylon cord exited the block, the upper horizontal bundle was allowed to fall. Pertinent parameters of the 1/27.5-scale and full-scale nets are presented in table III.

Energy Absorbers

The full-scale arrestment system uses a water turbine system (ref. 5) as the energy absorber system. This type of system is difficult to model at the 1/27.5 scale, so an anchor chain arrestment system similar to one used by the Air Force in the past was used. (See fig. 16.) The arrestment system for nets 1 to 3 (runs 1 to 43) is shown in figures 3, 6, and 16(a). The ends of both the upper and lower horizontal net bundles on one side of the runway were connected to a heavy chain, which was sized to simulate an appropriate stopping force profile for a water turbine. The stopping force buildup occurs when the net, caught on the model, begins to accelerate each link of chain, one at a time, to the speed of the model. Part of the stopping force is also due to the sliding friction of the moving chain links on the runway surface.

During the early testing (runs 1 to 39), a single weight chain was used as the energy absorber. As the arresting force became better defined, a graduated chain consisting of a length of small light chain followed by medium and then large heavy lengths

was used to more closely model the proper arresting force time history. Figure 16(b) is a sketch and figure 17 is a photograph of this chain. When the graduated chain was used with nets 4 and 5, a long nylon cord was attached to the net, then the chord was wrapped around a sheave and along the runway and attached to the light end of the chain, as shown in figures 16(b), 17, and 18.

For the last 1/27.5-scale tests (runs 57 to 59), the sheaves were moved upstream from the net (figs. 15 and 16(c)) to change the force angle as the net enveloped the model. Moving the sheave solved the problem of underwing engagements that occurred occasionally when the top horizontal bundle crossed the top of the fuselage but then fell down under the wing. For runs 57 to 59, the sheaves were located 87 in. (200 ft full scale) upstream and 87 in. (200 ft full scale) from the runway centerline.

Runway

The 80-ft-long runway was made of 0.75-in-thick plywood that was stacked two sheets high and secured to the concrete floor. The distance from the net to the rollout end of the plywood runway was 41 ft 6 in. The spacing between the plywood sheet edges was filled with dental plaster and then sanded to provide a smooth surface. The width of the plywood runway was 12 ft, but tape was placed on the plywood (figs. 3 and 4) to mark the runway width of 5.45 ft, which represented a 150-ft-wide runway (full scale). One of the four transatlantic abort site runways is 150 ft wide and the others are 200 ft wide. A 0.25-in. groove was cut into the plywood along the net line to recess the bottom horizontal bundle of the net during a run when desired. This groove was cut to prevent the scale-strength member of the 1/27.5-scale model nose gear from breaking due to the lack of adequate shock absorption of the model nose gear tires. Recessing the bottom horizontal bundle is also discussed in the section "Results and Discussion."

Instrumentation and Photographic Coverage

The tests were recorded with one panning video camera for quick-look purposes and four 16-mm cameras located at various positions to obtain film coverage for each test from different angles. Photographs were taken of the model after each test. The speed of the model was recorded by two miniature magnetic pick ups located 1 ft apart and mounted at the end of the catapult section of the runway. (See fig. 3.) Load cells, shown in figure 18, were used to measure the arresting load on each side of the net for only nets 4 and 5. No loads were measured for nets 1, 2, and 3.

Test Procedure

The 1/27.5-scale model was launched into the arresting system at three different net engagement speeds: 3.8, 11.4, and 19.1 knots (20, 60, and 100 knots full scale). Prelaunch preparations included hanging the net, checking its height and lateral position, and repositioning the energy absorber system. The model was then prepared, loaded into the launch system, and locked into place. After each run, the following information was recorded: model runout distance, model speed at net engagement, offset of nose gear from centerline, position of top bundle over payload bay doors, net entanglement of main and nose gears, whether nose or main gear failure occurred, number of net members broken, and for some runs, arresting system force. Still pictures and close-up videos were taken of the model after arrestment. Most runs were conducted with the model engaging the center of the net system to simulate a runway centerline engagement. Figure 19 is a sketch of the runway and net geometry. Nets 1, 2, and 3 were also used to test off-centerline engagements, and the dashed lines in figure 19 show the location of the net for these engagements. The only off-centerline engagement location tested was the extreme case where the vehicle was at the edge of the runway.

Results and Discussion

The data presented in this report are limited to the accuracy of the modeling of the parameters in the test hardware and technique. The scale relationships, although not pure Froude scaling, are accurate for this test. The arrestment forces, however, were not modeled precisely for the entire rollout and were changed during the test program to better, but still not completely, model the time history of the full-size force. For this reason, runout distance and lateral displacement values were not completely accurate, but they are considered adequate. Forces during the early portion of the test (net engagement) were considered to be adequately modeled so that net envelopment of the model represented full-scale dynamics. Also, items such as pneumatic tires and net member strength were not correctly modeled, but for some runs net strength was closer to the correct model values. In spite of these less than pure modeling techniques, the overall results of these tests were considered adequate to determine most of the problems that may be encountered on the full-scale orbiter arrestment. In addition, solutions to these problems would be satisfactory full-size solutions.

Net 1

The results of all 1/27.5-scale tests with net 1 are presented in table IV. Tests for net 1 included 10 on-centerline engagements and 3 off-centerline engagements at average speeds of 20, 60, and 95 knots (full scale). The average rollout distances for these speeds were 190, 517, and 761 ft (full scale), respectively.

Early in the test program, the simulated scale-strength nose gear would frequently fail when it crossed the lower horizontal bundle of net members, but when the horizontal bundle was recessed in the runway, no gear failure occurred. The fact that the scale-strength nose gear on the 1/27.5-scale model sometimes broke when it hit the horizontal bundle raised a question as to what the loads would be with the full-size orbiter pneumatic tire running over a full-size horizontal bundle. To answer this question, a brief full-size test was conducted at the Langley Aircraft Landing Dynamics Facility (ref. 6) in which a fully loaded shuttle nose tire was run at 100 knots across a bunched (not spread out) bundle of nylon straps that was the size of the lower horizontal bundle. The maximum measured vertical and drag forces were 31 000 lb and 6000 lb, respectively, for a nominal vertical load on the tire of 19 000 lb. The loads on the nose gear (with two tires) would be 62 000 lb vertical and 12 000 lb drag. The maximum nose gear capability was considered to be ≈71 600 vertical and ≈57 700 lb drag; thus, the measured forces of a loaded orbiter nose tire running over the horizontal bundle were not high enough to cause failure of the nose landing gear.

The solid rubber tires used in the model tests did not absorb the shock of hitting the bundle of net members like the actual orbiter inflated tires and thus did not properly respond to this bump input force. To conduct tests to determine whether vertical net members caught on the nose gear could cause nose gear failure, a groove was cut in the runway (fig. 20) to recess the lower horizontal bundle until the nose gear passed over it. The vertical net members were still exposed to being caught on the nose gear. As the net enveloped the model, the lower bundle was pulled out of the groove. For net 1, the nose gear did not fail during this test procedure.

For the on-centerline 20-knot (full scale) engagements, after nose gear penetration, the upper horizontal net bundle stopped moving rearward when it reached the area of the windscreen, as shown in figure 21. The rollout was short and the forces, although not measured, were obviously light.

For the on-centerline 60-knot (full scale) engagements, three of four arrestments resulted in net elements entangled around one or both main gear axles, as shown in figure 22. When entanglement was severe, binding of the main gear tires occurred; this binding caused the tires to slide, as indicated in figure 22 by the dark skid marks on the plywood runway surface. For tests with net 1, net member entanglement about one or more main gear tires was frequent and had the effect of applying brakes, which at times caused the vehicle to steer left or right and also affected the rollout distances and lateral displacements measured at the end of the rollout. Entanglement of the main gear was considered to be undesirable, but it was not known whether its occurrence resulted from the small size of the 1/27.5-scale model or the fact that most of the net members were overstrength and did not break. In general, the net spread out over the wing and loaded the wing fairly evenly along the leading edge. The top horizontal net bundle came to rest close to the joint between the third and fourth cargo bay doors, as shown in figure 23.

The simulated main landing gear doors are shown in figure 21. An attempt was made to hold these doors on with scale-strength fasteners, but the mechanism was not adequately scaled. Frequently the net pulled the doors off the model, as shown in figure 22. On rare occasions, the main gear hit the landing gear doors that were now laying on the runway. This impact affected the rollout of the model and in some cases, failure of the scale-strength main gear strut occurred. These tests with net 1 indicate that the nose and main gear doors will almost certainly be damaged or torn from the vehicle except for low-speed engagements.

Four on-centerline engagements occurred at ≈95 knots (full scale) with net 1. For two of the runs, a mild entanglement occurred on the right main gear and for one of these, the model moved to the right edge of the simulated 150-ft-wide (full scale) runway, as shown in figure 24. The top horizontal net bundle came to rest in the center of the fourth cargo bay door. The 6-in. (model scale) center of net 1 had 16 scale-strength vertical net members. For most arrestments, several of these members were broken; thus, in a full-scale arrestment, some net member breakage is possible. Table IV lists the number of scale-strength vertical members broken on each run. For all on-centerline tests, the model was successfully arrested. In general, the net slipped easily over the nose and fuselage and enveloped the wing. Less entanglement of net elements seemed to occur around the main gear for the 95-knot (full scale) arrestments compared with the 60-knot (full scale) arrestments. For all runs with net 1, the nose gear was locked (not free to castor) in a forward yaw angle position of 0°.

Off-centerline engagements were conducted at approximately 20, 60, and 95 knots (full scale) to determine how the net enveloped the vehicle and to determine the rollout behavior if the vehicle was at the edge of the runway when net engagement occurred. Figure 3 is a photograph of the apparatus set up for an off-centerline engagement. The net was laterally offset so that the model engaged the end of the net simulating a vehicle with its right main gear at the runway's edge at the point of engagement. Past arresting systems for aircraft equipped with a tail hook indicated that when vehicle engagement was off center, the vehicle tended to be brought back toward the runway centerline during arrested rollout. These tests were conducted to determine whether a net arrestment system would also bring the vehicle back toward the runway centerline. With the model in figure 3 considered to be at the right runway edge, any lateral movement to the right would mean the model would be off the hard surface runway. Because only the 6-in. (model scale) center of the test net had scale-strength vertical members, an area near the end of the net was held open for vehicle nose penetration. Thus, no net entanglement occurred on the nose gear to affect the rollout behavior. The object of the off-centerline engagements was to determine whether the vehicle would stay on the runway or go off the side. The net was held open to preclude nose gear entanglement or nose gear failure from raising questions about whether or not the vehicle would stay on the runway.

In spite of the opening in the net for vehicle nose penetration, a vertical net member was caught on the nose gear axle for the slow-speed engagement. For the 60-knot (full scale) engagement speed, the vehicle veered to the right (short side of the runway) and off the runway edge, as shown in figure 25. For this run, net entanglement occurred around the left main gear axle which was sufficient to slide the inboard tire. Normally for a centerline engagement, the vehicle would veer to the side of the entangled gear, but during this run the arrestment forces caused the vehicle to move to the right, off the runway, in spite of left gear braking due to entanglement. For 95-knot (full scale) engagements, no net entanglement occurred on the nose or main gear. The vehicle veered to the right and because of the longer run out, moved even farther off the right side of the runway, as shown in figure 26. The nose gear moved laterally 173 ft (full scale) from its initial runway track before net engagement.

Net 2

Results of the tests with net 2 are presented in table V. Net 2 had nine on-centerline engagements and three off-centerline engagements at average engagement speeds of 22, 61, and 94 knots (full scale). The runout distances for these speeds averaged 236, 520, and 697 ft (full scale), respectively.

For on-centerline engagement speeds of ≈22 knots (full scale) with net 2, the arrestment behavior of the net and model were similar to that of net 1. However, for the net 2 geometry, the main landing gear had a tendency to roll over the lower horizontal bundle. Figure 27 shows that most of the lower horizontal bundle fell aft of the left main gear and some entanglement occurred on both main gears. (See run 14 in table V.) For run 15 (table V) the right main gear failed, but the failure was due to a landing gear door falling in front of the gear. This failure occurred late in the rollout and thus does not invalidate the early portion of the arrestment. After the landing gear door failed, the remainder of the rollout was considered invalid.

For three of the four tests at ≈60-knot (full scale) engagement speed, a failure occurred in the main landing gear, as shown in figure 28. After the right main gear failed on run 17 (table V), the nose gear also failed. For high-speed engagements (94 knots full scale), one test was successful, but the other test resulted in a failure of both main gear struts. As indicated in table V, some scale-strength vertical net members were broken on seven of nine centerline engagements. In addition, the top horizontal bundle came to rest on the area of the third or fourth payload bay doors and sometimes spread over both doors.

Off-centerline engagements with net 2 resulted in the model departing the runway edge at speeds of 59 and 92 knots (full scale), and in two of the three tests, both main gear struts indicated failure.

In general, net 2 gave less desirable arrestments than net 1. Vehicle dynamics were about the same for both nets, but more arrestments caused gear failure with net 2. The net 2 geometry had longer vertical members and caused greater loads and more failures of the main gear than net 1. In general, net 2 also had more lower horizontal bundle members run over by the main gear.

Net 3

A total of 14 runs with net 3 were performed; these runs included 10 on-centerline engagements and 4 off-centerline engagements. The average speeds were 59 and 96 knots (full scale) with average runout distances of 498 and 747 ft (full scale), respectively. The test data for net 3 are presented in table VI.

Three of five runs at ≈59 knots (full scale) resulted in failure of the main gear, and two runs also

resulted in nose gear failure. Two of the runs with main gear failures also had entangled main gear, but one run with main gear failure was completely free of entanglement. (See fig. 29.) Figure 30 is a photograph of the net after a successful arrestment with no entanglement. For most of the engagement speeds of ≈59 knots (full scale), 10 or more of the scale-strength vertical net members were broken, and for some tests, several overstrength vertical net elements were also broken (table VI). In general, net envelopment of the vehicle and rollout behavior were similar to that of net 1 except net 3 had more broken main gear and more overstrength vertical net elements break.

In general, net 3 arrestments at ≈96 knots (full scale) were similar to nets 1 and 2. Landing gear failures occurred on two of five runs, but they only occurred when the net was entangled in the main gear. Presumably, if entanglement could be prevented for an optimum-sized net-opening geometry, then gear failures would not occur.

For off-centerline engagements with net 3, all runs tracked to the right, which meant they would be off the side of the runway. Neither the main nor the nose gear failed for off-centerline arrestments with net 3. For run 39 (table VI), the model initially turned to the right after engaging the net but then pulled back to the left probably as a result of the net entanglement of the left main gear. For runs with net 3, the top horizontal bundle came to rest on the third or fourth cargo bay doors.

In general, of the first three nets, net 1 is the geometry of choice because it resulted in no landing gear failures, whereas nets 2 and 3 each had several gear failures for on-centerline engagements. For off-centerline engagements, all three nets caused the model to depart the side of the runway if it engaged the net at the edge of the runway with nose gear fixed straight ahead and no differential braking. These tests showed that for slow speeds a runway edge arrestment could be made with a rapid steering maneuver back toward the runway centerline upon net engagement. However, if the pilot has adequate steering control, it should be used earlier in the rollout so that the vehicle would not be at the runway edge when it engages the net. If a runway edge arrestment is inevitable, then nets 1, 2, and 3 will certainly stop the vehicle.

Net 4

To determine how many vertical members may be caught on the nose gear as it passes through the net, 31 push-through tests were conducted with the 1/27.5-scale 36-element net configuration proposed by AAE. A push-through test consisted of pushing the nose of the model into the net by hand. Figures 31(a) and 31(b) are photographs of a front and side view of a typical push-through test. In the figures, one vertical net member was caught between the nose gear tires. In a dynamic high-speed arrestment, this member would either be rolled under the nose gear tire or it would break. The nose gear was determined to be able to structurally withstand having up to three vertical members caught on it. Slow-speed push-through tests were thought to result in more vertical elements being caught than would occur in a dynamic arrestment. Thus, if no more than three elements were caught in these tests, then arrestment without nose gear failure was considered a likely result. Although not shown in figure 31, small nose gear doors were used in some push-through tests to determine the likelihood of members being caught on the nose gear doors. An attempt was made to mount the doors so that they would come off at the scaled breaking force. The full-scale force was 430 lb and the model scale force was 0.5 oz. The modeling of the nose gear door breakaway forces was not considered adequate. In some cases, the nose gear was fixed straight ahead; in other cases, it was free to swivel as the model was pushed into the net.

Table VII presents the results from the push-through tests. For the first 21 runs, the nose gear was free swiveling. Seven of the these runs resulted in one or two vertical members being caught on the model nose at the stagnation point. One or two vertical members were caught between the nose gear tires during 9 of the 21 runs, and 1 vertical member was caught on the nose gear strut in 1 of these runs. Vertical net members were not caught on the stagnation point or the nose landing gear system during eight runs.

The nose gear was locked straight ahead (not free swiveling) for the next set of 10 runs. One vertical member was caught on the model nose stagnation point for one run, and during three other runs, one vertical member was caught between the nose gear tires. For seven runs, vertical net members were not caught on the stagnation point or the nose gear system.

Table VIII gives the data for the catapult tests with net 4. Runs 40 to 56 had average speeds of 62 and 98 knots (full scale) with average runout distances of 598 and 884 ft, respectively. These runs were made to determine the number of vertical members that caught on the nose gear, the initial loading of the energy absorber system on the model,

and the distribution of the top bundle on the payload bay doors.

Net 4 was modeled close to the final net configuration chosen for use at some Shuttle landing sites, but unlike the first three nets, it did not have a scale-strength section for the model nose to pass through; that is, all the net was overstrength. Long lengths of nylon parachute cord were used to attach the net to a graduated chain. This parachute cord passed through a stationary sheave so that the load application point (the sheave) would not vary throughout the arrestment. (See figs. 16(b), 17, and 18.) For tests with net 4, the nose gear strut was modified to exceed scale-strength requirements so that it would not break when vertical net elements caught on it. The nose gear was also fixed straight ahead. For the first 17 runs with net 4, the breakaways holding the net before engagement were not scaled. One of the prime objectives of these tests was to determine the number of vertical members caught on the model nose gear, and these data are given in table VIII. A net member was caught on the nose gear for 9 of the first 17 runs. Because the net members were overstrength, they did not break; thus, the net stayed at the front of the model (fig. 32) and did not envelop the wing. Although this type of arrestment would not occur normally (a scale-strength element would break), the model was still arrested with no unusual characteristics or failures. Only 4 of the first 17 runs resulted in a main gear failure. These failures could be partly due to the fact that the net forces acted only through the nose gear for 9 of the first 17 runs. The deviation from the launch centerline during the arrestment rollout (table VIII) is affected by the nose gear being fixed.

The maximum number of vertical net members caught on the nose gear was three, which was the maximum number allowed to keep from causing the nose gear to fail. When vertical members did not catch on the nose gear, the top horizontal net bundle generally spread over the third payload bay door, as shown in figure 33.

One concern was that the top horizontal net bundle could fall below the wing rather than envelop the wing at the slower engagement speeds, especially during off-centerline engagements. Figure 34 is a photograph of an underwing engagement. One attempt to alleviate this problem was to move the sheaves upstream and at the same time, use extended tearaways. The upstream sheave location is shown in figures 15 and 16(c). This modification moved the angle of the retarding force toward the rear of the model. The extended (or delayed) tearaway (fig. 15) was used to hold the top net bundle up until the net had time to envelop the wing. The delayed tearaway was crudely modeled with a parachute cord passed through a groove in a wooden block. The tightness of the grooved block to its base was varied to produce the desired friction on the parachute cord for the tearaway force, and the length of cord was varied to control the amount of time needed to hold the net up until wing envelopment was assured. Data from runs 57 through 59, which used this revised configuration, are given in table VIII. Arrestments for the two 60-knot (full scale) tests (runs 58 and 59) resulted in the top horizontal bundle staying above the wing with good net envelopment of the model. (See fig. 35.) For the slow-speed engagement (run 57), the net fell in front of the wing in spite of the extended tearaways. However, the extended tearaways and the movement of the sheave upstream resulted in better net envelopment of the vehicle than the earlier net set up.

Arrestment forces were measured for nets 4 and 5 with a force transducer (load cell), which is shown in figure 18 mounted between the net and the nylon cord that was attached to the graduated chain. Figures 36(a) and 36(b) show typical traces of the arrestment forces acting on the model and theoretical arrestment forces from a computer program of the water twister arrestment system proposed for use on the Space Shuttle orbiter. The arrestment forces are presented for engagement speeds of ≈12 and ≈20 knots (≈60 and ≈100 knots full scale). The measured arrestment loads obtained at both speeds during the initial portion of the arrestment were similar to the theoretical forces. Thus, the energy absorber system (graduated chains attached to the net by a long nylon cord and sheave system) adequately modeled the initial portion of the performance curve of the expected performance for the full-scale arrestment system. The initial portion of the arrestment is important because during this time the net envelops the vehicle. Although no scale-strength vertical members were used with net 4, it was considered to exhibit essentially the same good qualities as net 1. Four runs occurred during which one or both main gears failed and this appeared to be a potential problem that must be solved.

Net 5

Net 5 was constructed of fine nylon thread with elongation characteristics similar to the proposed full-scale nylon net. Figure 14 is a photograph of net 5, and figure 16(b) is a sketch of the energy absorber system for net 5. The primary purpose of the single test conducted with this net was to determine the likelihood of a zipper effect that might allow the

model to pass through the net without stopping. The idea of the zipper effect was that a few vertical net members would overload and break and thus allow the load to be picked up by other members, which in turn would overload and break and so on until the vehicle broke through the net and continued down the runway unarrested. Only one test was conducted with net 5 and that test was conducted at a speed of 19.7 knots (103 knots full scale). The model was still slowly moving after a 40-ft roll distance; a backup arresting system kept it from hitting the end of the building. No zipper effect occurred and only two vertical and one horizontal net members were broken (substantially fewer breaks than for nets with the scale-strength cotton net members). This lower number of breaks was attributed to significant elongation with the nylon instead of the cotton, which had little elongation. Figures 37(a) and 37(b) are photographs of the scale-strength nylon net (net 5) after arrestment. Figure 37(a) shows the net pattern on top of the right wing and across the cargo bay doors, and figure 37(b) shows the net pattern under the model. The net was disturbed only slightly by pivoting the model nose up to take the photograph in figure 37(b). The vehicle deviation from the runway centerline was only 13.8 ft (full scale). One horizontal net member wrapped around the right main gear axle and three vertical elements were under the left main gear axle. Neither nose or main gear failed and the top horizontal bundle came to rest on the third cargo bay door.

Conclusions

Scale model studies of the Shuttle orbiter arrestment system (SOAS) have been completed. The system was tested with a 1/27.5-scale model at the NASA Langley Research Center. The following conclusions were made from the model studies.

1. For all nets tested, the 1/27.5-scale model was caught and arrested during every test run.
2. The best results were obtained when the vehicle engaged the net on or near the runway centerline. For engagements at the edge of a 200-ft-wide runway (88 ft from runway centerline), the possibility is high that the vehicle will depart the side of the runway during rollout with the possible exception of a quick steering input back toward the runway centerline at initial engagement with the net. If the pilot can make successful steering inputs, steering earlier in the rollout so that engagement is near the runway centerline would be best. If steering is not possible and inadequate braking has allowed the vehicle to reach the net, then a net arrestment system would stop the vehicle.
3. The net arrestment system should be considered for use only in landing abnormalities during aborts, and every effort should be made to stop before reaching the net. At least some damage to the orbiter can be expected for any engagement even if the damage is only to the nose or main gear doors.
4. The top horizontal net bundle of nylon members is likely to contact the orbiter windshield. For slow-speed arrestments, the top bundle may stay on the windshield and not envelop the orbiter wing, but this event poses no known structural problem.
5. For all tests with all five net configurations, three vertical net elements were the most ever caught on the nose gear during an arrestment. Furthermore, separate analyses have shown that three vertical elements will not cause nose gear failure.
6. Of the nets tested in this investigation, nets 1 and 4 had the best overall characteristics. Although not proven by these tests, net 4 appeared to have a better design to distribute the loads more evenly over the orbiter.
7. The problem with the top bundle going under the wing for some tests was alleviated by moving the force vectoring sheaves and using extended tearaway straps to hold the net up longer to allow full net envelopment before complete release from the net supports.

NASA Langley Research Center
Hampton, VA 23681-0001
September 16, 1993

Table I. Scaling Factors for 1/27.5-Scale Model

$[\lambda = 1/27.5]$

Definition	Symbol	Scaling factor
Length	L	λL
Acceleration	a	$1a$
Mass	m	$\lambda^{2.85} m$
Area	A	$\lambda^2 A$
Volume	V	$\lambda^3 V$
Force	F	$\lambda^{2.85} F$
Weight	w	$\lambda^{2.85} w$
Velocity	v	$\sqrt{\lambda}\, v$
Time	t	$\sqrt{\lambda}\, t$
Inertia	I	$\lambda^{4.85} I$

Table II. Pertinent Parameters for Model Scale, Full Scale, and Orbiter

Parameter	1/27.5-scale value	Full-scale value	Orbiter value
Mass, slugs	0.71	9 036	8 074
Mass, lbm	21.25	268 800	260 000
Body:			
Length, in.	52.25	1 437	1 466
Wing span, in.	34.10	938	936
Tail height, in.	24.60	676	682
Center of gravity:			
Height, in. (from runway)	6.35	175	≈197
Distance from nose, in.	30.75	846	≈850
Yaw moment of inertia, slugs-ft^2	0.8453	8 087 000	≈8 617 000
Nose landing gear:			
Distance from nose, in.	5.25	144	154
Tire spacing (center to center), in.	0.75	20.6	22
Tire diameter, in.	1.13	31.1	31
Tire width, in.	0.31	8.5	8.7
Main landing gear:			
Distance from nose, in.	34.62	952	947
Gear spacing, in.	9.88	272	272
Tire spacing (center to center), in.	1.25	34.4	36
Tire diameter, in.	1.47	40.4	44
Tire width, in.	0.52	14.3	16
Drag load at wheel axle to fail main gear, lb	7.9	100 000	100 000
Drag load at wheel axle to fail nose gear, lb	4.6	58 000	57 700

Table III. Pertinent Parameters for 1/27.5-Scale Nets

Net	Vertical strap				Bottom bundle offset		Width of scale-strength center section		Net length (chain to chain)		Net or stanchion height		Number of net elements	Breaking strength of net member (strap)	
	Length		Spacing												
	m.s., in.	f.s., ft	m.s., in.	f.s., ft	m.s., in.	f.s., ft	m.s., in.	f.s., ft	m.s., ft	f.s., ft	m.s., in.	f.s., ft		m.s., lb	f.s., lb
1	14.5	33.2	12.1	27.7	6.0	13.7	6.0	13.8	12	330	10.9	25	30	1.5	19 000
2	16.0	36.7	10.6	24.3	7.7	17.6	6.0	13.8	13	358	10.9	25	30	1.5	19 000
3	13.0	29.8	13.6	31.1	4.3	9.9	6.0	13.8	12	330	10.9	25	30	1.5	19 000
4	14.3	32.8	(fig. 12)		3.0	6.9	None		[a]14.2	[a]390	11.3	26	36		
									[b]13.6	[b]374					
5	13.3	30.2	(fig. 12)		3.0	6.9	Entire net		[a]14.2	[a]390	11.3	26	36	0.5	6 000
									[b]13.6	[b]374					
Actual Shuttle		32.8		15.1–26.8		7.0				424		25.8	36		6 000

[a]Upper horizontal bundle.
[b]Lower horizontal bundle.

Table IV. Test Data for 1/27.5-Scale Model With Net 1

[Off-centerline engagements at 2.6 ft m.s. (71 ft f.s.) from net centerline]

Run	Aim point position on centerline	Engagement velocity, knots		Rollout, ft		Nose gear deviation from launch centerline		Number of scale-strength straps broken	NLG failure	MLG failure		Top bundle location, payload bay door no.	Remarks
		m.s.	f.s.	m.s.	f.s.	m.s., in.	f.s., ft			Left	Right		
1	On	3.7	19.4	7.8	215	8.6	19.8		No	No	No		Top bundle on crew cabin window
2	On	4.2	22.0	7.7	211	27.0	61.9	2	No	No	No	3, 4	Right MLG entangled
3	On	11.5	60.3	20.7	569	18.5	42.4	6	No	No	No	4	Right MLG axle entangled by net
4	On	11.5	60.3	18.0	494	7.0	16.0	9	No	No	No	4	Right MLG axle entangled
5	On	11.5	60.3	18.5	509	25.0	57.3	10	No	No	No	4	Right MLG locked-up and axle entangled
6	On	11.8	61.9	19.7	541	34.5	79.1		No	No	No	4	
7	On	18.1	94.9	28.3	779	21.5	49.3		No	No	No	4	Right MLG entangled
8	On	17.8	93.3	28.9	795	3.0	6.9	16	No	No	No	4	Right MLG axle entangled
9	On	18.1	94.9	27.5	756	30.0	68.8		No	No	No	4	Right MLG axle entangled
10	On	18.1	94.9	29.0	797	15.0	34.4		No	No	No	4	
11	Off	3.4	17.8	5.2	144	10.0	22.9		No	No	No		Free NLG passage in net; top bundle on crew cabin window; one vertical strap on NLG axle; model tracked to right[a]
12	Off	11.6	60.8	17.2	472	47.0	107.7		No	No	No	3	Free NLG passage in net; left MLG axle entangled; model tracked to right[a]
13	Off	18.1	94.9	24.8	680	75.5	173.0		No	No	No		Free NLG passage in net; model tracked to right[a]

[a]Because model engaged net on right runway edge and moved to right during arrestment, it would have come to rest off right side of runway.

Table V. Test Data for 1/27.5-Scale Model With Net 2

[Off-centerline engagements at 2.6 ft m.s. (71 ft f.s.) from net centerline]

Run	Aim point position on centerline	Engagement velocity, knots		Rollout, ft		Nose gear deviation from launch centerline		Number of scale-strength straps broken	NLG failure	MLG failure		Top bundle location, payload bay door no.	Remarks
		m.s.	f.s.	m.s.	f.s.	m.s., in.	f.s., ft			Left	Right		
14	On	4.1	21.5	8.5	233	4.8	10.9	5	No	No	No	3	Both MLG entangled
15	On	4.3	22.6	8.5	234	10.5	24.1	2	No	No	Yes	3	Right MLG door fell in front of right main gear and caused it to fail
16	On			8.2	226	1.5	3.4	1	No	No	No	3	Left MLG entangled by net
17	On	11.5	60.3	18.5	508	11.0	25.2	7	Yes	No	Yes	4	NLG failed after right MLG failed; no net around NLG when it failed
18	On	11.7	61.4	17.6	483	31.3	71.7		Yes	No	Yes	3, 4	Right MLG failed at end of rollout; net wrapped around left MLG axle
19	On	11.6	60.8	19.0	522	3.3	7.5	8	No	No	No	3, 4	
20	On	11.7	61.4	23.6	648	0.5	1.2		No	Yes	Yes	4	Both MLG entangled
21	On	18.0	94.4	29.2	804	1.8	3.9	18	No	No	No	4	
22	On	18.1	94.9	24.5	674	6.5	14.9	17	No	Yes	Yes	3	Both MLG entangled
23	Off	Slow		9.2	253	7.0	16.0		No	No	No	3	Horizontal elements were in front and behind MLG struts; model tracked to left
24	Off	11.3	59.3	15.9	438	23.0	52.7		Yes	Yes	Yes	3	Both MLG entangled; NLG broke when right wing hit runway; then left MLG broke; model tracked to right[a]
25	Off	17.5	91.8	22.3	614	16.5	37.8		No	Yes	Yes	3	Both MLG entangled; model tracked to the right[a]

[a]Because model engaged net on right runway edge and moved to right during arrestment, it would have come to rest off right side of runway.

Table VI. Test Data for 1/27.5-Scale Model With Net 3

[Off-centerline engagements at 2.6 ft m.s. (71 ft f.s.) from net centerline; bottom horizontal bundle bunched to see whether NLG fails when it hits bundle for runs 37 and 38]

Run	Aim point position on centerline	Engagement velocity, knots		Rollout, ft		Nose gear deviation from launch centerline		Number of scale-strength straps broken	Number of overstrength vertical net straps broken	NLG failure	MLG failure		Top bundle location, payload bay door no.	Remarks
		m.s.	f.s.	m.s.	f.s.	m.s., in.	f.s., ft				Left	Right		
26	On	11.2	58.7	20.7	568	8.5	19.5	10		No	No	No	4	
27	On	11.1	58.2	16.7	459	5.8	13.2	10	2	No	Yes	Yes	3	Bottom horizontal bundle broke MLG; both MLG entangled
28	On	11.1	58.2	17.4	478	28.5	65.3	11	2	No	No	Yes	4	Nose wheel steering; model veered to edge of runway; RMG entangled
29	On			16.3	447	15.8	36.1	18	3	Yes	Yes	Yes	4	
30	On	11.7	61.4	19.9	548	21.5	49.3			Yes	No	No	4	Bottom bundle bunched; model veered to right; NLG failed after NLG was over bottom bundle
31	On	18.8	98.6	23.3	642	2.3	5.3	16		No	Yes	Yes	4	Both MLG entangled
32	On	17.9	93.9	28.8	793	5.5	12.7			No	No	No	4	
33	On	18.0	94.4	27.0	742	21.5	49.3			Yes	Yes	No	4	Scale-strength vertical members not repaired for this run; NLG failed when it hit bottom bundle; MLG entangled
34	On	18.1	94.9	28.3	777	14.5	33.2			Yes	No	No	4	NLG failed when it hit bottom bundle
35	On	18.2	95.4	28.6	786	2.3	5.3			No	No	No	4	Scaled strength verticals not repaired
36	Off	Slow		6.8	186	2.3	5.3			No	No	No		Top bundle on crew cabin window; two vertical straps caught on NLG
37	Off	11.5	60.3	17.8	490	42.0	96.2			No	No	No	4	Right MLG entangled; model tracked to right[a]
38	Off	18.4	96.5	27.5	756	32.5	74.5			No	No	No	4	Model tracked to right and pulled back to left[a]
39	Off	18.2	95.4	25.9	712	8.0	18.3			No	No	No	4	Left MLG axle entangled; model tracked to right and pulled back to the left[a]

[a]Because model engaged net on right runway edge and moved to right during arrestment, it would have come to rest off right side of runway.

Table VII. 1/27.5-Scale Model Push-Through Tests With Net 4

Run	Number of vertical elements caught—				Nose gear doors broken off
	By model nose	Between nose tires	By nose strut	By nose gear doors	
Nose gear free swivelling; nose gear doors off					
1	0	0	0		
2	1	2	0		
3	0	0	0		
4	1	0	0		
5	1	0	0		
6	0	0	0		
7	0	1	0		
8	1	1	0		
9	2	0	0		
10	0	2	0		
Nose gear free swivelling; nose gear doors on					
11	0	0	0	0	
12	0	0	0	0	
13	1	1	0	2	
14	0	2	0	1	
15	0	2	0	1	
16	0	2	0	2	Left
17	0	0	0	1	Left
18	0	0	0	0	
19	1	0	1	2	
20	0	0	0	2	Left
21	0	1	0	2	Left
Nose gear fixed straight ahead; nose gear doors on					
22	0	0	0	1	Left
23	0	0	0	1	Left
24	0	0	0	1	
25	0	1	0	1	
26	0	0	0	0	
27	0	1	0	1	Left
28	0	0	0	0	
29	1	1	0	1	Left
30	0	0	0	1	
31	0	0	0	0	

Table VIII. Test Data for 1/27.5-Scale Model With Net 4

[Used pulleys for lead-off sheaves, parachute cord to attach net to chains, 2 ft small, 2 ft medium and the remainder heavy chain; all vertical net members were overstrength; NLG fixed, bottom bundle not buried, breakaways not scaled, and used two stanchions]

Run	Aim point position on centerline	Engagement velocity, knots		Rollout, ft		Nose gear deviation from launch centerline		Number of vertical members caught on nose gear	MLG failure		Top bundle location, payload bay door no.	Remarks
		m.s.	f.s.	m.s.	f.s.	m.s., in.	f.s., ft		Left	Right		
40	On	11.6	60.8	16.0	440	6.5	14.9	0	Yes	Yes	2, 3	MLG broke at end of rollout; right MLG axle entangled
41	On	12.1	63.5	27.0	741	3.5	8.0		No	No	3	Open passage for NLG in net to see top bundle spread over cargo bay
42	On	11.8	61.9	17.4	479	15.0	34.4	0	Yes	Yes	3	Both MLG entangled
43	On			24.3	669	38.5	88.2	3	No	No	1	Three vertical members across NLG strut
44	On	10.6	55.6	22.0	605	0.5	1.1	3	No	No	1	One vertical member across NLG strut; two verticals between NLG tires
[a]45	On	12.0	62.9	24.3	669	24.8	56.8	1	No	No	1	Left MLG entangled
[a]46	On			16.3	448	55.5	127.2	0	No	No	3	Both MLG entangled
[a]47	On			21.0	576	57.3	131.2	3	No	No	1	One vertical across NLG strut; two verticals between NLG tires; left MLG entangled
[a]48	On	12.0	62.9	16.2	446	22.5	51.6	0	No	Yes	3	Both MLG entangled
[a]49	On	11.8	61.9	23.6	648	7.5	17.2	2	No	No	1	Two verticals around NLG axle
[a]50	On	11.8	61.9	24.0	659	29.0	66.5	0	No	No	3	Both MLG entangled
[a]51	On	11.9	62.4	21.3	585	45.2	103.6	1	No	No	1	One vertical caught between NLG tires; one vertical on left MLG
[a]52	On	11.9	62.4	23.5	646	7.2	16.6	1	No	No	1, 2	One vertical around NLG axle; left MLG entangled
[a]53	On	11.8	61.9	23.2	639	9.2	21.2	1	No	No	1	One vertical between NLG tires; MLG entangled
[a]54	On	12.0	62.9	26.2	722	37.5	85.9	0	No	No	3	Right MLG entangled
[a]55	On	18.6	97.5	28.0	769	22.0	50.4	3	Yes	No	1	NLG steering engaged; three verticals around NLG axle; three verticals on left MLG
[a]56	On	18.6	97.5	36.3	999	10.0	22.9	0	No	No	3	Open passage for NLG in net; model stopped by instrumentation cord
[b]57	On	5.3	27.8	9.8	270	0.8	1.8		No	No	1	One vertical around NLG axle
[b]58	On	11.5	60.3	24.5	675	17.5	40.1		No	No	3	Overwing engagement; right MLG entangled; model yawed to the right
[b]59	On	11.7	61.4	24.5	674	10.0	22.9		No	No	3	Both MLG entangled; overwing engagement

[a]Runs 45–56 used two 2 ft medium size chains in parallel between medium and large chains to alter retardation force.

[b]Runs 57–59 sheaves moved upstream 7.27 ft, simulated extended tearaways installed.

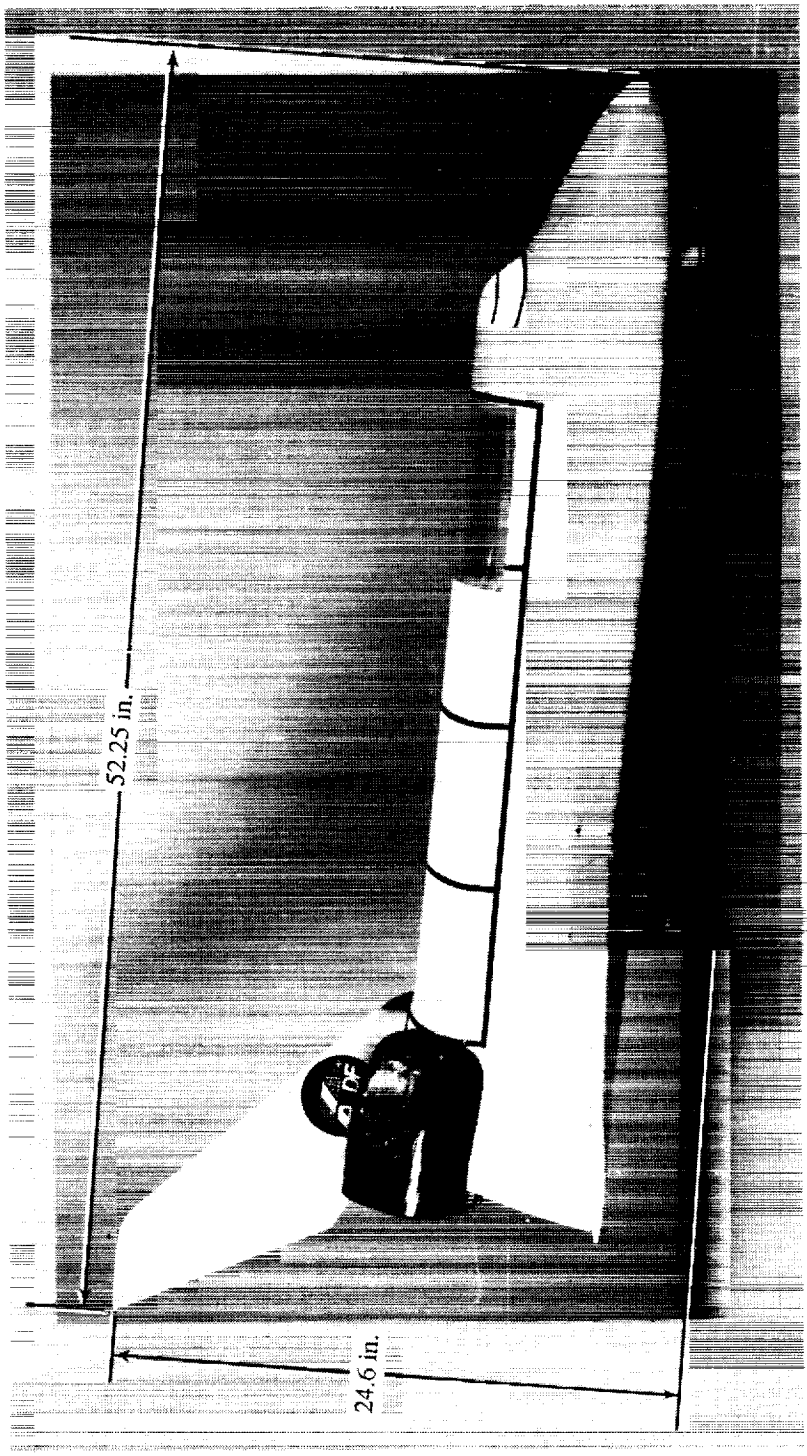

L-88-6082

Figure 1. 1/27.5-scale model of Space Shuttle orbiter.

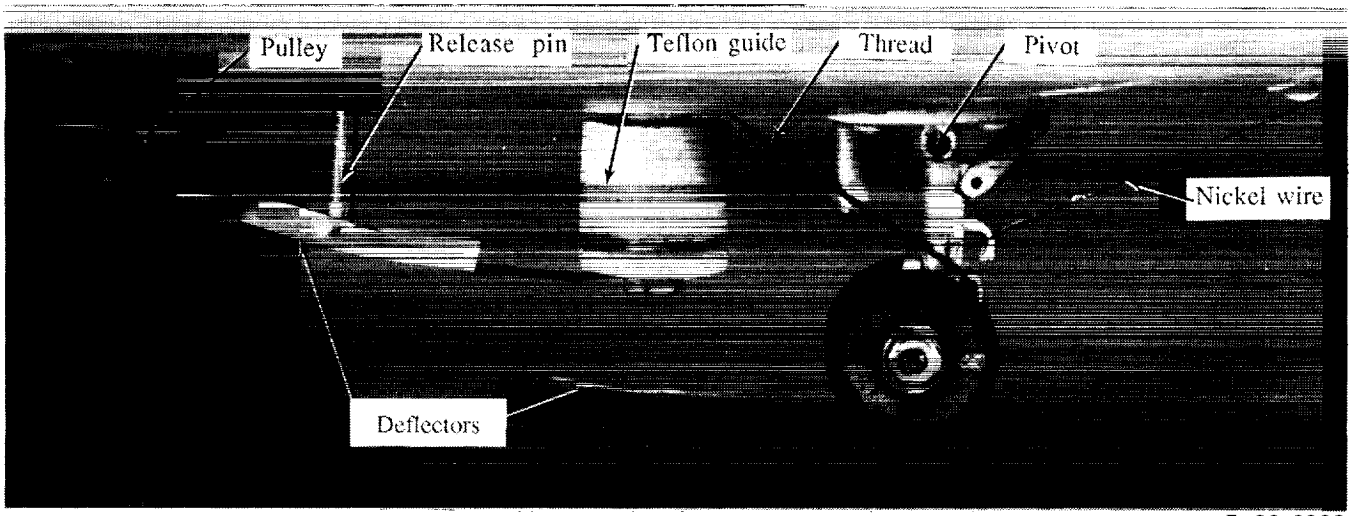

L-88-6082

(a) Nose landing gear.

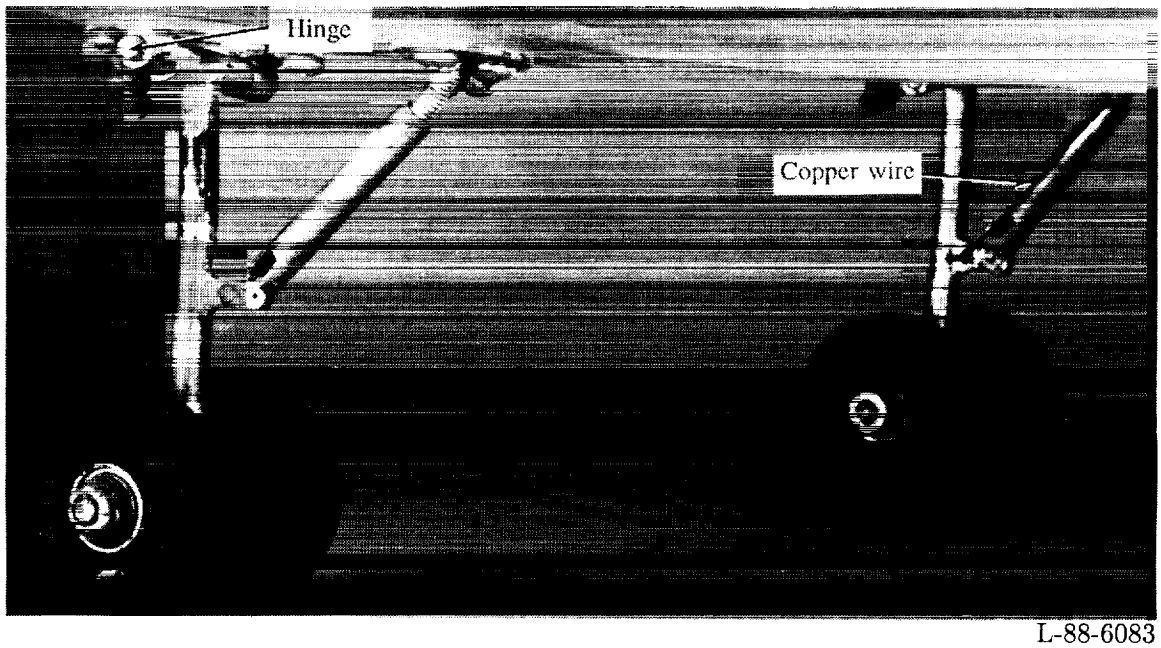

L-88-6083

(b) Main landing gear.

Figure 2. Landing gear for 1/27.5-scale model.

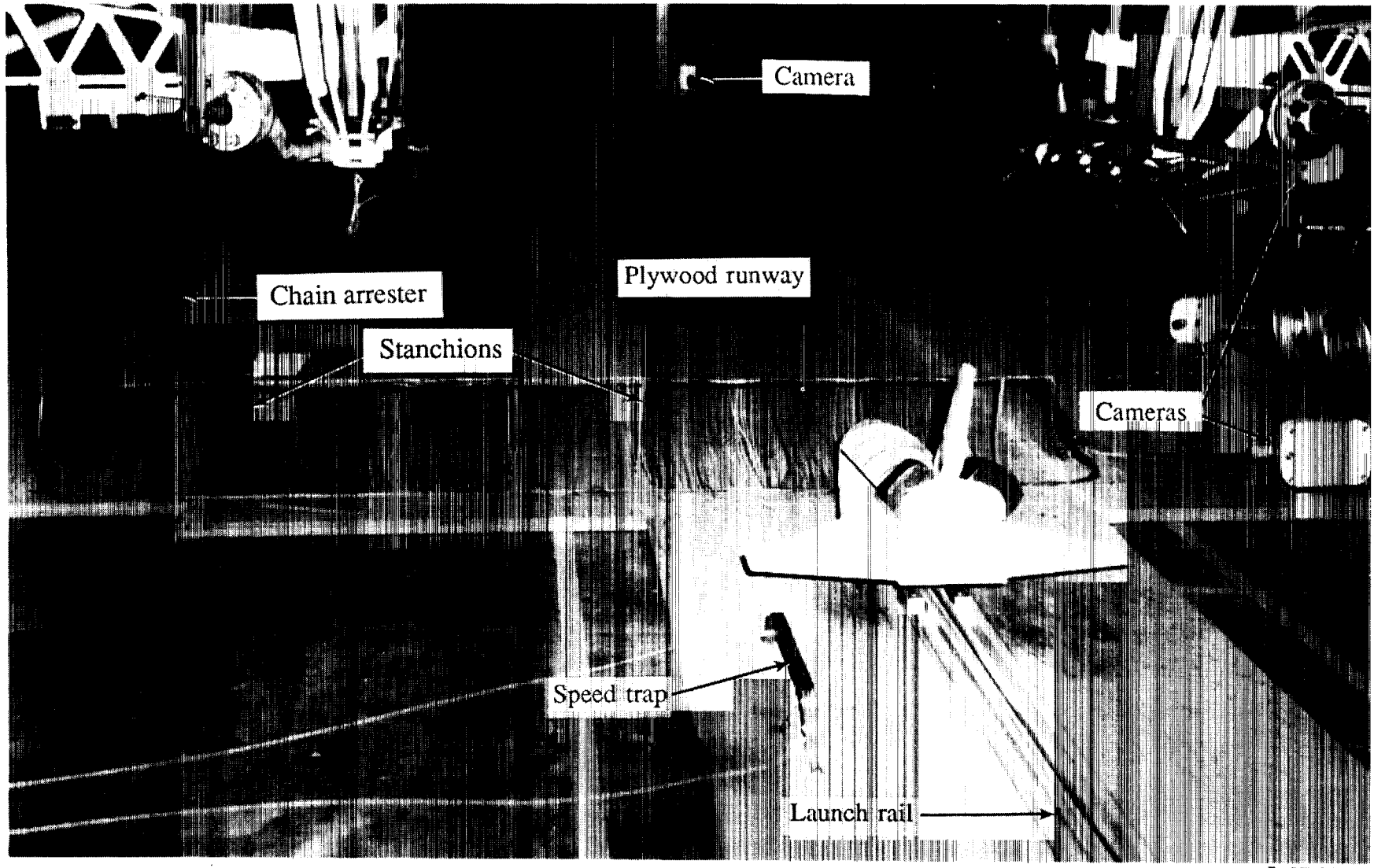

L-87-02898

Figure 3. Net setup for off-centerline engagement.

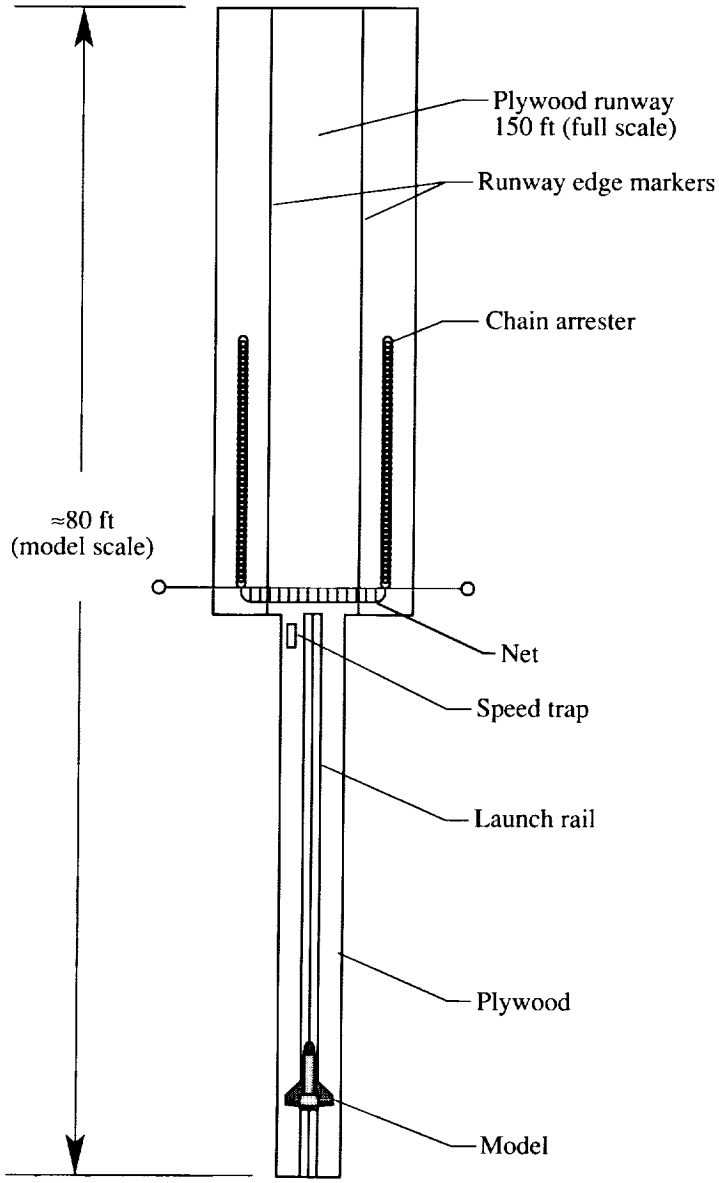

Figure 4. Plan view of 1/27.5-scale test setup.

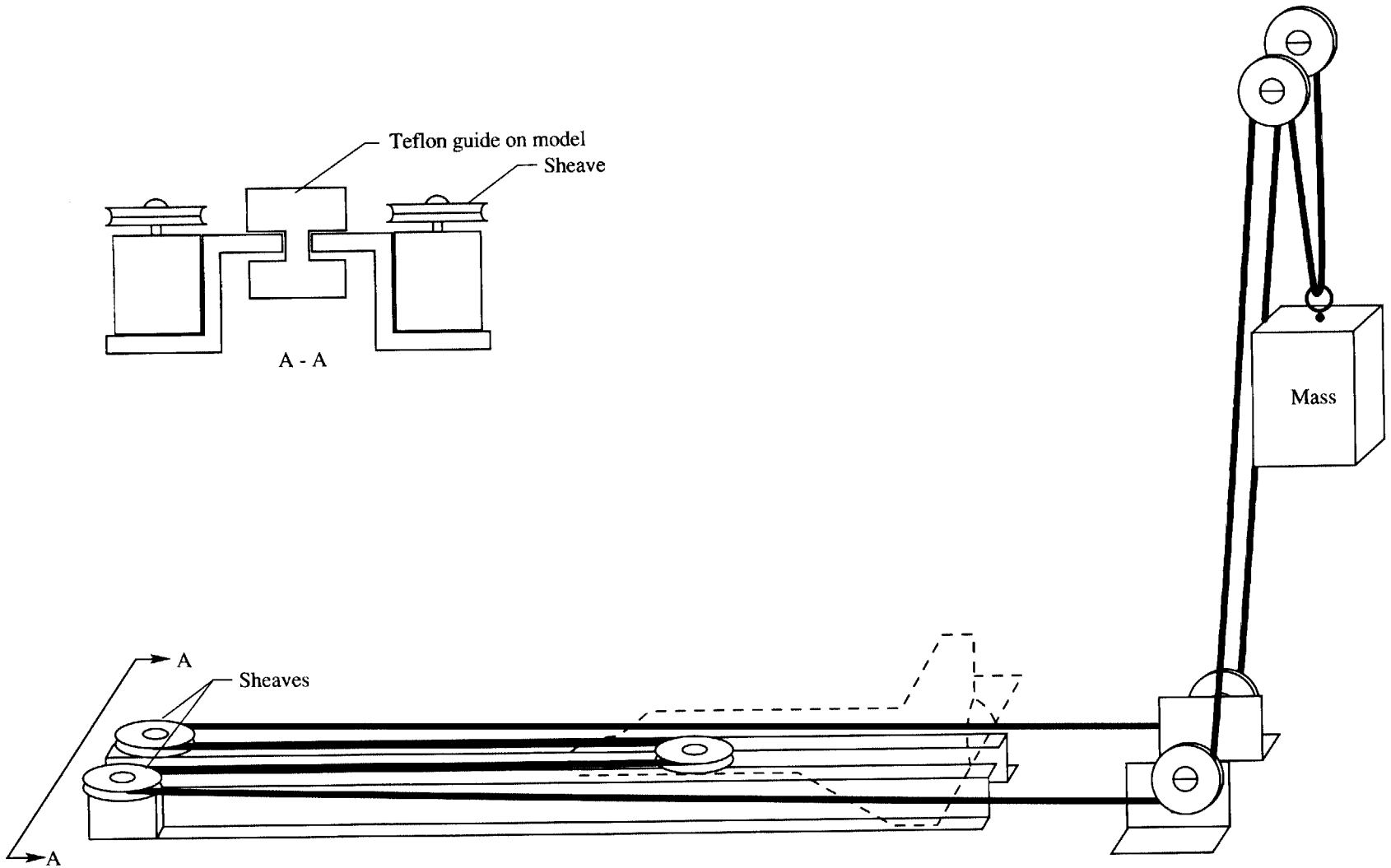

Figure 5. Launch mechanism.

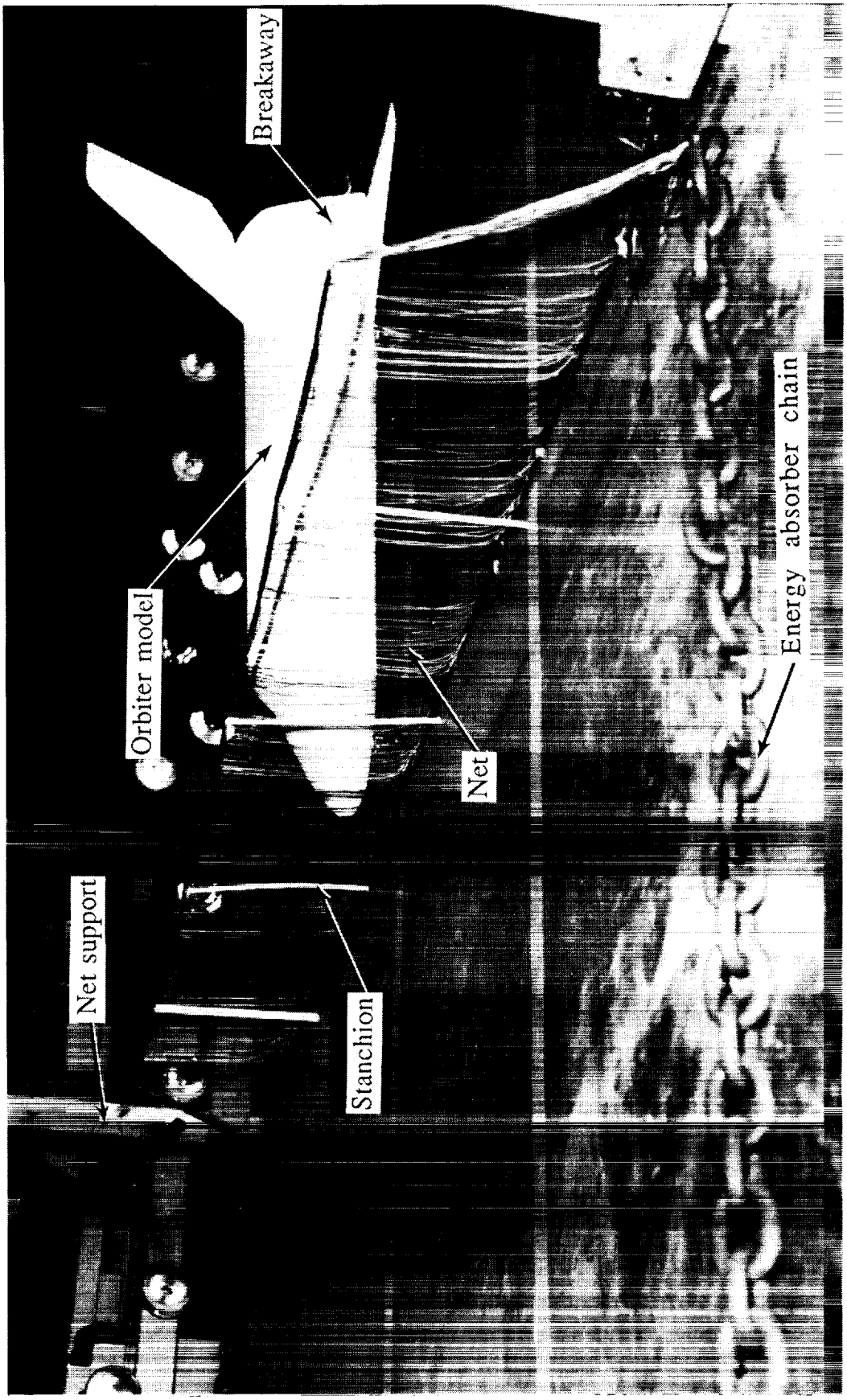

Figure 6. Early version of 1/27.5-scale arrestment system.

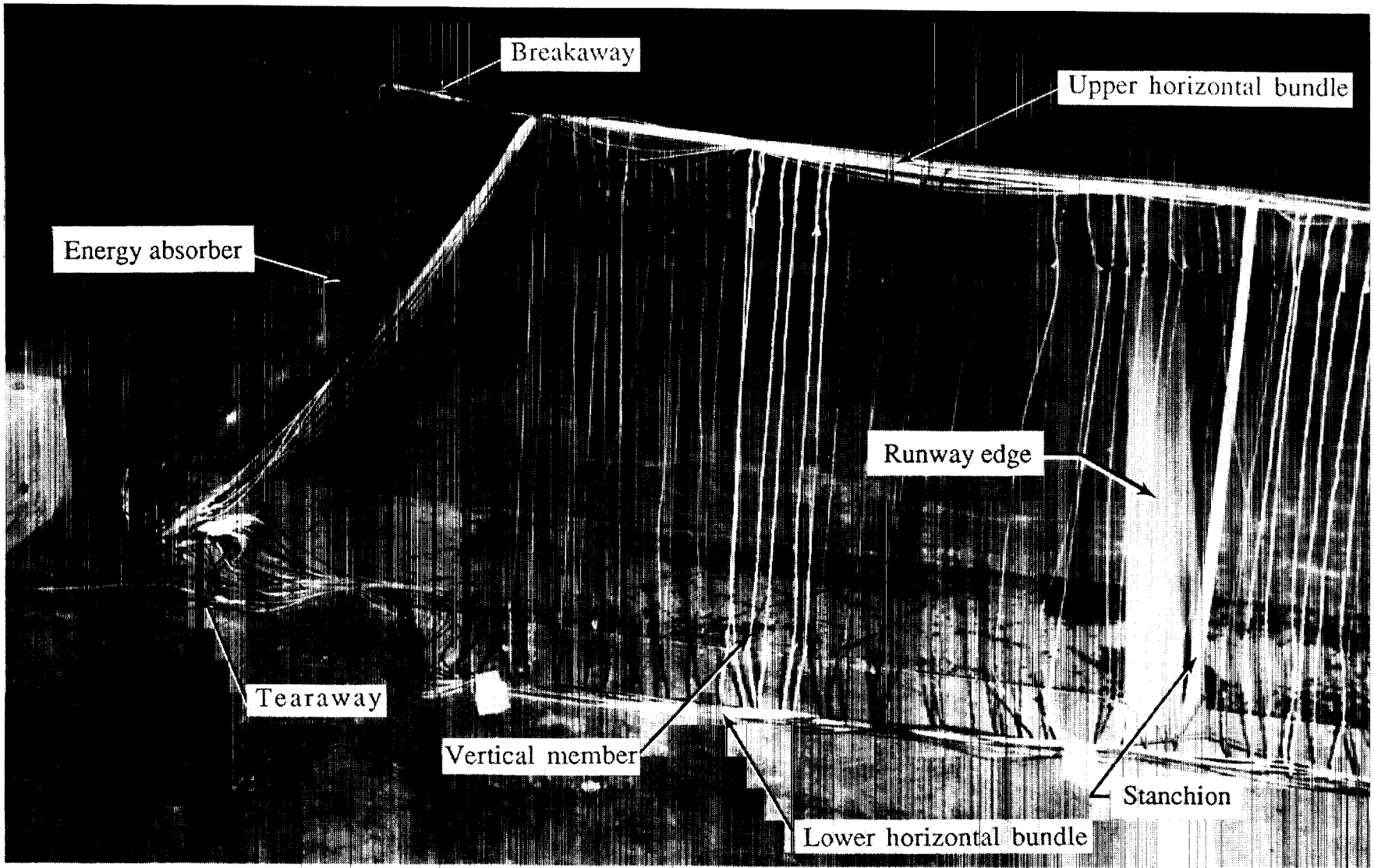

Figure 7. Net, supports, and energy absorber chain.

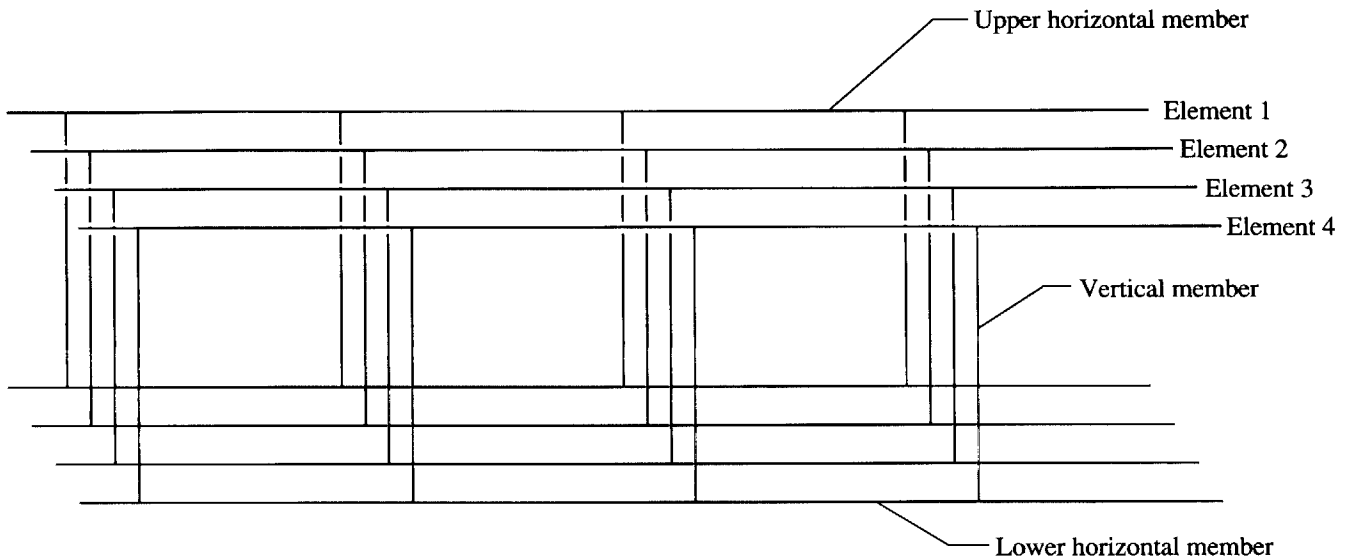

Figure 8. Partial schematic of multiple-element net.

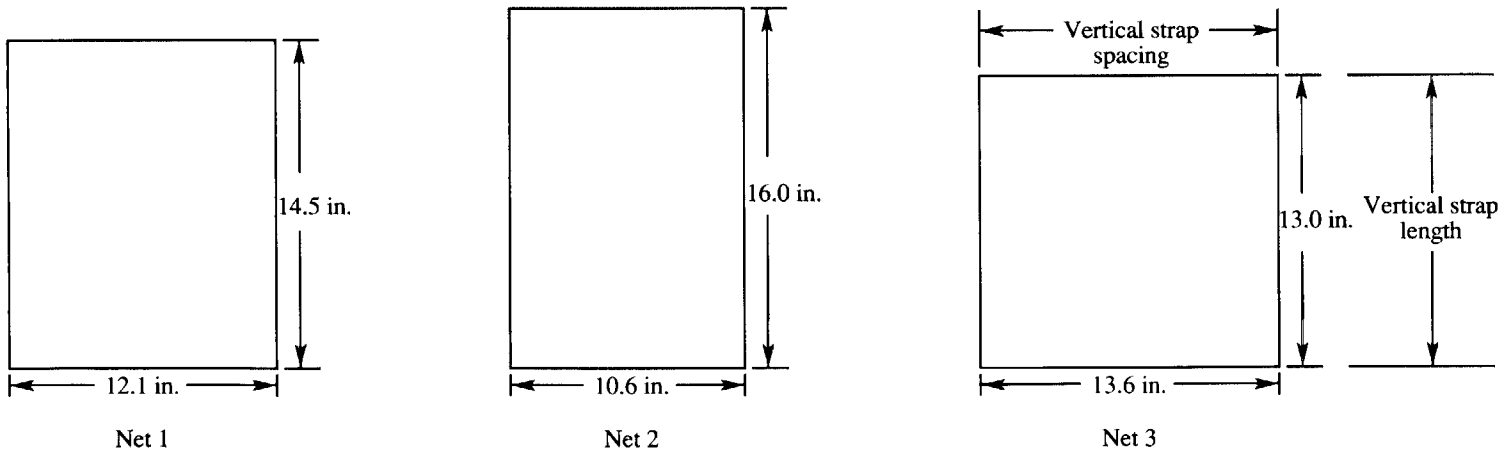

Figure 9. Window geometries for nets 1 to 3. Dimensions are in model scale.

	Bottom bundle offset	
	Model scale	Full scale
Net 1	6.0 in.	13.7 ft
Net 2	7.7 in.	17.6 ft
Net 3	4.3 in.	9.8 ft

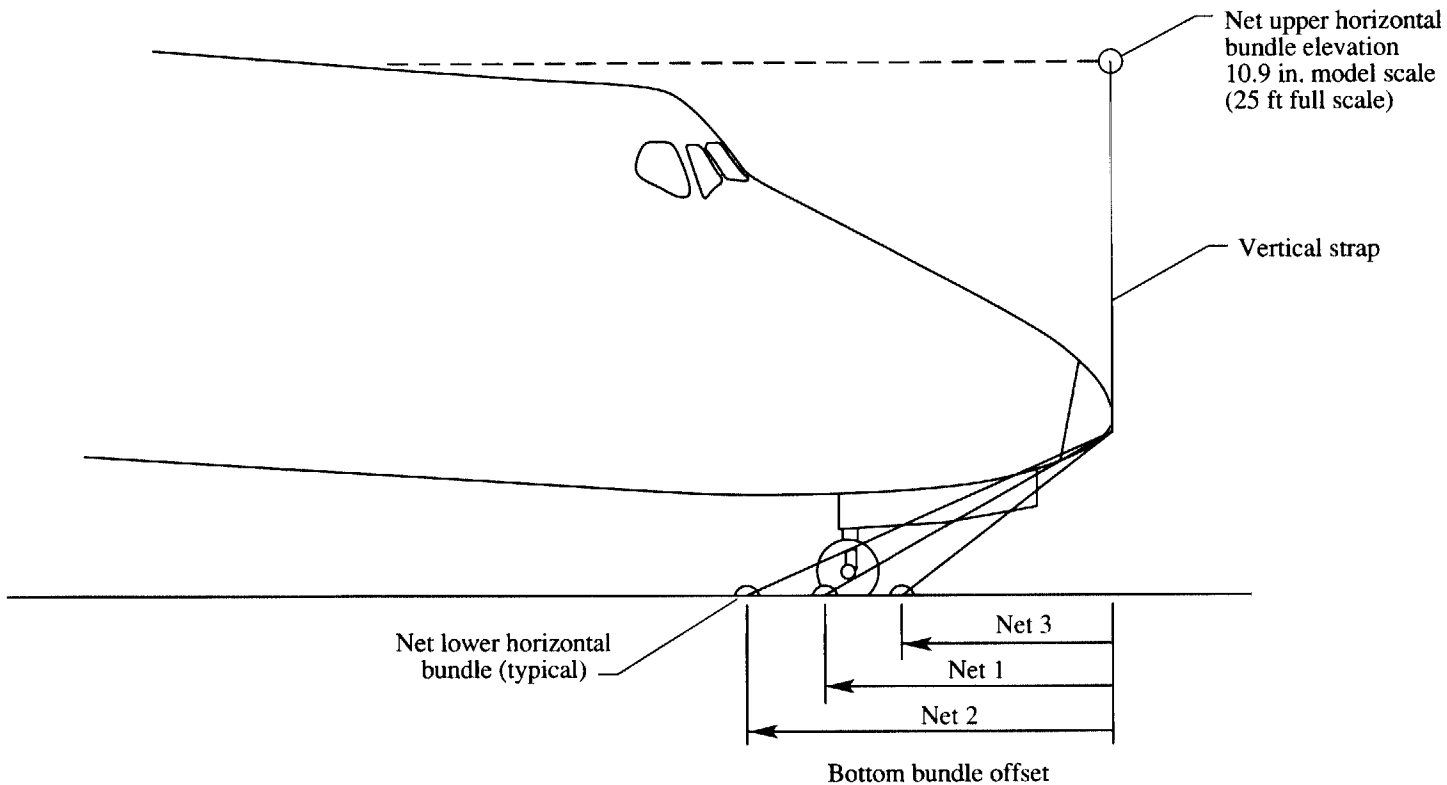

Figure 10. Geometry of L-shape for nets 1 to 3.

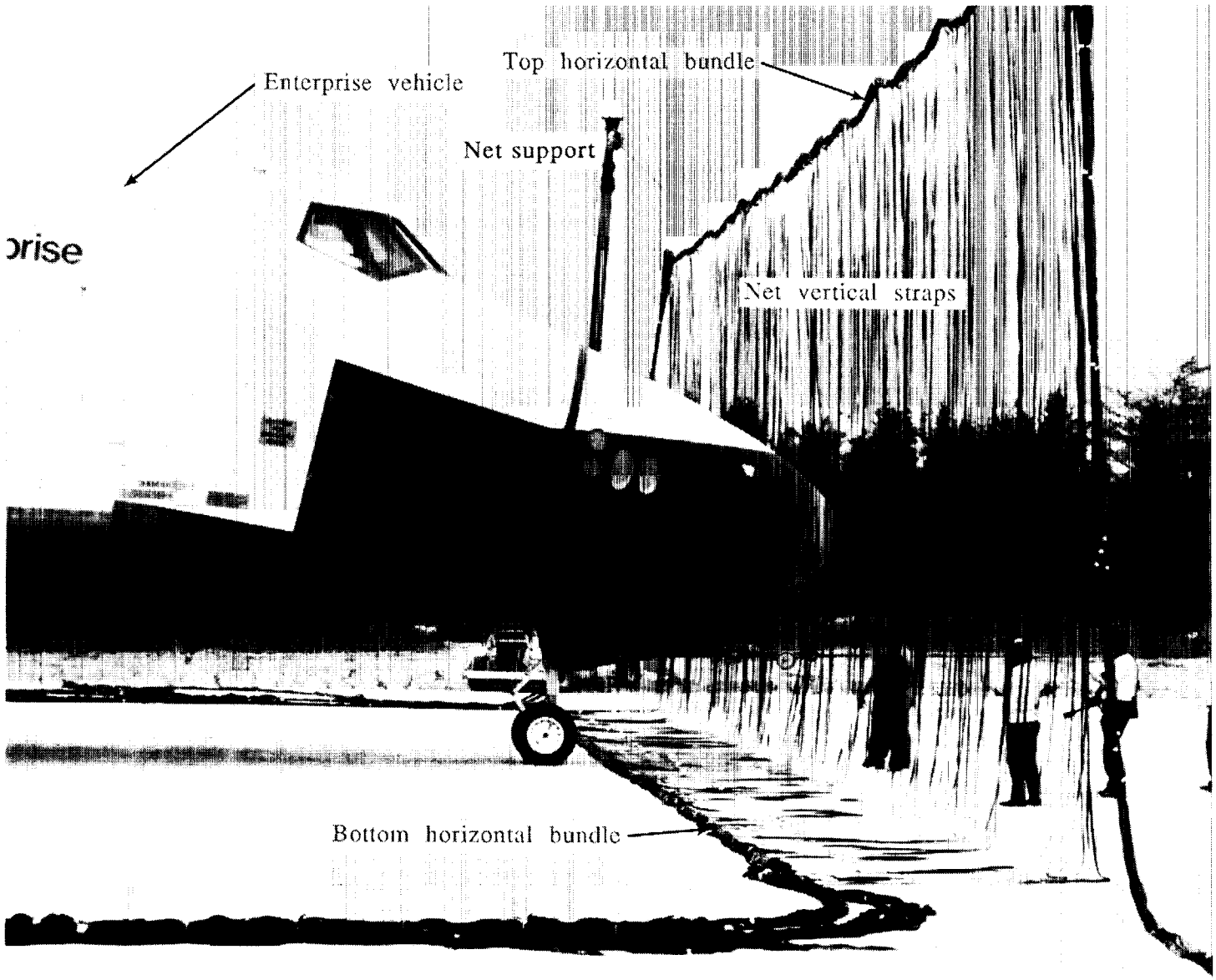

Figure 11. Space Shuttle *Enterprise* with nylon net in L-shaped configuration.

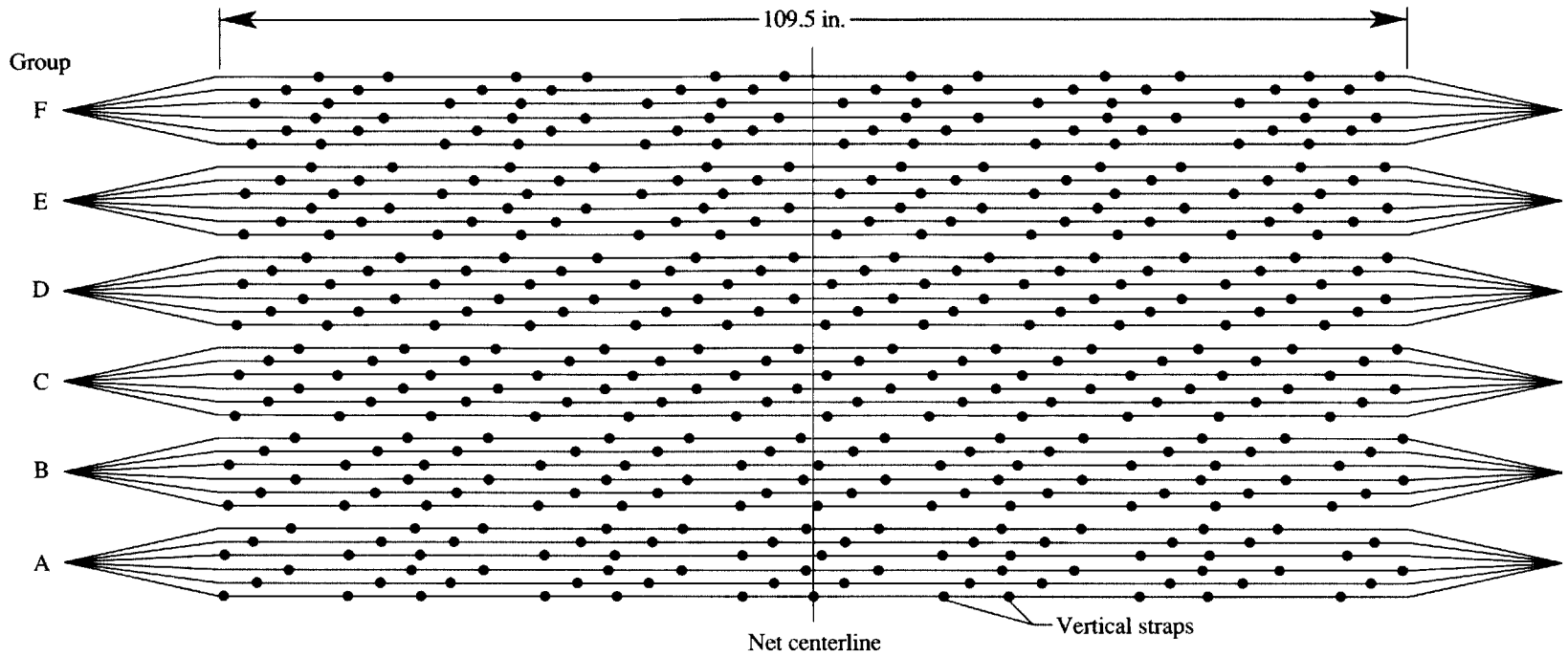

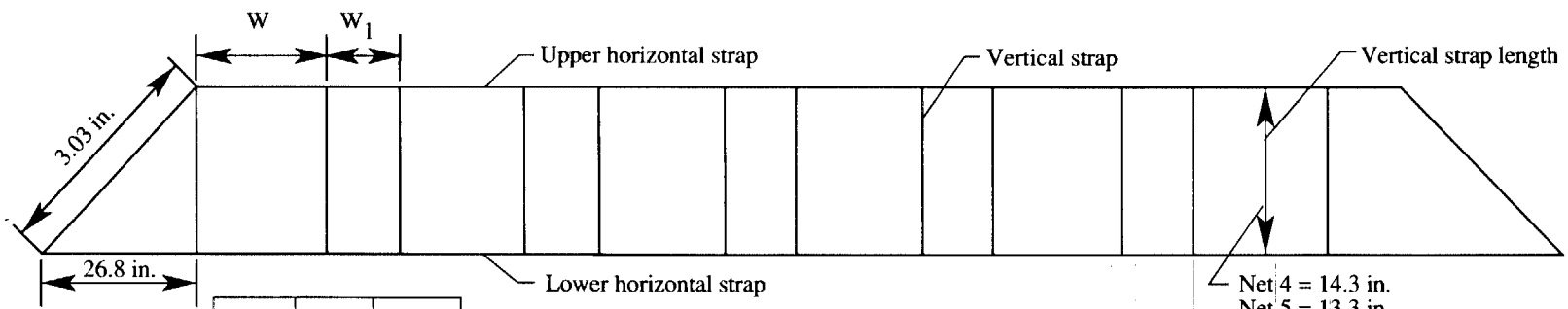

Group	W, in.	W_1, in.
A	11.7	6.6
B	10.7	7.6
C	9.7	8.6
D	9.7	8.6
E	10.7	7.6
F	11.7	6.6

Figure 12. Arresting net geometry for nets 4 and 5. Dimensions are in model scale.

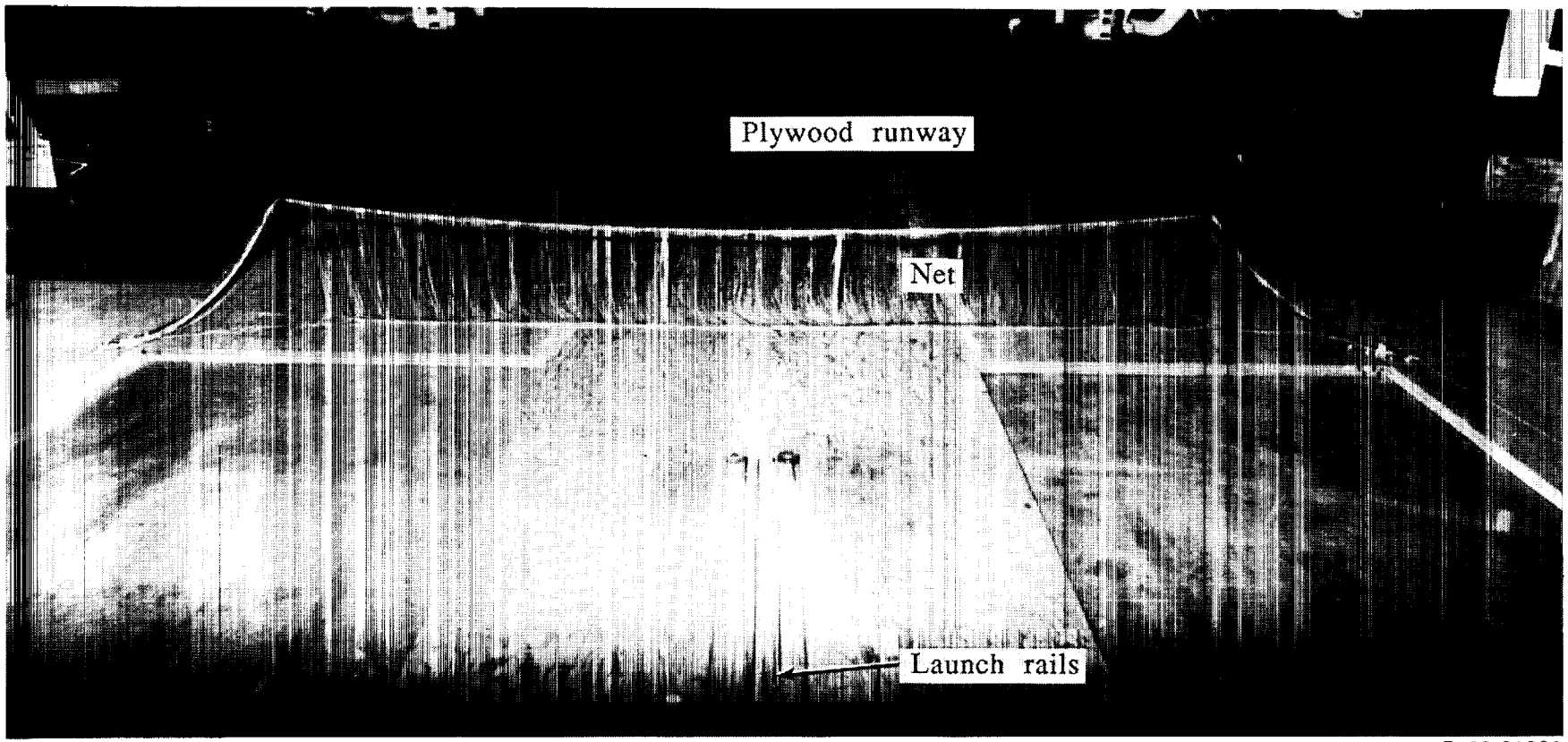

L-88-01991

Figure 13. Net 4, with varying window widths, used for 1/27.5-scale tests.

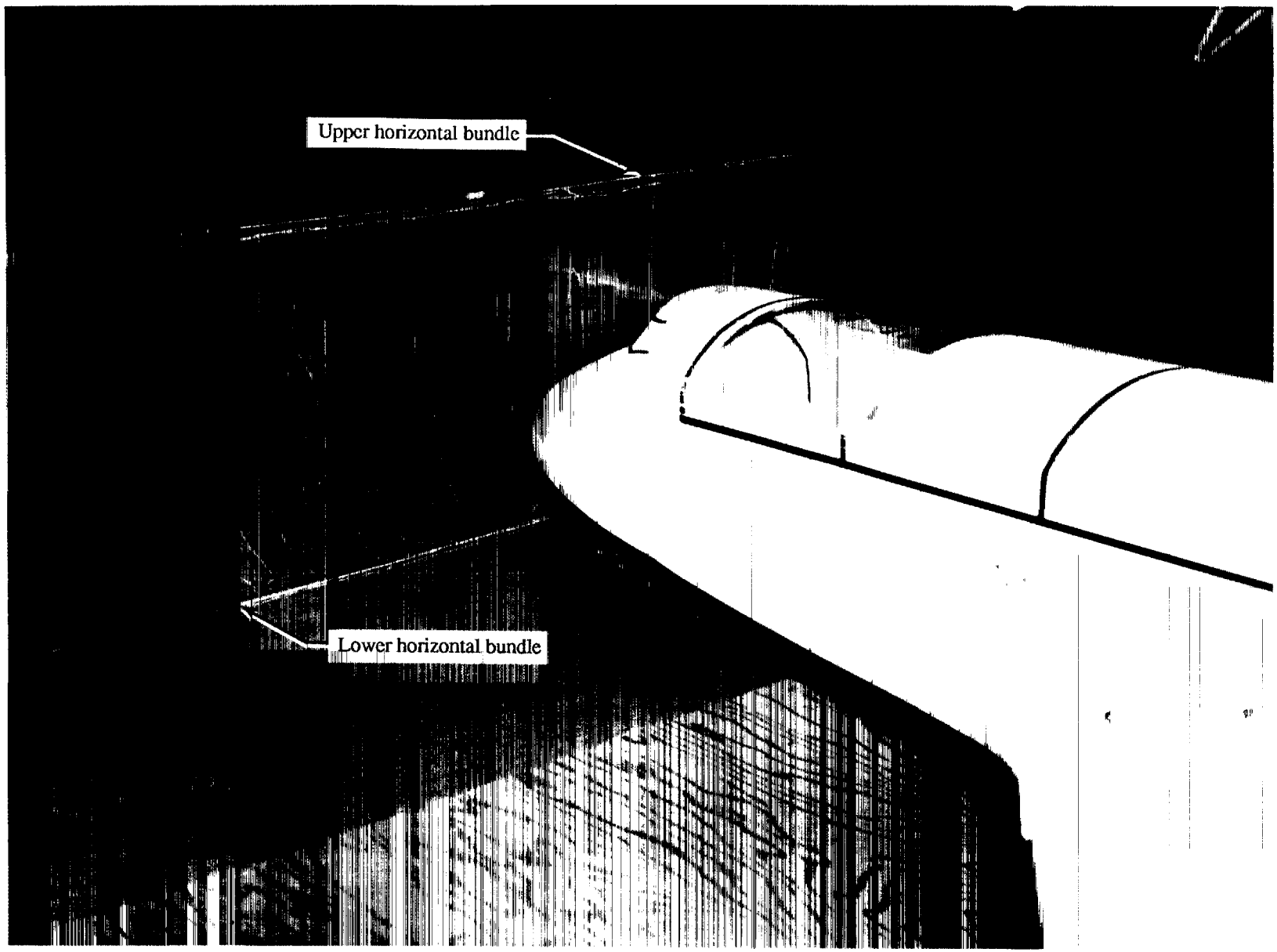

L-87-11023

Figure 14. Scale-strength net 5 constructed with nylon thread.

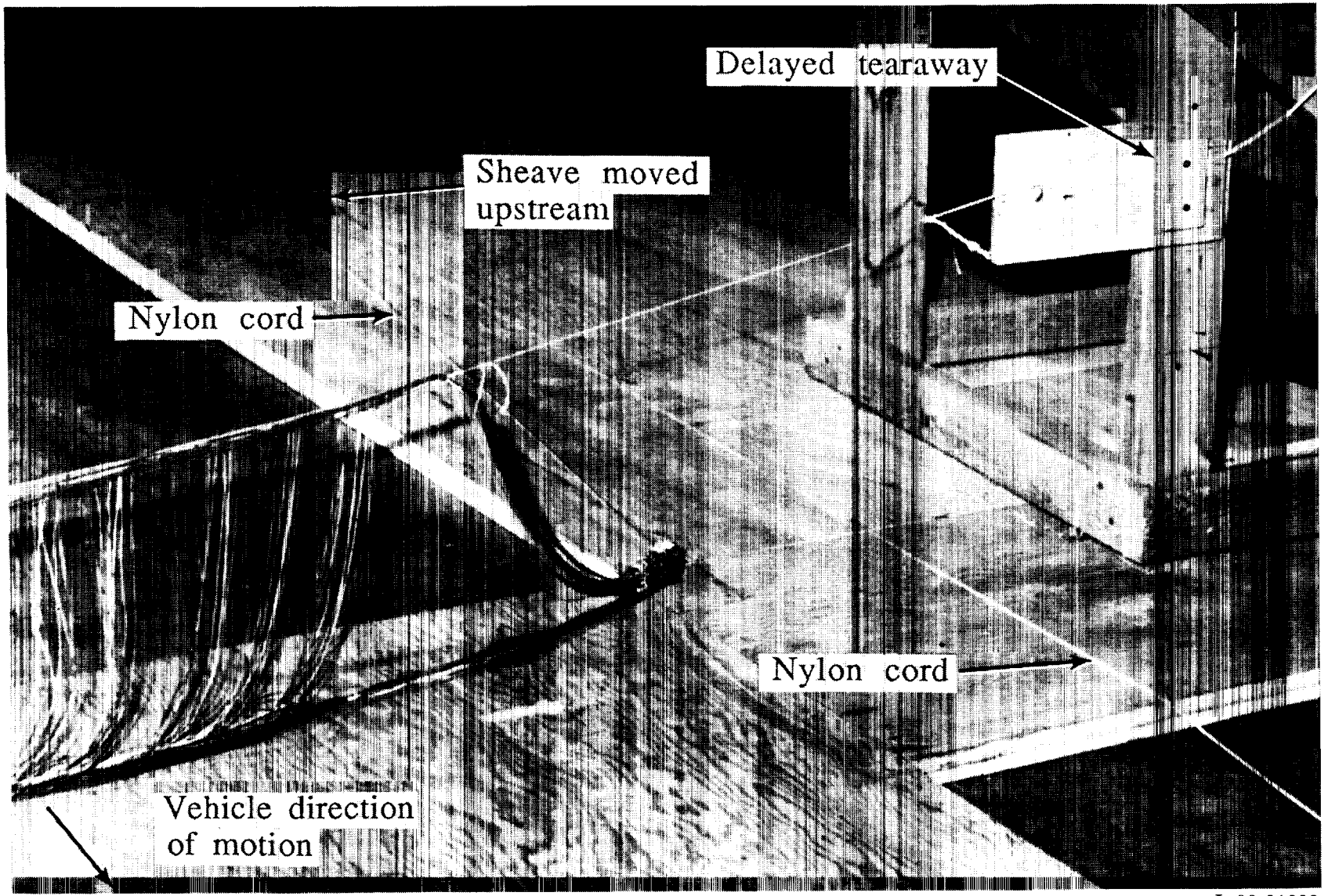

L-88-01992

Figure 15. Upstream sheave location for runs 57 to 59.

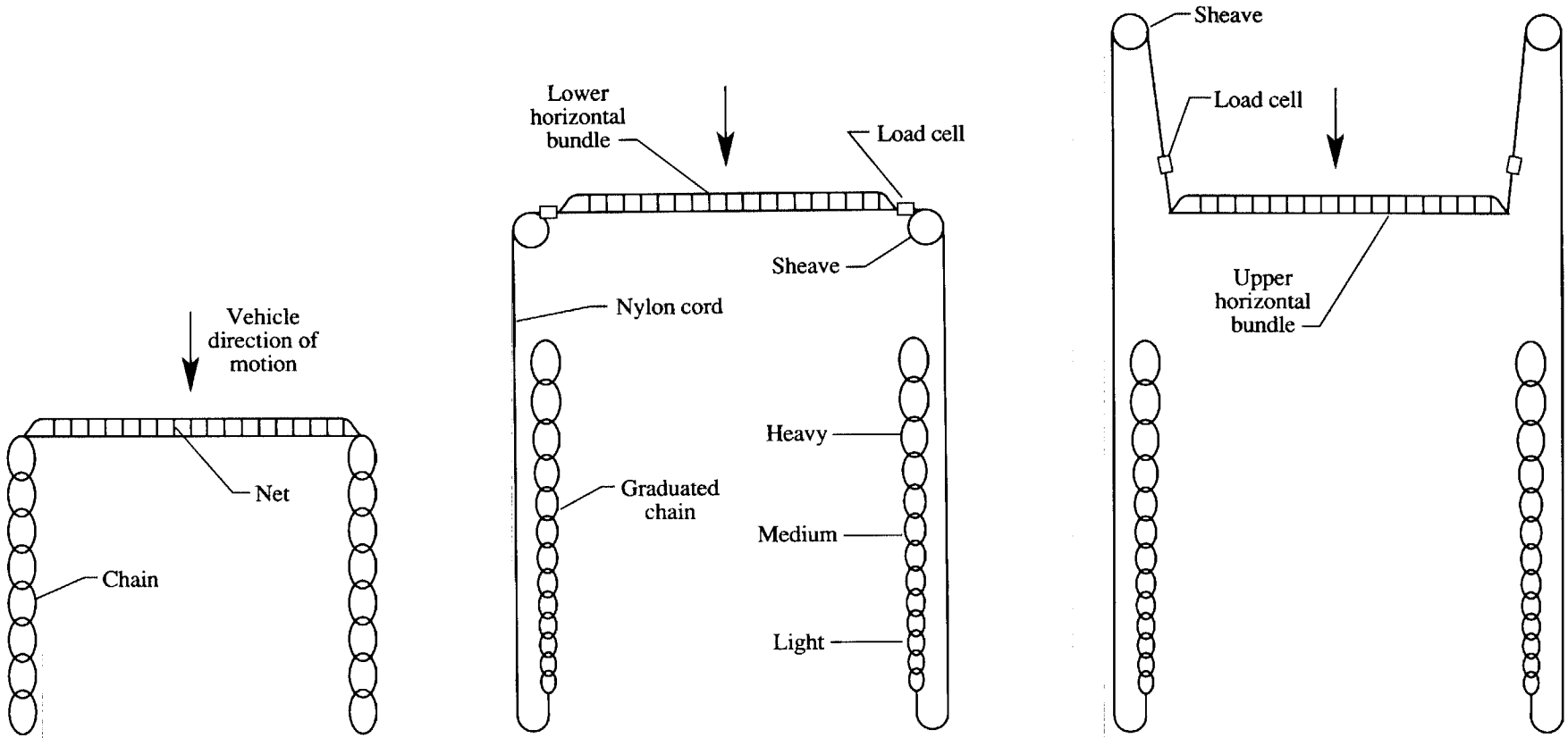

(a) Energy absorber system for nets 1 to 3 (runs 1–39).

(b) Energy absorber system for nets 4 and 5 (runs 40–56).

(c) Energy absorber system for net 4 (runs 57–59).

Figure 16. Anchor chain arresting system for 1/27.5-scale tests.

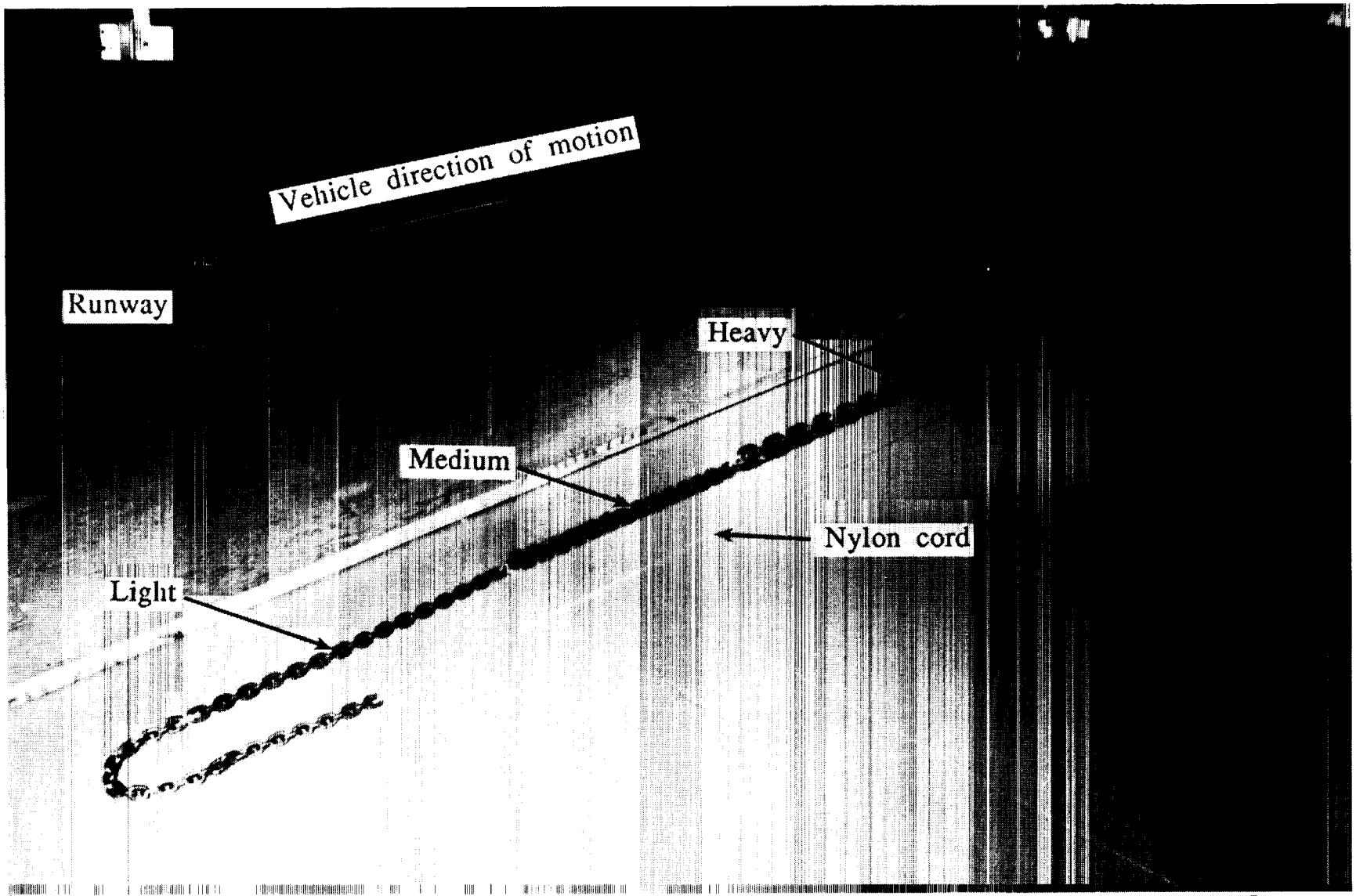

L-88-01995

Figure 17. Graduated weight energy absorber chain for nets 4 and 5.

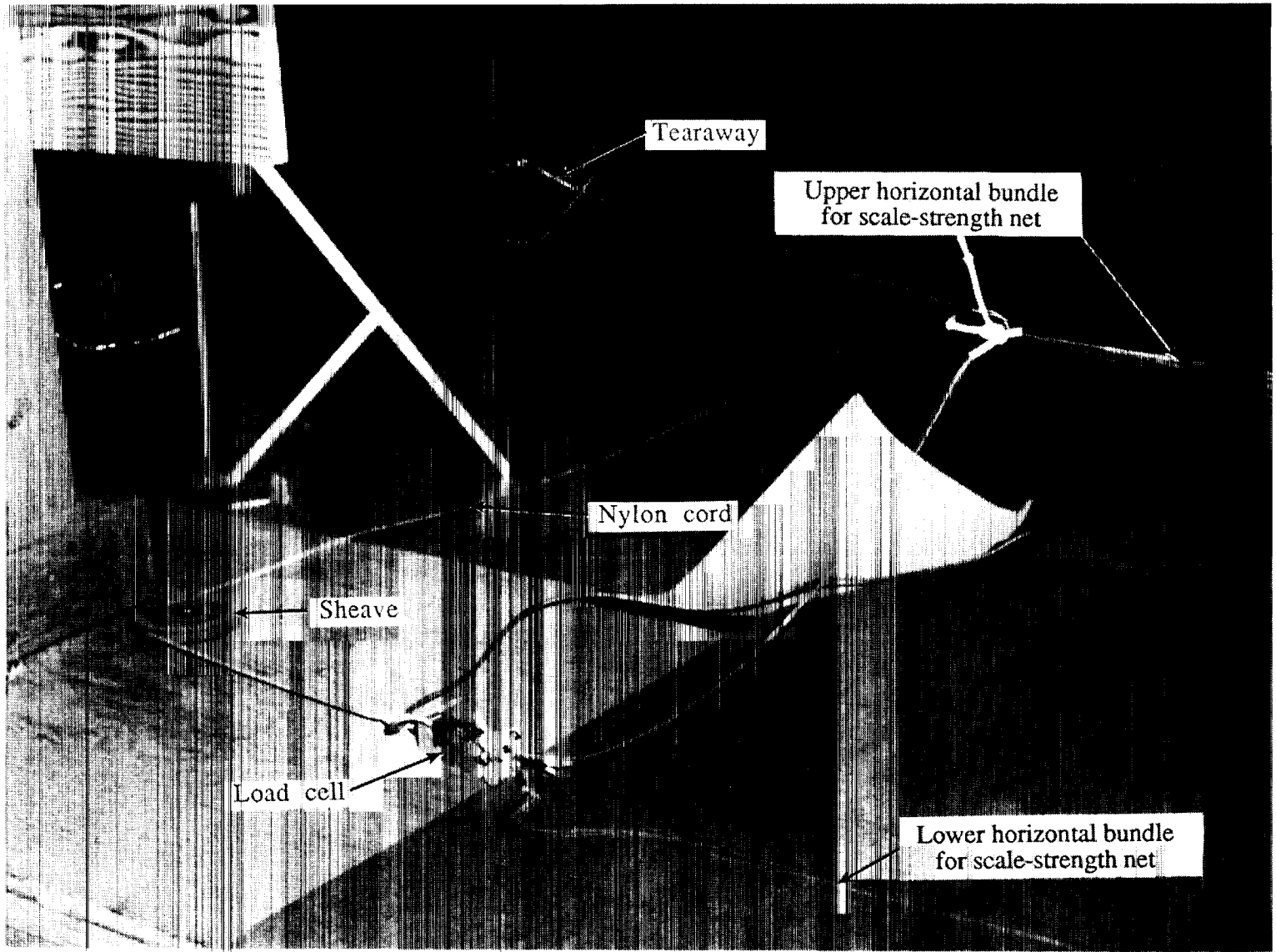

L-87-11019

Figure 18. Nylon cord sheave system for energy absorber chain system used for runs 40 to 56.

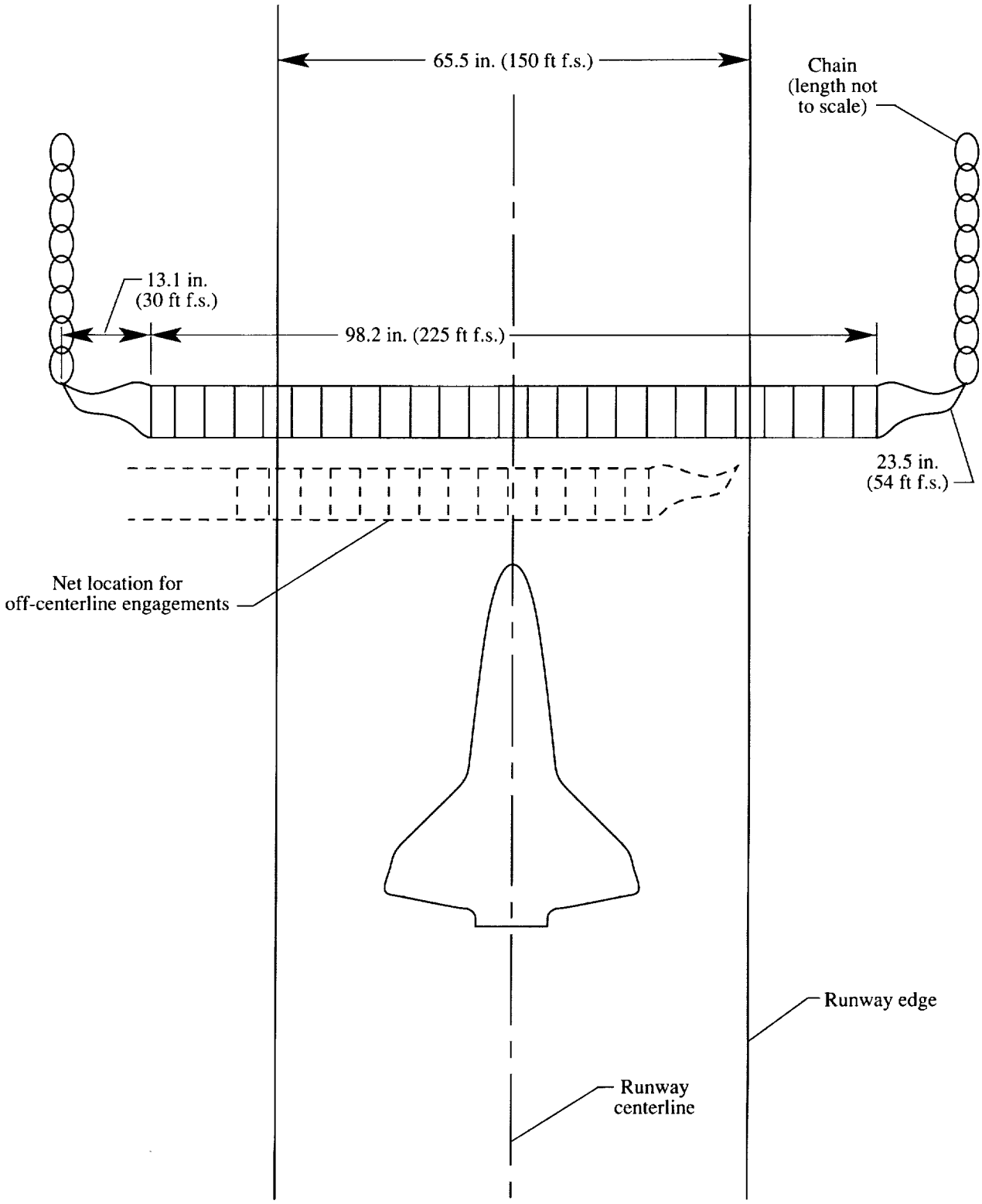

Figure 19. Typical geometry for on-centerline and off-centerline net engagements.

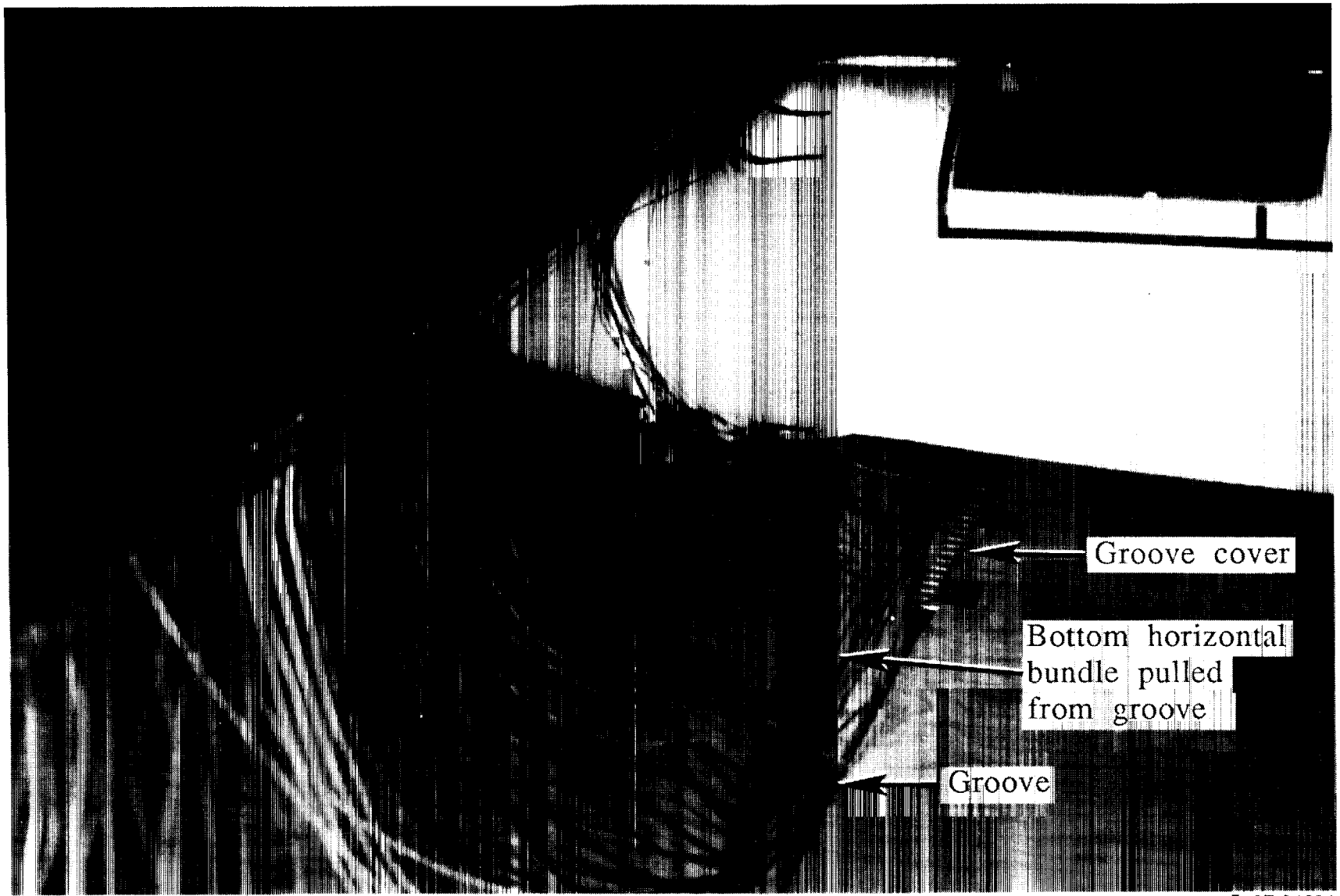

(a) Side view.

Figure 20. Groove cut into runway surface to recess lower net bundle.

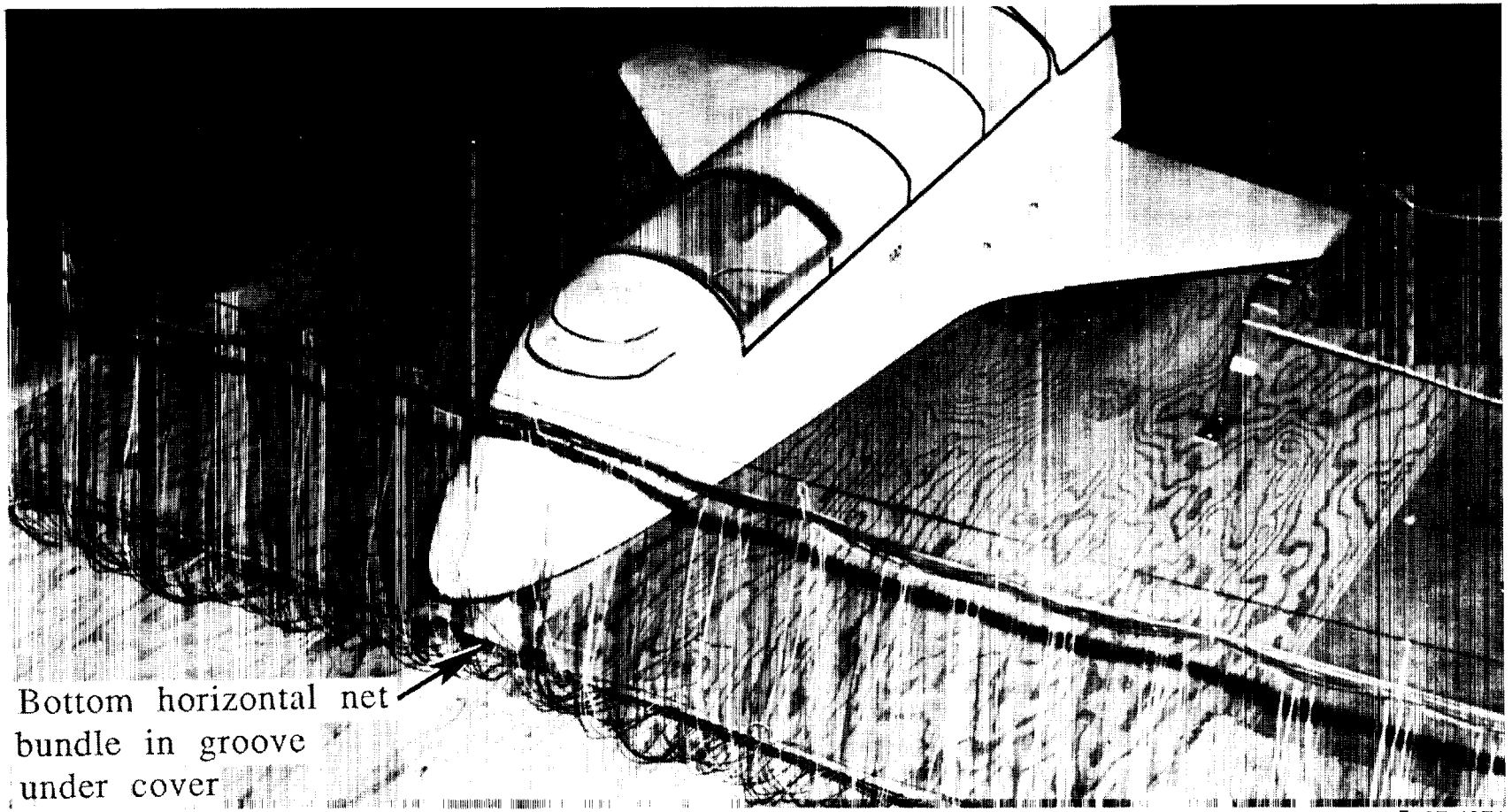

L-87-4974

(b) Front view.

Figure 20. Concluded.

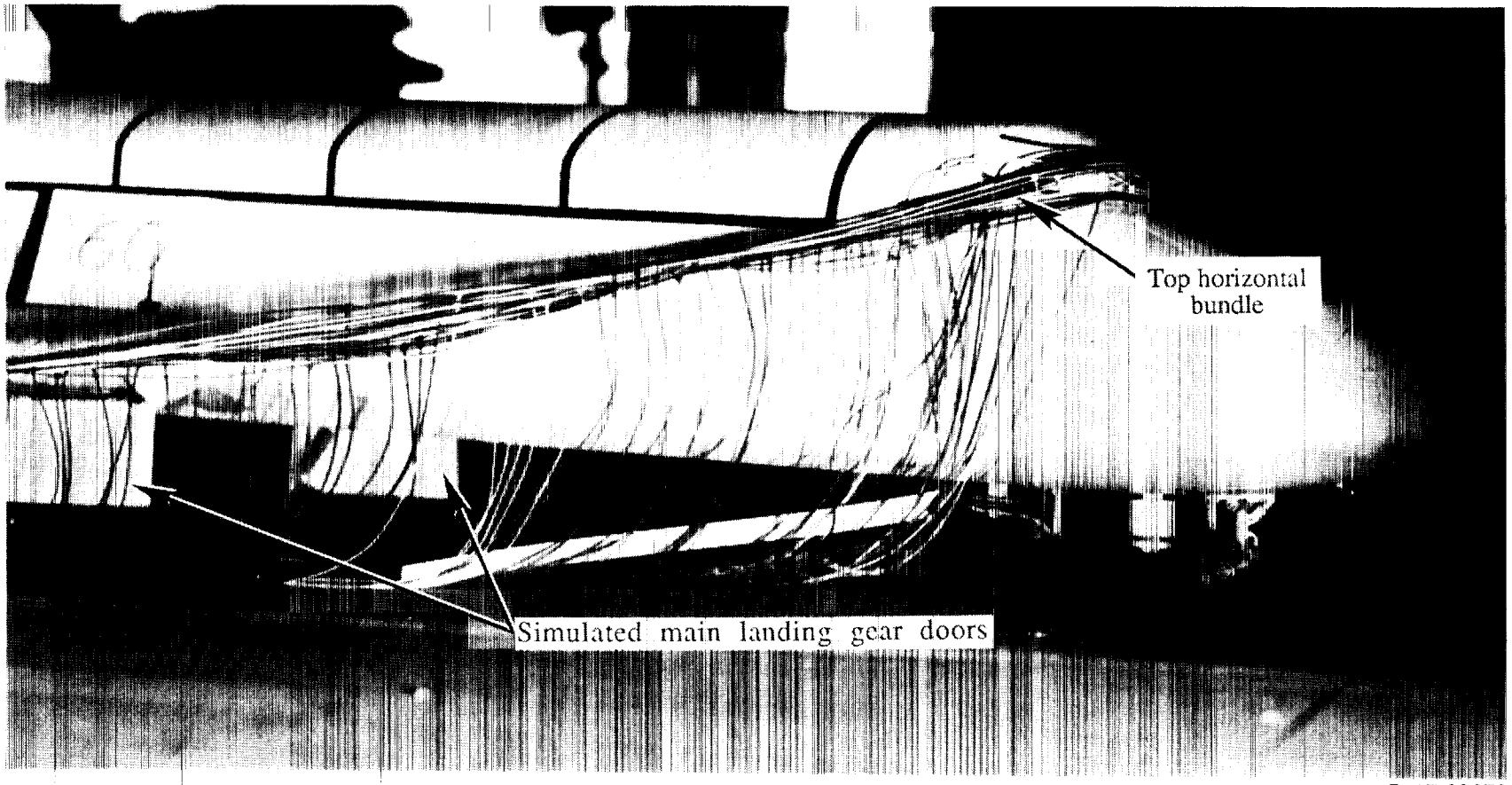

L-87-02676

Figure 21. Slow speed engagement with net top horizontal bundle on windscreen area.

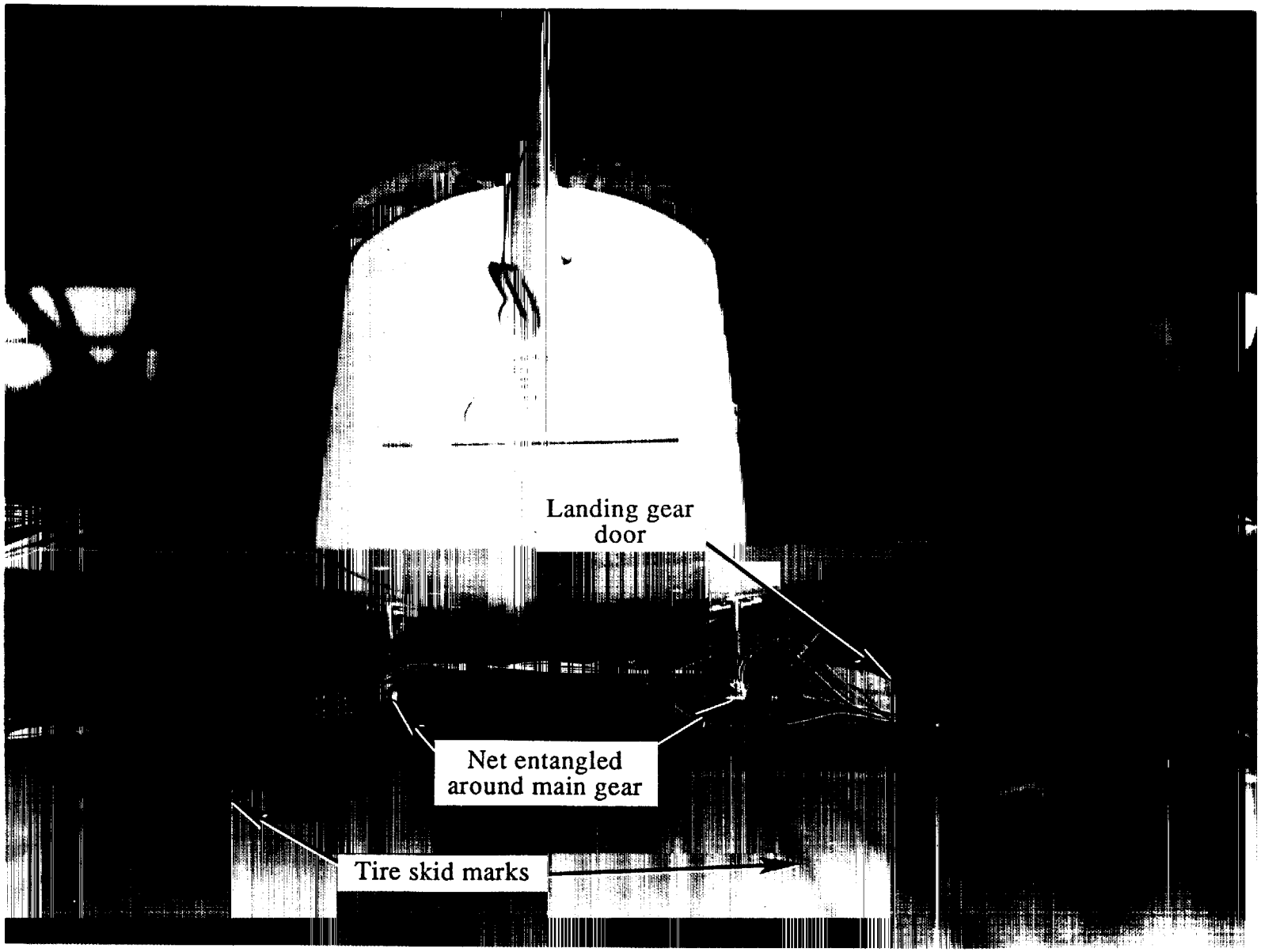

L-87-2423

Figure 22. Net elements entangled around main gear producing tire skidding.

ORIGINAL PAGE
COLOR PHOTOGRAPH

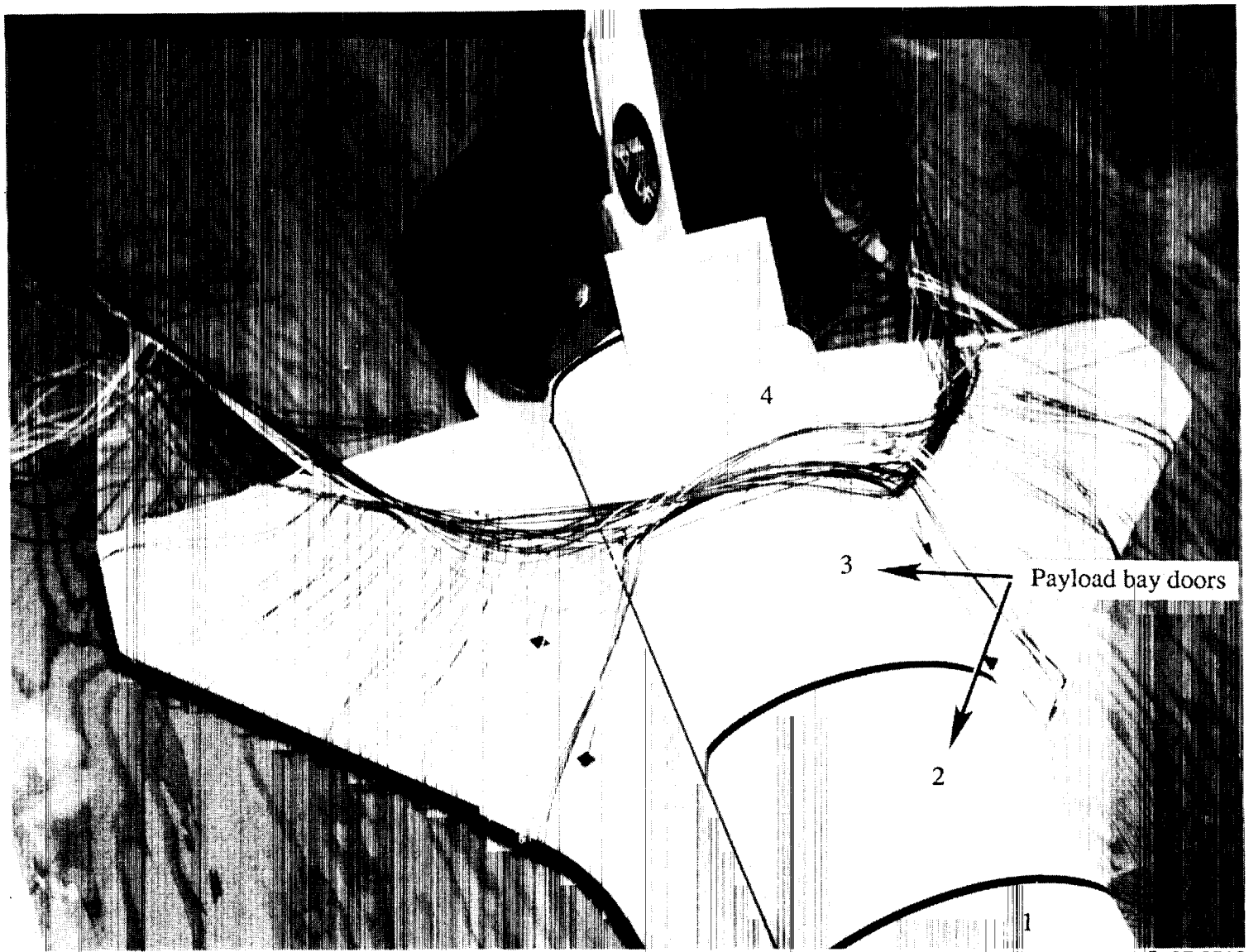

Figure 23. Location of net top horizontal bundle on payload bay doors.

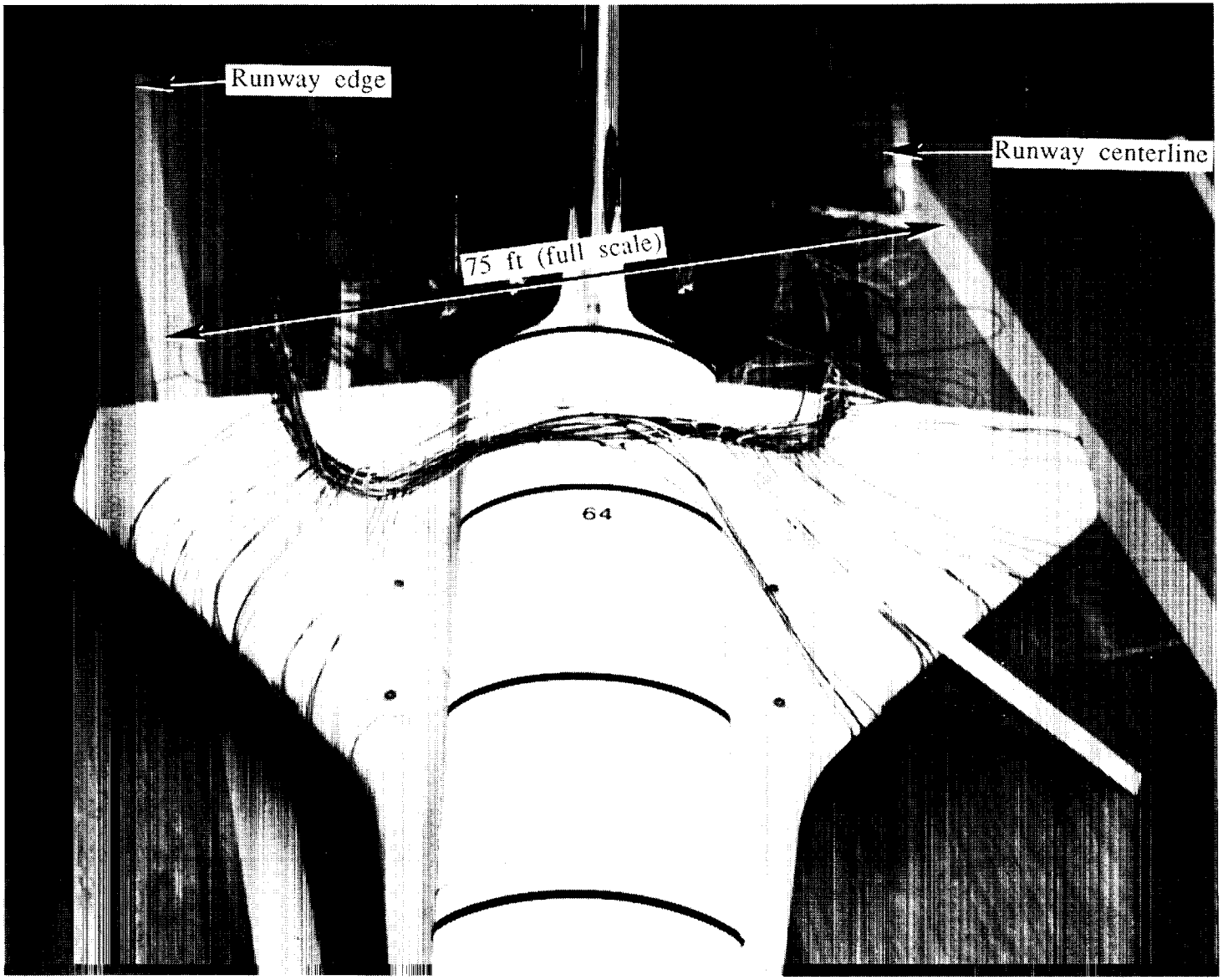

L-87-02899

Figure 24. Vehicle nose landing gear off edge of runway because of right main landing gear entangled by net.

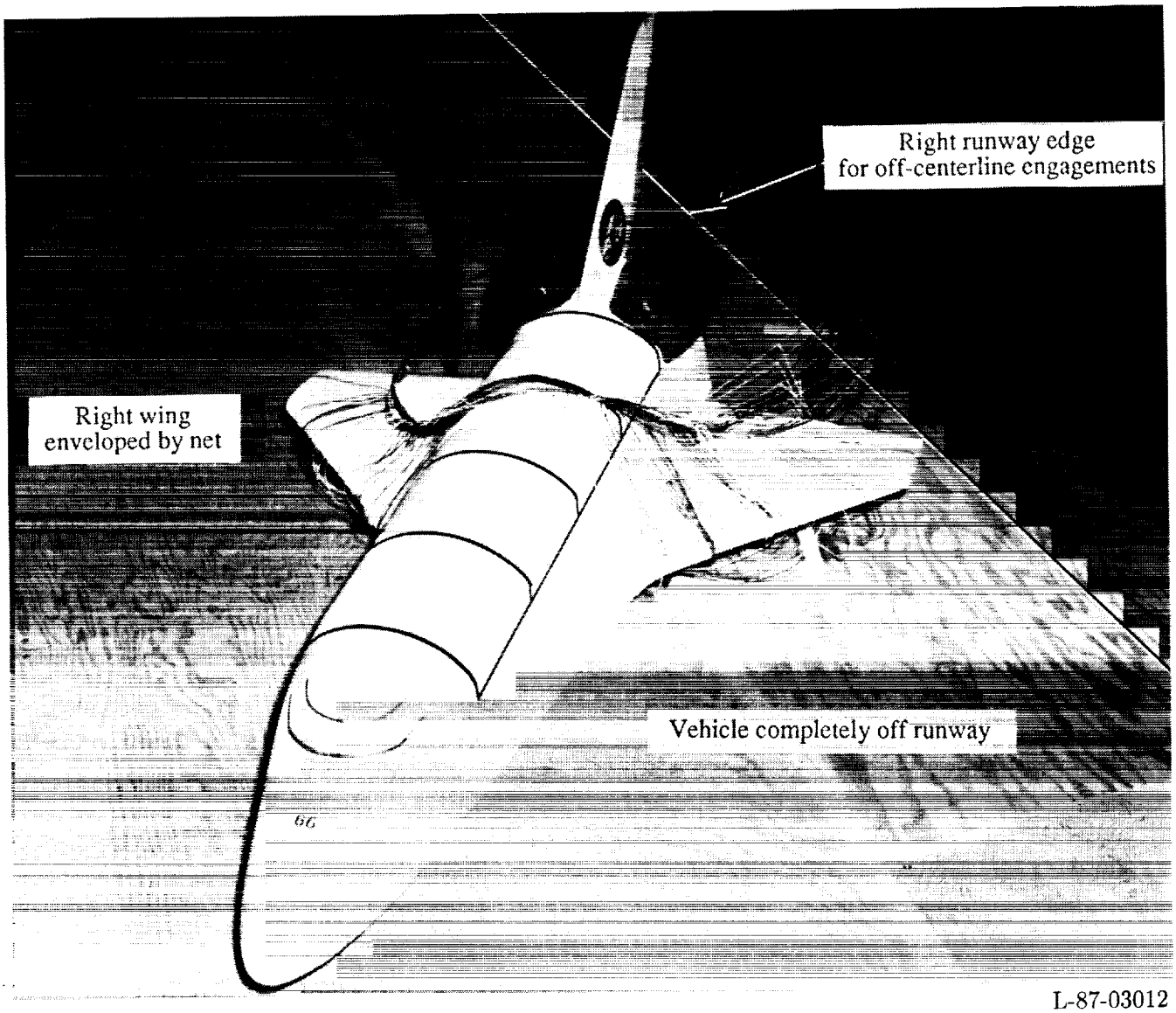

L-87-03012

Figure 25. Vehicle tracked to right side of runway during runway off-centerline engagements.

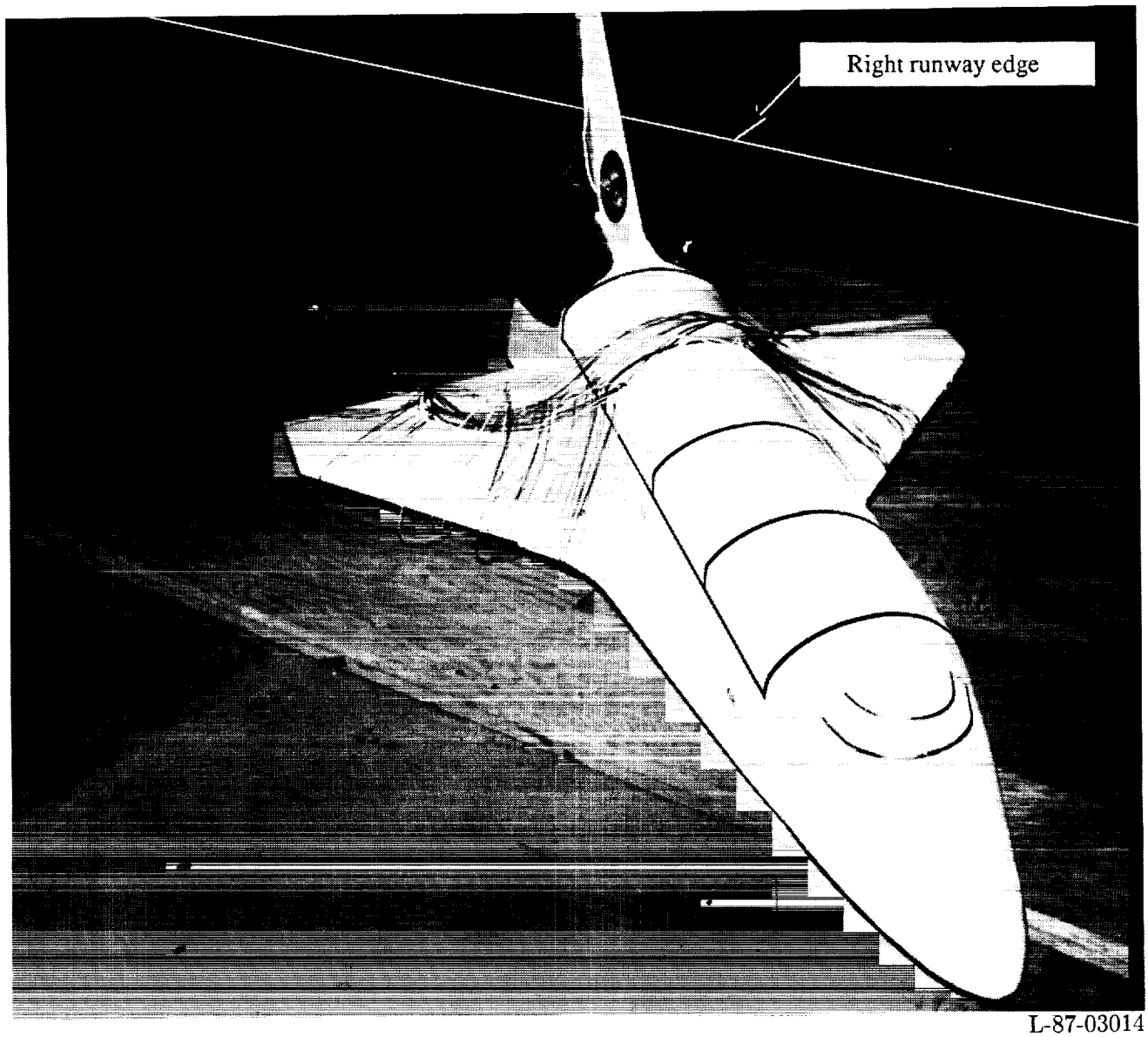

L-87-03014

Figure 26. High-speed arrestment along edge of runway with net 1.

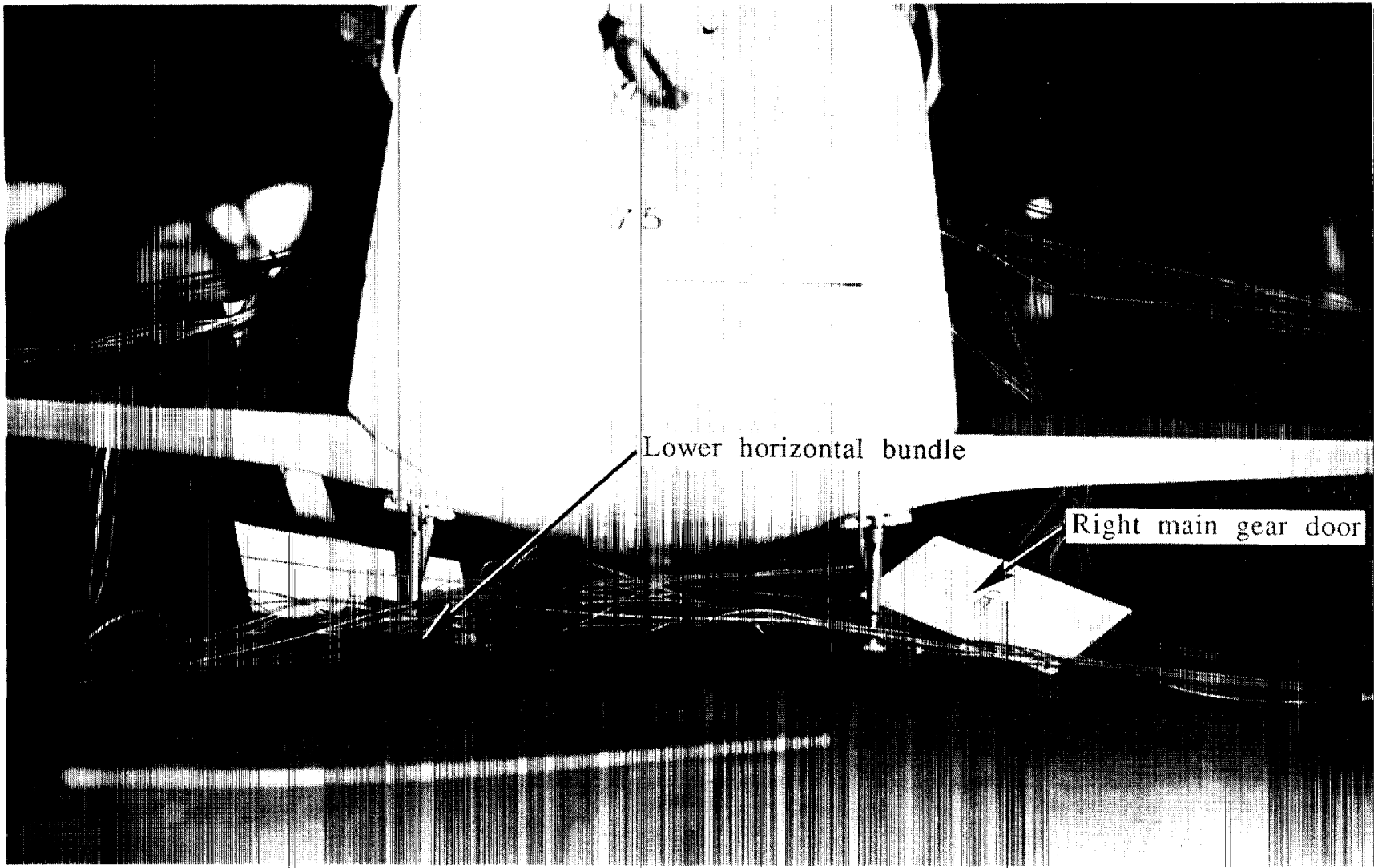

L-87-03428

Figure 27. Majority of lower horizontal bundle behind main gear for net 2.

L-87-03423

Figure 28. Typical main landing gear failure during arrestment for net 2.

L-87-04105

Figure 29. Main landing gear failure without gear entanglement by net 3.

L-87-3578

Figure 30. Typical good arrestment with no main landing gear net entanglement about wheels or axles.

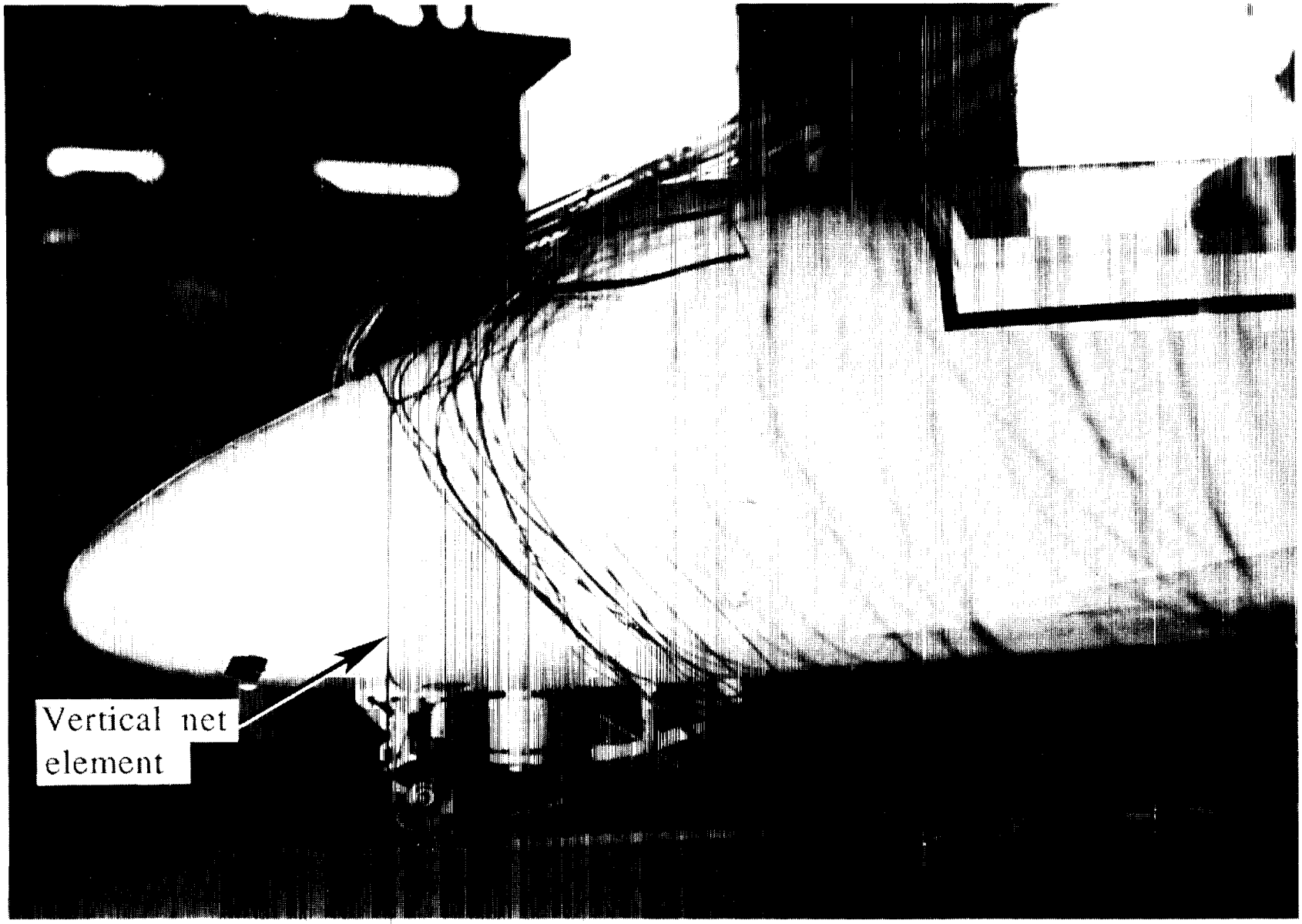

(a) Side view.

Figure 31. Vertical net element caught between nose landing gear tires for push-through tests.

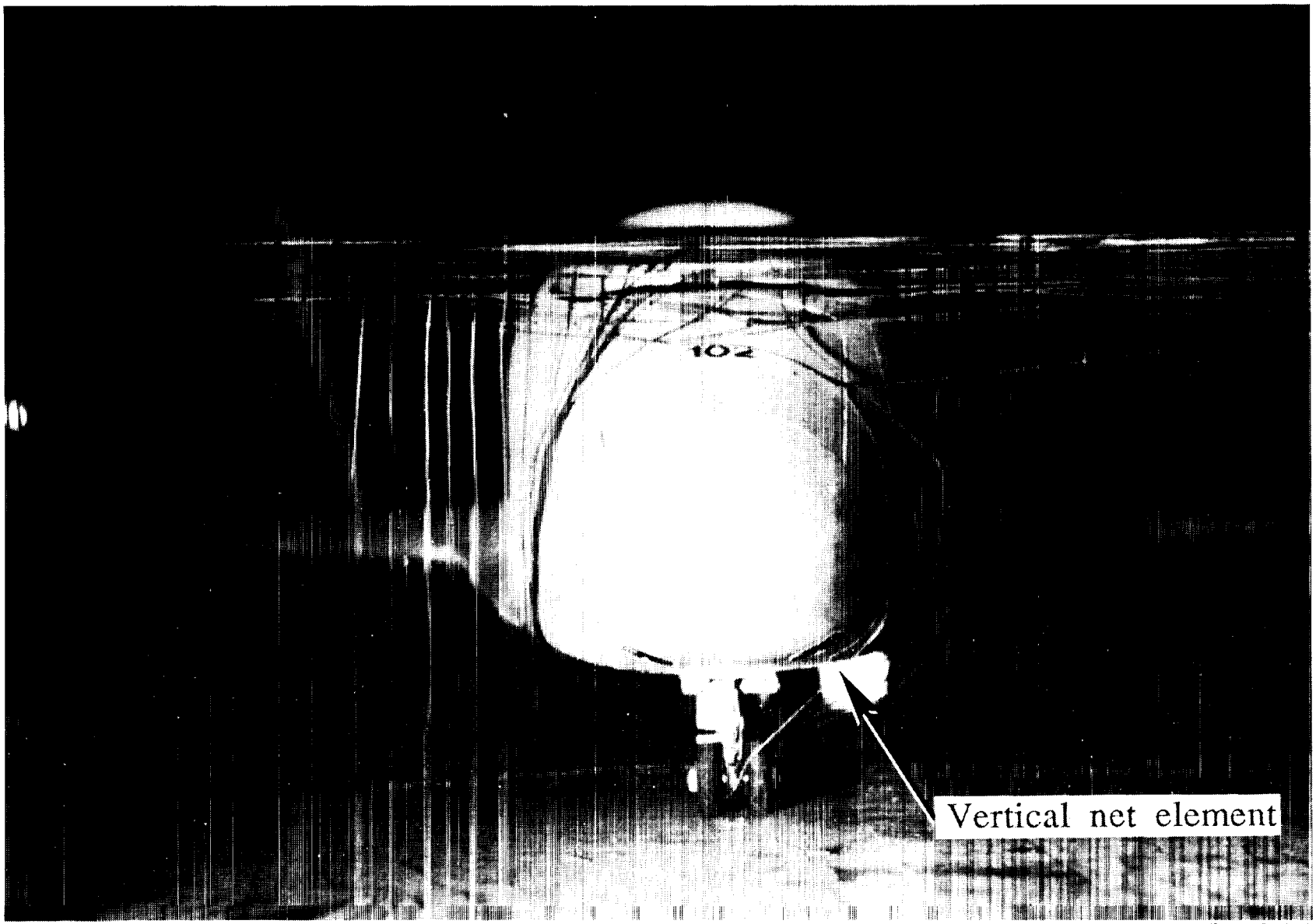

(b) Front view.

Figure 31. Concluded.

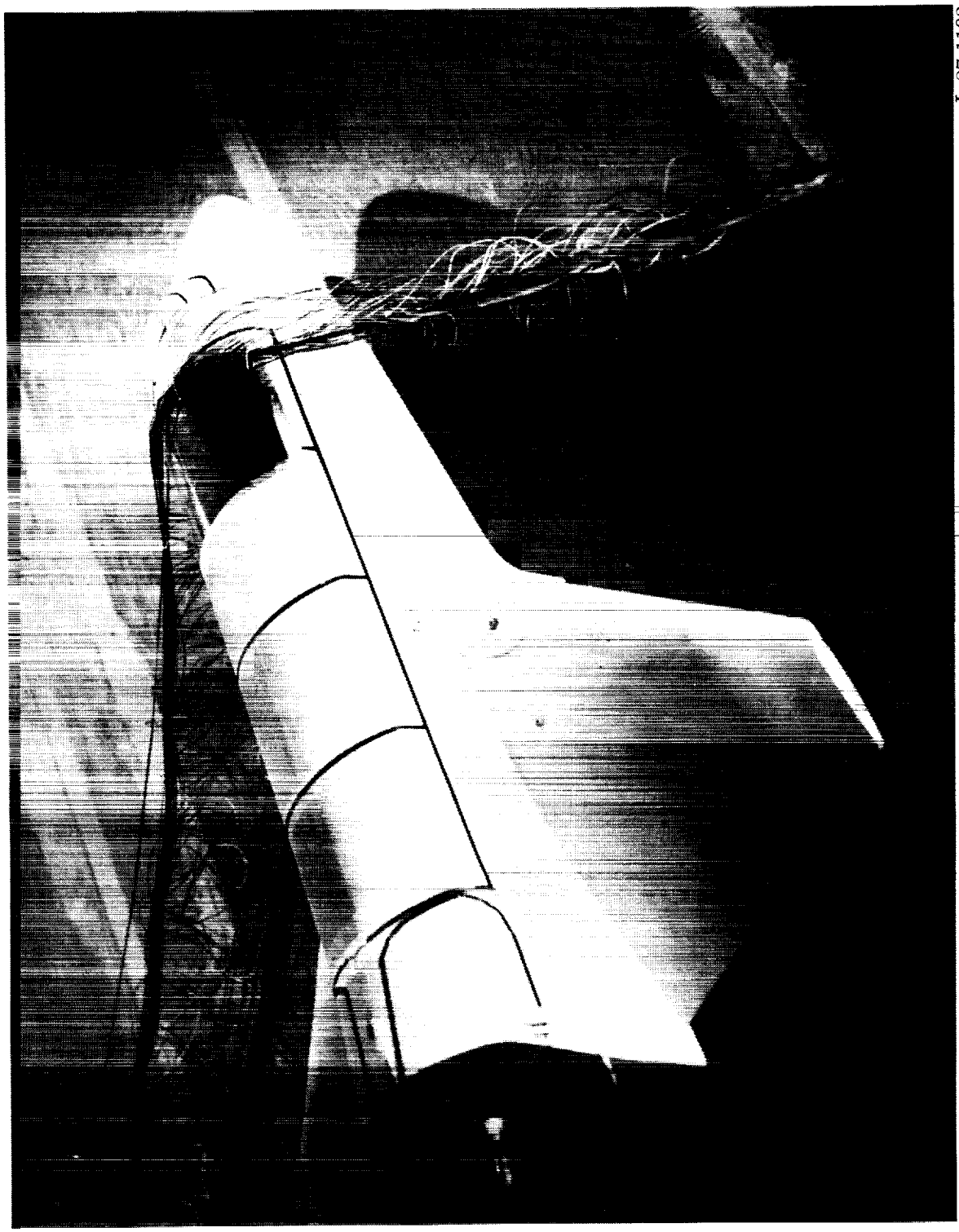

L-87-1102

Figure 32. Overstrength net caught on nose landing gear resulted in net staying on nose instead of enveloping wing.

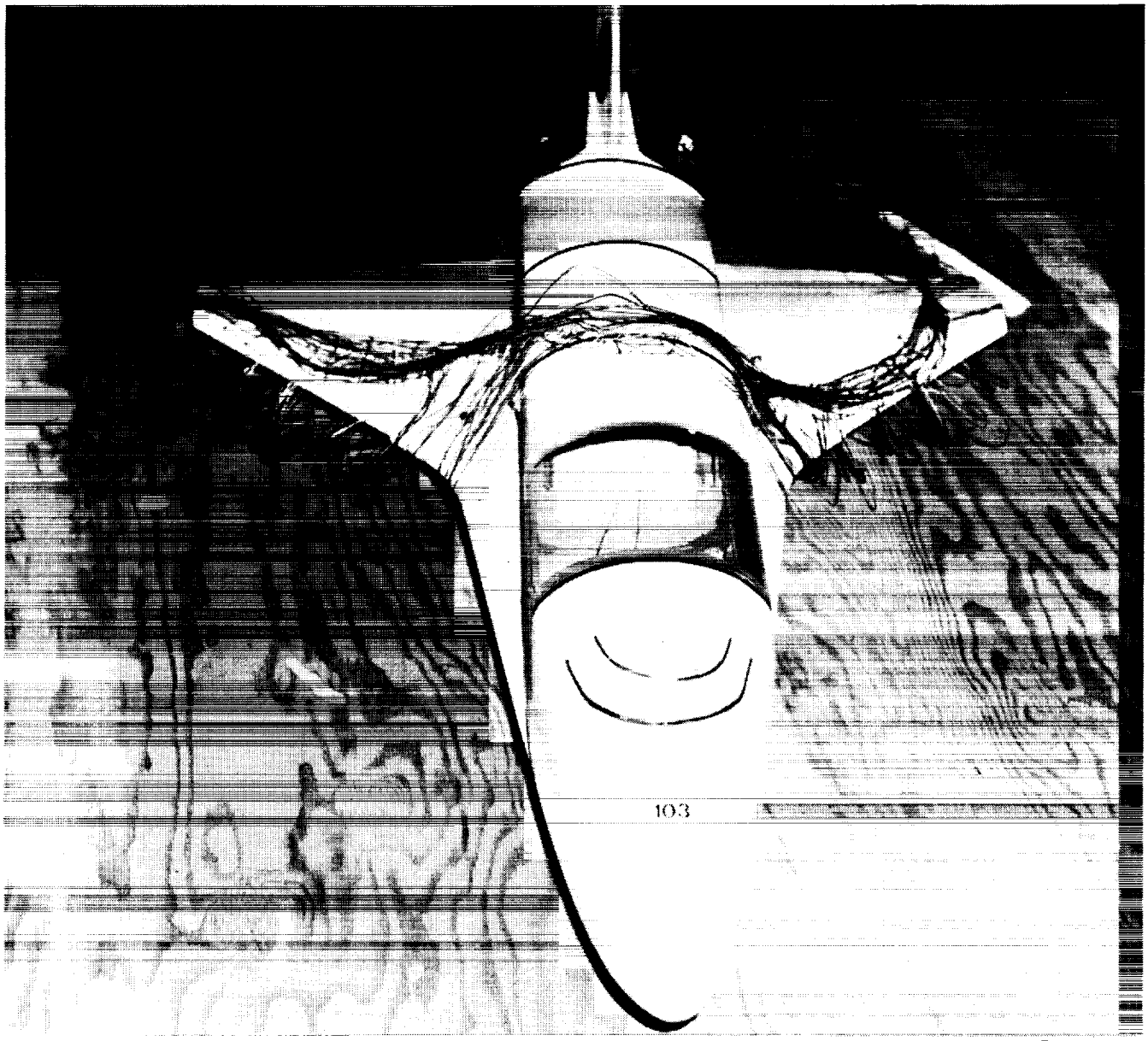

L-87-5193

Figure 33. Top horizontal bundle for net 4 generally came to rest on third cargo bay door area.

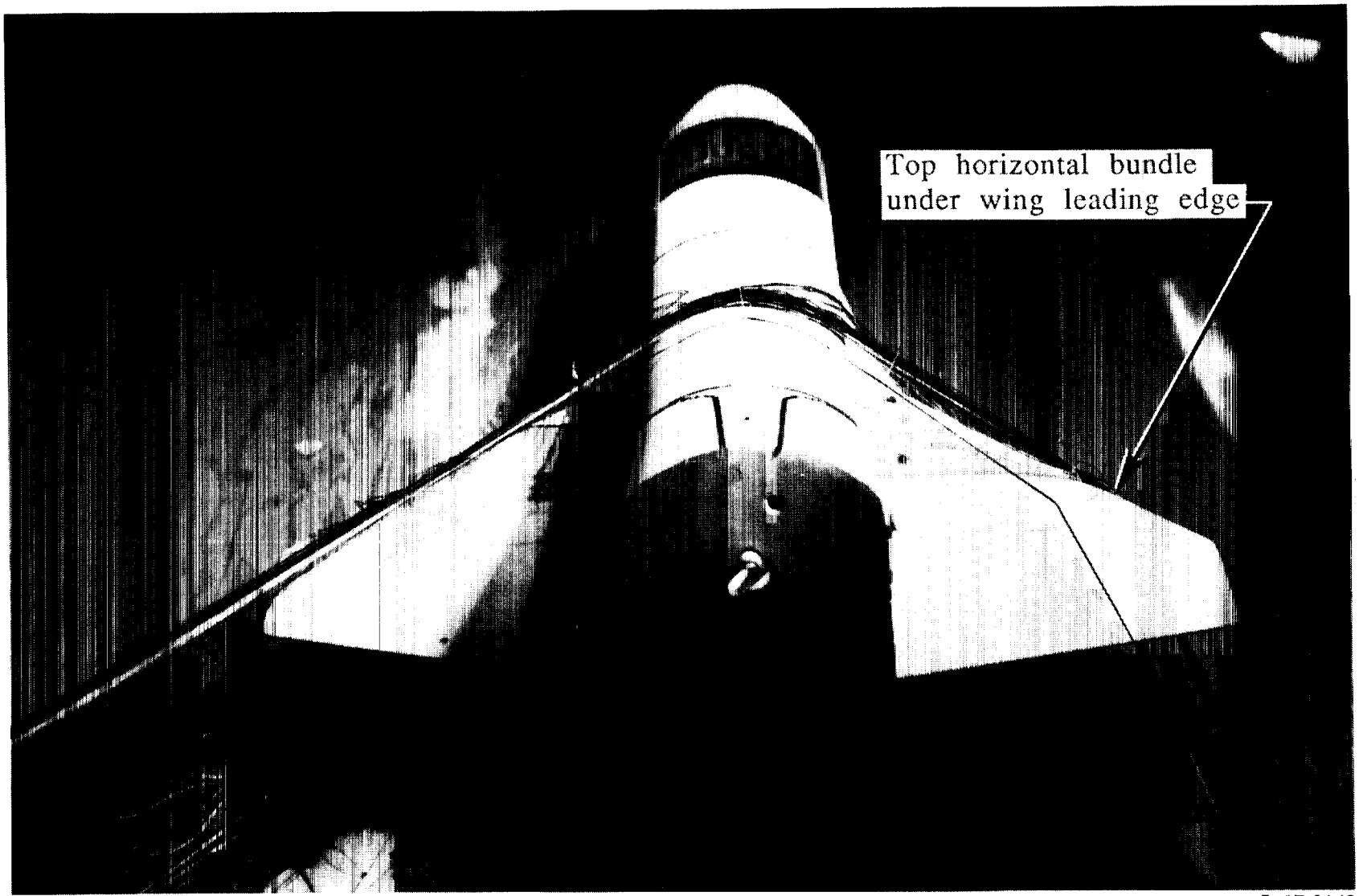

L-87-9143

Figure 34. Example of underwing engagement.

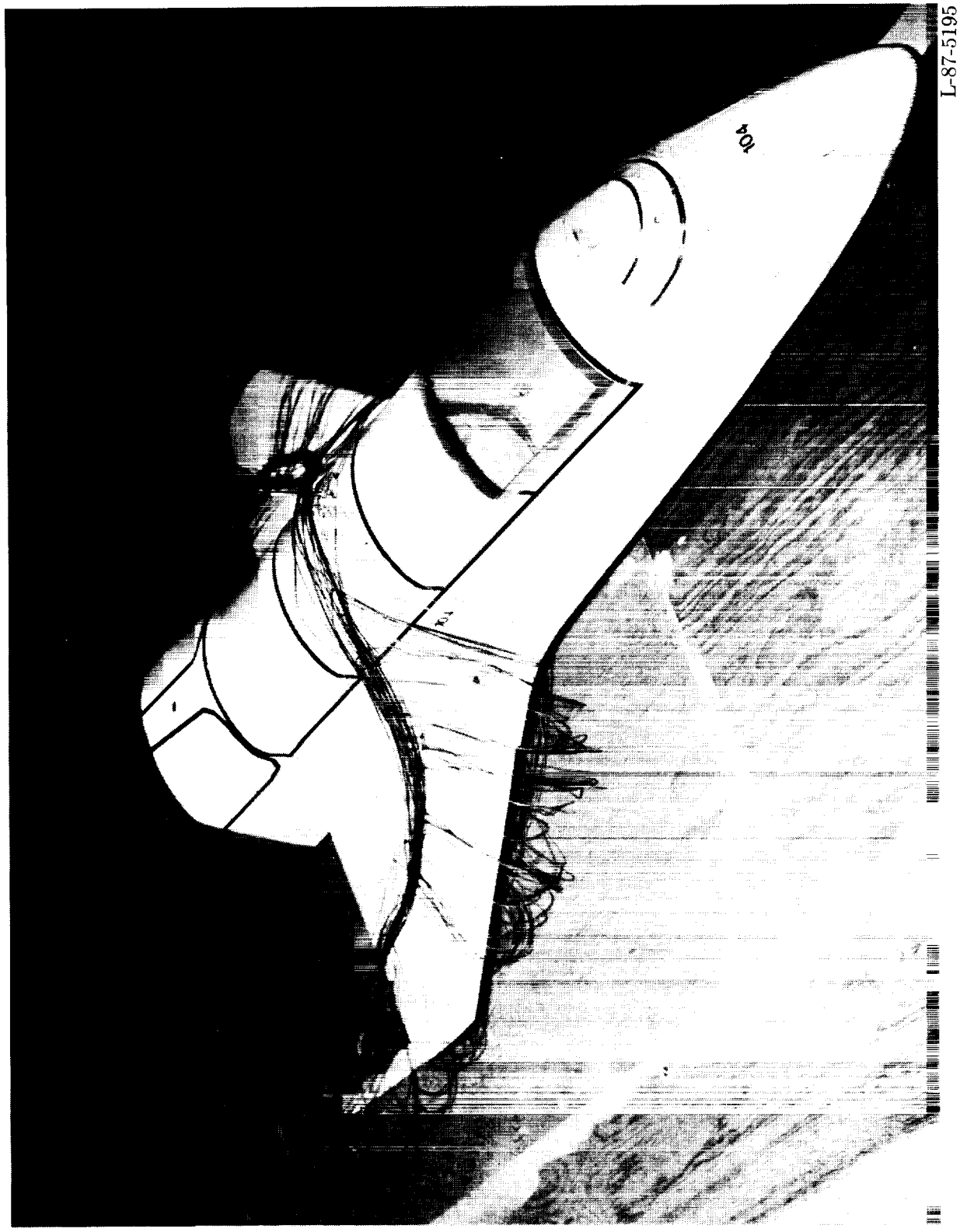

L-87-5195

Figure 35. Typical good wing envelopment by net.

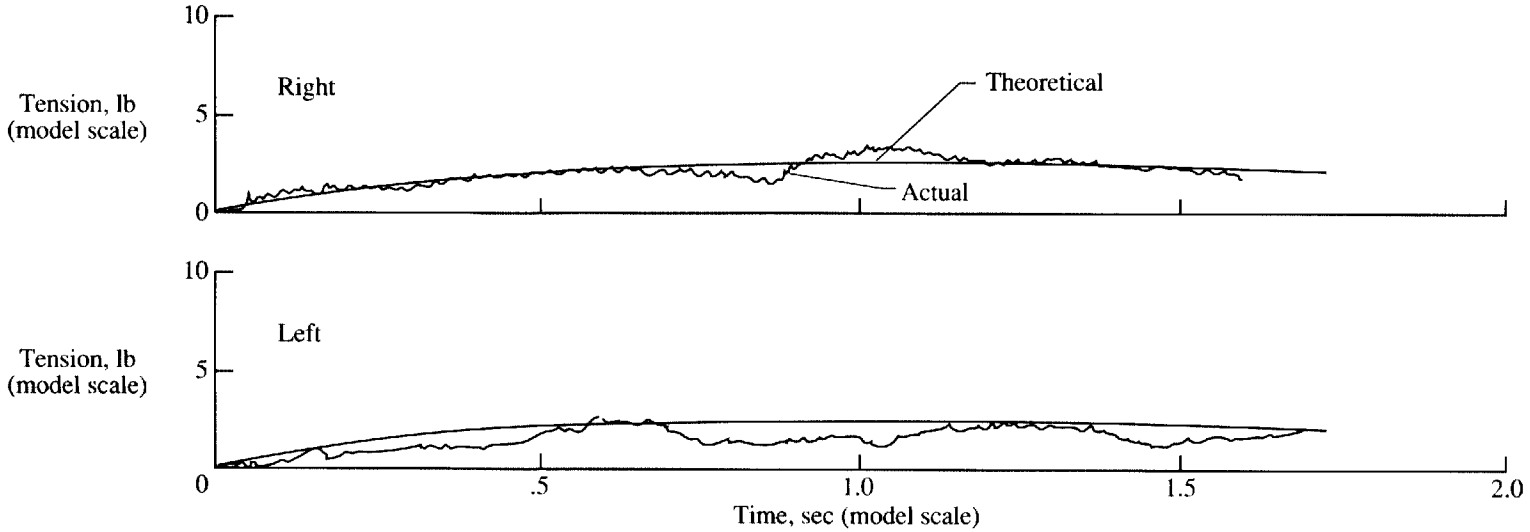

(a) ≈12 knots model scale (≈60 knots full scale).

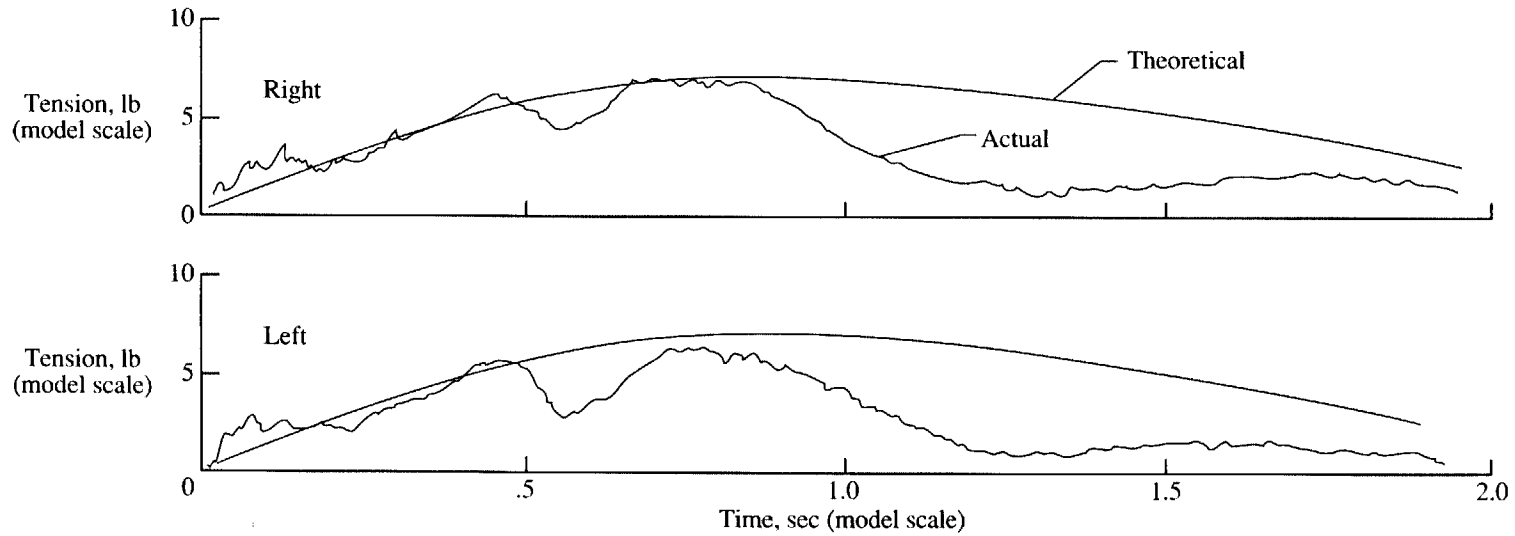

(b) ≈20 knots model scale (≈100 knots full scale).

Figure 36. Arresting net tension loads.

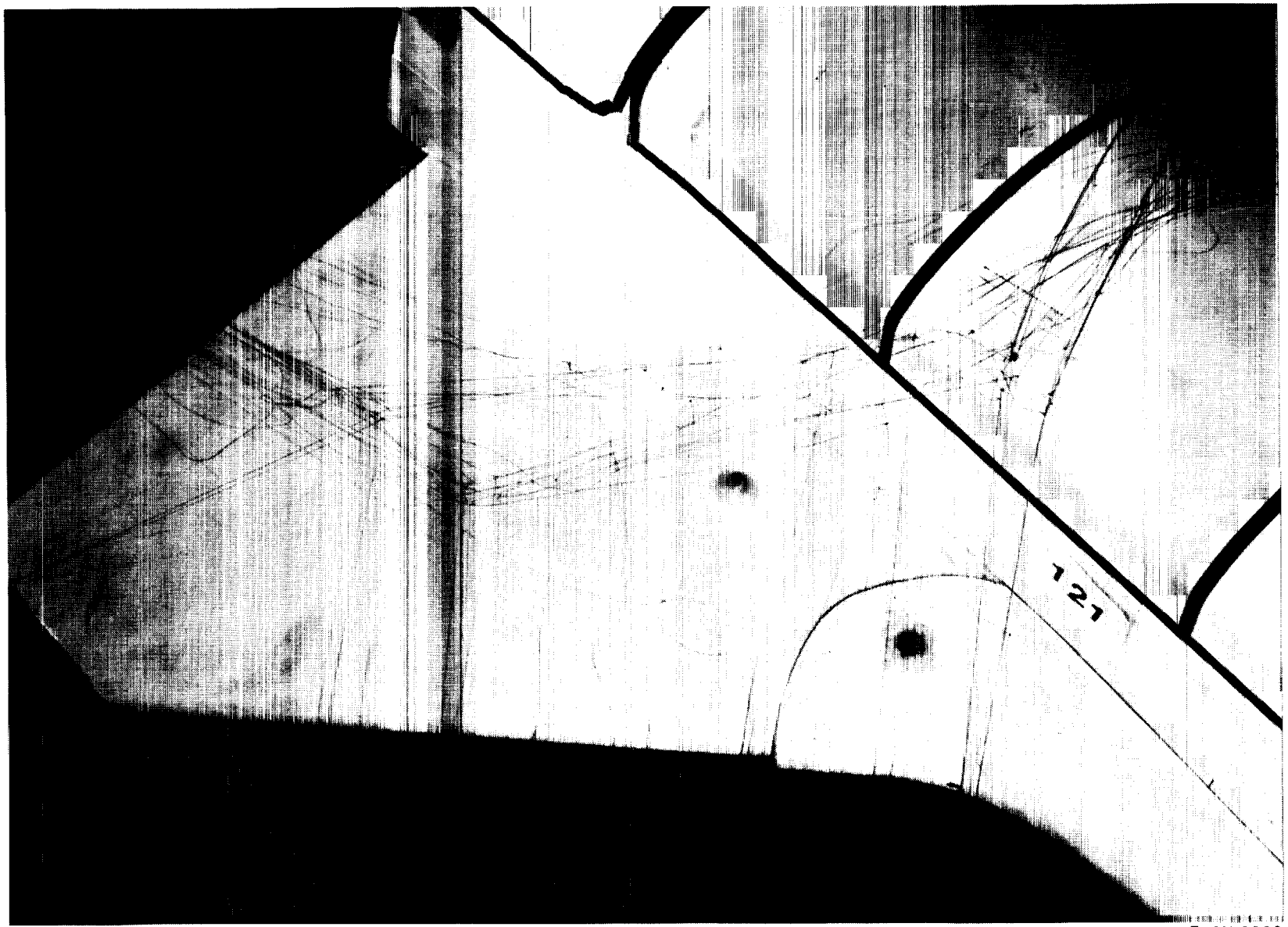

L-87-8280

(a) Net pattern on top of wing and cargo bay.

Figure 37. Net 5 after arrestment.

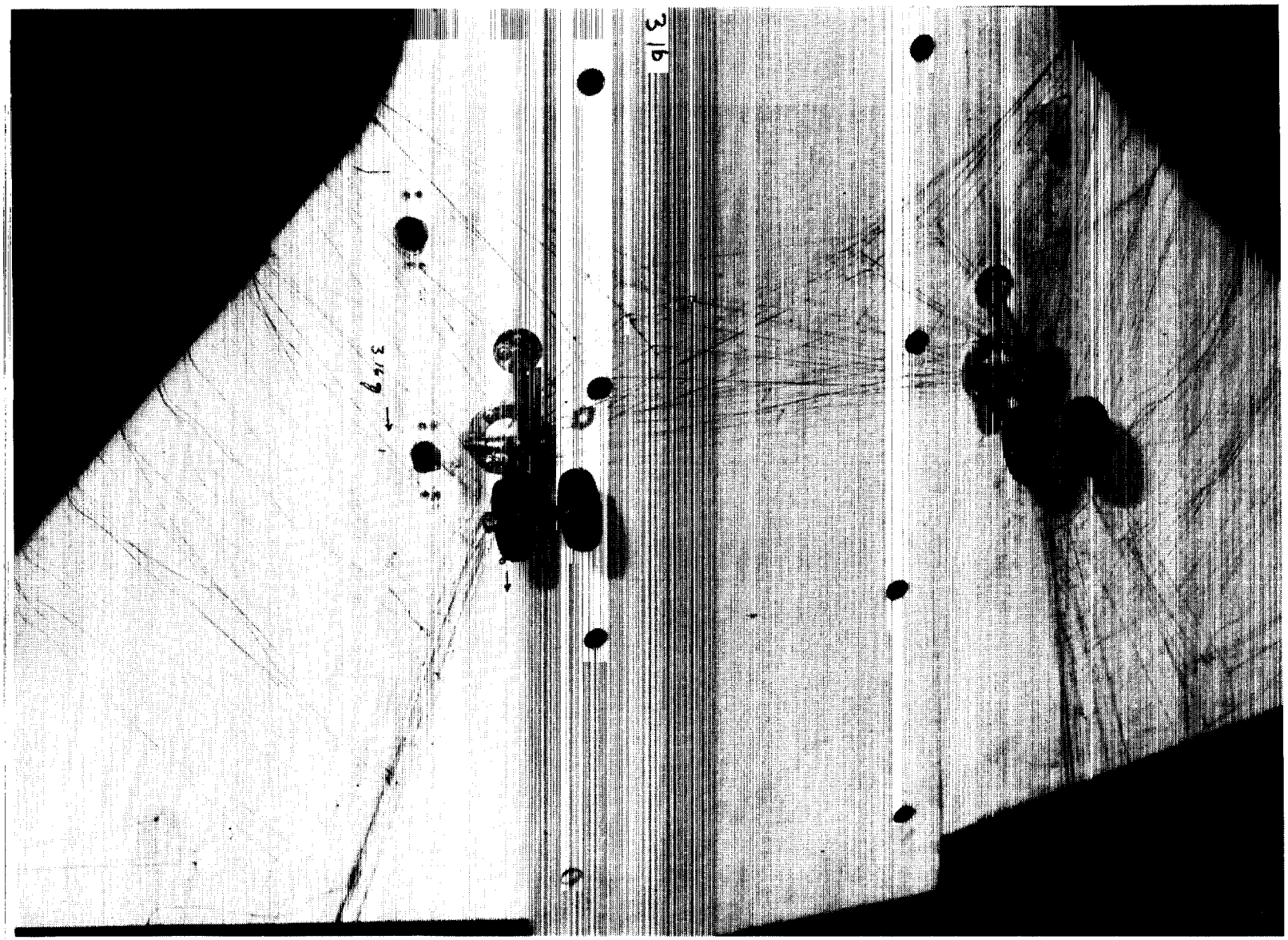

L-87-08281

(b) Net pattern under wing and around main gear.

Figure 37. Concluded.

Appendix

1/8-Scale Tests of Shuttle Orbiter Arrestment System

Introduction

Before the orbiter arrestment system tests were conducted by NASA Langley with a 1/27.5-scale model, All American Engineering Company (now Engineered Systems, a Division of Daytron, Inc.), the contractor for the Shuttle net arresting system, believed that a full- or large-scale test program was necessary to assure a successful orbiter arrestment and develop confidence in the arrestment system. Because a full-scale vehicle was prohibitively expensive, a 1/8-scale model was considered sufficiently large enough to accomplish the objectives. The test program presented in this appendix was conducted by All American Engineering Company (AAE) under NASA contract NAS9-17774 for Johnson Space Center. Some details of the test program are not included in this appendix; however, the information considered essential to understanding the results are presented.

The purpose of the 1/8-scale model tests was to determine the characteristics of various conditions such as on-centerline, off-centerline, maximum-speed, and low-speed net engagements. Of primary concern during these tests was the verification of complete and proper penetration of the net assembly by the orbiter and the proper envelopment of both wings under all conditions of engagement. Unless otherwise indicated, the values in this appendix are presented in 1/8 scale. If full-scale values are presented, they are labeled as such.

Apparatus

Figure A1 is a photograph of the 1/8-scale model on the launch apparatus, and table AI presents the Froude scale relationships for the model. Because the 1/8-scale model was built to Froude scale relationships, modifying the relationships as was done for the 1/27.5-scale model was not necessary. Pertinent parameters of the 1/8-scale model, the full-scale values, and the orbiter values are presented in table AII. Although no geometric dimensions of the model are presented in this appendix, the overall model body and gear geometry were presumably scaled correctly from NASA drawings of the orbiter. The tires on the landing gear for the 1/8-scale model were composed of solid rubber and were cut to the proper cross-sectional profile. The landing gear struts were stronger than the orbiter gear and are thus referred to as overstrength. No attempt was made to determine whether the gear would fail during these tests, but arresting system forces, some of which were applied to the landing gear, were measured. The nose gear for the 1/8-scale model was fixed (not free to castor). The full-size yaw moment of inertia of the model was close to that of the orbiter, but the roll moment of inertia was greater than that of the orbiter. (See table AII.) For arrestment system tests, the yaw moment of inertia was considered to be of primary importance and the roll moment of inertia secondary.

The launch apparatus, shown partially in figure A1, was a pneumatic-powered launcher designed for launching remotely piloted vehicles. The orbiter model wheels ran on tracks above the launcher that were at the same elevation as the concrete floor that served as the runway.

The arrestment system consisted of a net used to capture the vehicle, net supports, tearaway straps to hold the net up until the wing was fully enveloped by the net, breakaways to release the net from its supports, and energy absorbers to bring the vehicle to a stop. The net was a 36-element net and it is shown in figures A2 to A4. Each element consisted of several vertical members attached to upper and lower horizontal members. Groups of individual elements were bundled together to form one net assembly of 36 elements. For the 1/8-scale test, the vertical and horizontal members were made of nylon thread with a breaking strength of 17.5 lb. The vertical members were tied to the horizontal members, and the actual breaking strength at the tie point was $\approx$12.0 lb. The 1/8-scale net included 324 of the 439 vertical members planned for the full-scale net on a 200-ft-wide runway. The omitted vertical members were in an area of the net to the right of the center where vertical members were not contacted by the vehicle during on-centerline and off-centerline (left-side) engagements. Some of the vertical net members were omitted to reduce net fabrication costs. Two lengths of nylon rope weighing 2.33 lb/100 ft were used to ballast the upper and lower horizontal net bundles to achieve a net mass of 4.0 lb. These nylon ropes, which are shown in figures A3 and A4, helped to obtain the proper net inertia. The ropes were tied to the upper and lower horizontal bundles with wraps of copper wire (not twisted) in a manner which prevented the rope from carrying tensile load. Pertinent parameters of the arrestment system are shown in table AIII.

Figures A5 and A6 show the net and the suspension system. Some of the net suspension system is also shown in figures A3, A4, and A7. The net

was supported primarily by a Kevlar suspension line (breaking strength 180.0 lb) that was attached to a tearaway strap on both sides of the runway, the tearaway strap in turn was attached to a net-tensioning line cord connected to the net support. The tearaway strap was designed to tear for its full length. While tearing, the strap maintains a force of 15.5 lb to hold the net up while at the same time allowing the arresting tape to unwind. The net-tensioning line had a breaking strength of 95.0 lb. Net ties of varying lengths, shown in figure A4, were used to hold the upper horizontal bundle to the net suspension line. An inner suspension line on each side was used to secure the net laterally and thus prevent movement along the main suspension line. The inner suspension lines had a breaking strength of 0.5 lb. An auxiliary suspension line, shown in figure A4 was used on each side to maintain tension on the upper horizontal bundle to hold the net up while the tearaway was tearing to assure the upper horizontal bundle remained over the top of the vehicle wing. The auxiliary suspension line had a breaking strength of 95.0 lb. Breakaway occurred when the tearaway reached the end of its tear stroke and broke and thus separated the net completely from the net support stanchion.

The lower horizontal bundle, shown in figures A4 and A6, was attached to a lower bundle tearaway strap that was anchored to the runway. This strap was designed to put a controlled tension on the lower horizontal bundle and thus cause it to lift and catch the main landing gear strut above the tires to minimize tangling of the net in the main gear wheel assembly. The force to tear the lower bundle tearaway was the same 15.5 lb as that of the upper tearaway strap.

The lower horizontal bundle was held to the runway by loops of commercial polyester thread attached to ground anchor straps, which in turn were attached to ground anchors. (See fig. A3.) The ground anchors were $\approx$1.2 ft apart. The ground anchor system, in addition to keeping the net in place when it was windy, also held the net down until the model nose and nose gear passed over the lower horizontal bundle; thus, the anchor system prevented the nose gear from catching on the lower horizontal bundle. The polyester thread for the 1/8-scale model had a breaking strength of 2.75 lb, which took the place of the designed configuration of six ties with 0.5-lb breaking strength each.

The main suspension line, net tensioning line, and auxiliary suspension lines were designed not to fail. However, failure of the upper and lower tearaways, the lower bundle net tie downs, the inner suspension lines, and net vertical members were scale strength and were expected to fail at the correct load level during an arrestment.

Figures A5 and A6 show the layout of the complete arresting system. The net height (upper horizontal bundle) above the runway was 38.75 in., and the height of the net support was 67.5 in. The net support stanchions were 50.75 ft apart, and the energy absorbers were $\approx$53 ft apart. A pair of 14-in-diameter energy absorbers were used for this test because they were available and designing and building 6-in-diameter scale-strength energy absorbers was considered too costly. A typical force (tape tension) time history produced by the energy absorbers tests is shown in figure A8. The solid line in the figure is from the model test at a 33.8-knot engagement, and the dashed line is the full-scale theoretical tape tension from a symmetrical centerline engagement scaled to 1/8 scale for comparison. The scaled engagement speed for the dashed curve is 35.4 knots. Overall, performance of the energy absorbers was not considered to be a primary concern for these tests. The purpose of this program was to verify proper envelopment of both wings under all specified conditions of engagement. Essentially, all actions that must occur to effect envelopment occur before energy absorber rotation begins or becomes significant. Differences between the actual and theoretical force time histories affect the run out dynamics to some degree; thus, both longitudinal and lateral rollout distances are not exactly the same as those for the full-size vehicle. The energy absorbers were placed 25 ft upstream (fig. A6) from the net and were connected by a tape leader to the upper and lower horizontal bundles. Figure A9 is a photograph of the 14-in. energy absorbers. During arrestment, the tape unwinding rotates the tape spool which rotates a paddle wheel and causes a churning action of water in the water twister to dissipate energy. Tape from the spool is fed through a tensiometer to measure retardation forces during arrestment.

Vehicle speed at engagement with the net was measured from the time to trip a pair of infrared light sources (fig. A3) until the time to trip sensors located on the opposite side of the runway and in front of the net. Longitudinal and lateral accelerometers were mounted at the vehicle's center of gravity to measure accelerations. Main gear wheel revolutions were recorded in addition to tape tensions on both sides of the net. The number of broken vertical and horizontal net members was recorded for each test. Figure A10 is a typical time history of the data recorded during a test run. Some of the data provided in table AIV came from this type of oscillograph recording.

Results and Discussion

Table AIV presents the data for this discussion of the 1/8-scale test. The tests consisted of 15 centerline engagements, which included 10 runs with the vehicle entering the net at an angle of 90° and 5 runs with the vehicle entering the net at an angle of 85°. Figure A11 shows the test layout for the vehicle entering the net at an angle of 85°. The launcher was not changed for 5° off-centerline angle net penetration. Instead, the net was skewed 5°, which is illustrated in figure A11 by the skewed centerline. The test speed ranged from 11 to 33 knots (31 to 93 knots full scale). Eight engagements were made with the model entering the net 5.44 ft (43.5 ft full scale) left of the runway centerline. Two of these runs were with the net skewed 5° from perpendicular to the runway centerline. Six engagements were made with the model entering the net 10.88 ft (87 ft full scale) left of the runway centerline; all were made with the net perpendicular to the runway centerline. In this appendix, all run numbers for on-centerline engagements are numbered with the prefix 1 starting with run A101. All net engagements made 5.44 ft off-centerline are numbered with the prefix 2 starting with run A201, and all net engagements made 10.88 ft off-centerline are numbered with the prefix 3 starting with run A301.

On-centerline engagements. The first three engagements (runs A101 to A103) were accomplished at 11 knots (31 knots full scale). Although the model was successfully arrested in each case, the lower horizontal bundle did not clear the main landing gear wheels. The bundle became entangled with the wheels and caused extensive damage to the net. (See figs. A12 and A13.) Also several lower horizontal straps caught on one of the primary anchor clips (fig. A14) and resulted in additional damage to the net during run A102. This problem was eliminated by covering the six outermost clips with plastic tape. Following run A101, the initial attempt to resolve the wheel entanglement problem of the main landing gear was to reduce the strength of the primary anchor ties from 11.00 lb to 2.75 lb.

The second attempt to resolve this problem was to tie and clip the lower bundle at closer intervals to prevent the individual horizontal straps from spreading apart immediately at the net engagement. Following run A103, the lack of tension in the lower bundle was determined to be the primary cause of the bundle contacting the wheels. Figure A15 shows slack in the lower bundle. Installation of tearaway straps between the lower bundle and an auxiliary ground anchor (figs. A4 and A16) was determined to be an effective solution to this problem. Figure A16 shows the lower bundle maintaining tension by means of the tearaway strap, which in this photograph is shown torn approximately one-half of its tear length. The lower horizontal bundle is shown above the wheels on the main gear struts with no entanglement around the main gear wheels. No entanglement of the main gear occurred in any of the subsequent tests with the lower bundle tearaway.

Run A104 (the fourth engagement) was accomplished at 14.1 knots (40 knots full scale) with lower bundle tearaway straps installed. Also during this engagement, the auxiliary suspension lines were tied to a length of 84 in., and the tape leaders were shortened to 162 in. The arrestment was completely successful with the lower horizontal bundle contacting the main landing gear struts clear of the wheels. Two vertical straps were broken by the nose landing gear, which was verified by a study of the videotape, and two upper horizontal straps were broken. Total wing envelopment occurred in spite of vertical straps being captured and broken by the nose landing gear. The vehicle stopped 8 in. right of the runway centerline.

Run A105 was an engagement at 17.8 knots (50 knots full scale). Run A105 and all subsequent engagements were performed with lower bundle tearaway straps installed and the auxiliary suspension lines tied at 78 in. (±6 in.). In addition, the tape leaders remained tied at 162 in. During this engagement, the lower bundle contacted the drag brace of the main landing gear at approximately the midpoint, and the upper bundle spread uniformly over the cargo bay doors. Two vertical straps were broken by the nose landing gear, and one upper horizontal member was broken. The vehicle stopped 3 in. right of the runway centerline.

Run A106 was an engagement at 24.2 knots (68.5 knots full scale) with six vertical straps on each side of the centerline tied back to allow the nose landing gear to pass through the net without entanglement. At the completion of the runout, the upper bundle appeared to be less spread out over the cargo bay door area than on previous runs. This difference may have been a result of the bundle ties being wrapped too tightly. No vertical or horizontal straps were broken, and the bottom bundle again contacted the main landing gear drag brace. The vehicle stopped 9 in. left of the centerline.

Run A107 was accomplished at 10.9 knots (30.8 knots full scale) with six vertical straps tied back on each side of the centerline. This run was an attempt to determine whether main landing gear entanglement would occur with the lower bundle when

vertical strap entanglement of the nose landing gear was not a factor. The top bundle of the net did not spread over the cargo bay door area because the bundle was tied too tightly to the 0.31-in. nylon ballast rope. Consequently, the dynamics of the upper bundle ballast rope was more pronounced than for previous runs. The lower horizontal bundle cleared the main landing gear tires and contacted the struts without hitting the drag braces. No straps were broken on this arrestment. The vehicle stopped 11 in. left of the centerline.

Run A108 engaged the net at 33.8 knots (95.6 knots full scale). On this engagement, the center vertical straps were not tied back but were positioned to allow entanglement of the nose landing gear. No straps were broken. Again, the ballast rope was secured tightly to the upper bundle; this configuration made the dynamics very pronounced but restricted spread over the payload bay door area. During this engagement, the nose landing gear bounced ≈3 in. after contact with the lower bundle and ballast rope. The rubber on the right nose landing gear separated from the wheel hub and departed the vehicle model after the bounce. Other than the tire problem with the nose landing gear, the arrestment was uneventful, and the vehicle stopped 13 in. left of the centerline.

Run A109 was another arrestment at 33.8 knots (95.6 knots full scale). On this run, the vertical elements were angled slightly in an attempt to improve the chances of catching vertical elements with the nose landing gear. One vertical and one horizontal strap were broken, and the break was evidenced on the video by a momentary and localized dip down of the top bundle at engagement. Again, on this run the lower bundle appeared to contact only the main landing gear strut and not contact the drag brace. The nose landing gear bounced ≈2 in. and shed the tire from the wheel hub again. However, the tire moved toward the nose landing gear strut and remained loose on the axle. The vehicle stopped 1 in. right of the centerline.

Run A110 was a 5°-skewed engagement at 14.8 knots (41.9 knots full scale). Three vertical straps and one horizontal strap were broken. Tracking of the vehicle was off to the right even before contact with the net because of an inadvertent slight steering offset in the nose landing gear, which probably occurred when the tire rubber was reattached to the wheel hub. The vehicle stopped 10.6 ft right of the launcher centerline, which was only 2.67 ft right of the 5°-skewed centerline.

Run A111 was a repeat of the previous run except that the verticals were tied back to prevent the nose landing gear from catching them. Engagement velocity was 15 knots (42.4 knots full scale). The vehicle tracked on-centerline both before and after engagement, and it stopped 3 in. right of the 5°-skewed centerline.

Run A112 was an engagement at 25.2 knots (71.3 knots full scale) also with a 5°-skewed net. Tracking of the vehicle appeared to be on the launcher centerline before the net, then a slight correction toward the 5°-skewed centerline. The vehicle stopped 1.8 ft right of the launcher centerline (4.7 ft left of 5°-skewed centerline). No straps were broken on this run.

Runs A113 to A115 were on-centerline runs that were conducted following the 5.44-ft and 10.88-ft off-centerline runs. These on-centerline runs were performed because of a change to the tape lengths, which was made during the off-centerline tests. For these engagements, the tapes were 15 ft longer than for previous on-centerline runs.

Run A113 was a 25.2-knot (71.3 knots full scale) engagement with the net positioned 90° to the launcher centerline. All aspects of this arrestment looked good. No straps were broken and the vehicle stopped 1.9 ft left of the centerline.

Run A114 was an engagement at 11.3 knots (32 knots full scale) with a 5°-skewed net. No straps were broken on this run. The vehicle stopped 2.12 ft left of the launcher centerline (7.6 ft left of the 5°-skewed centerline).

Run A115 was an engagement at 33.8 knots (95.6 knots full scale) with a 5°-skewed net. On this run, no straps were broken and the arrestment looked good. A tracking correction from the launcher centerline toward the 5°-skewed centerline was pronounced after the vehicle engaged the net. (See fig. A17.) A sketch showing the relationship between the launcher centerline and the skewed centerline is shown in figure A11. The vehicle stopped 4.4 ft right of the launcher centerline (3.7 ft left of the 5°-skewed centerline).

Off-centerline engagements. Run A201 was the first 5.44-ft off-centerline engagement, with an engaging speed of 12 knots (33.9 knots full scale). On this run, the vehicle appeared to track left from the time of launcher release until the end of the runout. However, when the vehicle was manually pushed on the runway centerline, the nose landing gear tracked appropriately. The vehicle stopped 2.2 ft left of the launcher centerline. No straps were broken on this engagement.

Run A202 was an engagement at 19.7 knots (55.7 knots full scale). Like run A201, the arrestment looked good except for the tendency for the vehicle to veer left immediately after leaving the end of the launcher. The vehicle stopped 4.8 ft left of the launcher centerline. No vertical or horizontal straps were broken. Further investigation into the tracking problem revealed a slight left bow in the nose landing gear rails of the launcher. The launcher was realigned before the next run.

Run A203 was an engagement at 12.2 knots (34.5 knots full scale) with the net set to 90° from the launcher centerline. The vehicle appeared to track straight from the launcher to the net. During the runout, the vehicle drifted slightly to the left and stopped 10 in. left of the launcher centerline. (See fig. A18.) One horizontal strap was broken during this engagement; this strap was coincident with the vertical strap that was on the launcher centerline.

Run A204 engaged the net at 19.4 knots (54.9 knots full scale). Vertical straps of the net were gathered near the location of the nose landing gear contact point to improve the chances of catching vertical straps. The vehicle tracked straight from the launcher to the net, then drifted to the left and stopped 6.2 ft left of the launcher centerline. Two vertical straps were broken during this arrestment; one on the vehicle centerline, the other 2.5 ft right of vehicle centerline.

Run A205 was performed with a steering vector set in the nose landing gear. Manual pushing of the vehicle placed it 5 in. right of the launcher centerline when the nose landing gear reached the net lower bundle, a distance of ≈25 ft. Engagement velocity was 15.2 knots (43 knots full scale). After engagement, the vehicle drifted slightly right before drifting left to stop 1 ft left of the launcher centerline. Thus, even with a small steering vector to the right, the action of the arresting system for an off-centerline arrestment tended to pull the vehicle to the left (short) side of the runway. The vehicle appeared to pull the top bundle downward on initial engagement, but no straps were broken. The lower bundle appeared to also come up and ride along the bottom of the fuselage until it contacted the main landing gear drag brace. It then slid down the drag brace and seated against the main landing gear strut.

Run A206 included a steering vector for the nose landing gear of 1 ft right from the launcher to the net. Engagement velocity was 24.6 knots (69.6 knots full scale). The vertical straps were gathered near the projected location of the nose landing gear contact to enhance the probability of catching vertical straps with the nose landing gear. After engagement, the vehicle moved to the right ≈13 in. before drifting left and coming to rest 6 in. left of the launcher centerline. No straps were captured by the nose landing gear.

Before run A207, the arresting tapes were lengthened in an attempt to soften the energy absorber dynamic loads occurring early in each arrestment. Lengthening the tapes increased the tape stack diameter on the tape spool. This increase reduced the rotational speed of the energy absorber and thus reduced the arrestment forces early in the runout. Runs A207 and A208 were conducted with tapes that were 20 ft longer than they were for previous engagements.

Run A207 was an engagement at 15.2 knots (43 knots full scale) without a steering vector; this run was performed for comparison with run A205. No straps were broken on this run, although the top bundle did move downward on initial engagement as though one or more straps were momentarily caught. The vehicle drifted left after engagement and stopped 2.4 ft left of the launcher centerline.

Run A208 duplicated run A206 without the steering vector but with arresting tapes that were 20 ft longer. The engagement velocity was 25.2 knots (71.3 knots full scale). The vehicle appeared to drift ≈4 in. left of the launcher centerline by the time it reached the net. Following the engagement, the vehicle continued to drift left and stopped 7.8 ft left of the launcher centerline. The nose gear and the left main gear were off the edge of the runway. One vertical strap was caught and broken by the nose landing gear. The lower bundle appeared to contact the main landing gear drag brace near the lower end and slid down to the strut.

Runs A301 to A306 were performed with the arresting tapes 5 ft shorter than they were for runs A207 and A208. The tapes were shortened because the effective tape drum radius exceeded the radius of the tape drum flanges. For these remaining runs, the tapes were 15 ft longer than the original length. In an attempt to soften the energy absorber dynamic loads, the nylon cord tape leaders were changed from four strands of 115 lb breaking strength to two strands of 225 lb breaking strength. This material exhibited somewhat greater stretch characteristics than the 115 lb material.

Run A301, the first 10.9-ft off-centerline engagement, was at 12.2 knots (34.5 knots full scale). The vehicle was set for no steering vector. The envelopment of the wing was good, even for the right (long) side. No straps were broken during this

arrestment. The vehicle stopped 4 in. left of the launcher centerline.

Run A302, again without a steering vector, engaged at 14.8 knots (41.9 knots full scale). Wing envelopment was good, and no vertical straps were caught by the nose landing gear in spite of a positive attempt. The vehicle drifted to the left after engagement and stopped 2.8 ft left of the launcher centerline. At the end of the run, the nose landing gear was 1.1 ft left of the runway edge, and the right main landing gear was 1.8 ft right of the runway edge.

Run A303 was an engagement at 19.2 knots (54.3 knots full scale) without a steering vector. No problem occurred with wing envelopment and no net straps were broken. The vehicle stopped 8.6 ft left of the launcher centerline with the nose landing gear positioned 6.92 ft left and the right main landing gear positioned 3.8 ft left of the runway edge. These results indicate that for an engagement at the edge of the runway, the vehicle will depart the runway.

Run A304, also without a steering vector, engaged the net at 24.5 knots (69.3 knots full scale). All aspects of the arrestment were good except for the vehicle tracking after engagement. One upper horizontal strap was broken, coincident with a vertical strap on the centerline of the vehicle. The nose landing gear came to rest 12.1 ft left of the launcher centerline, which was 10.5 ft off the runway. The right main gear was 8.4 ft left of the launcher centerline, which was 6.8 ft off the runway.

Run A305 had a 12.5-in. steering vector (displacement) at the net, which placed the model 12.5 in. to the right of the launcher centerline after pushing it 25 ft. Engagement velocity was 24.6 knots (69.6 knots full scale). Three adjacent vertical straps were broken on this arrestment at 12 in. right of the launcher centerline. The vehicle stopped with the nose landing gear positioned 6.2 ft left of launcher centerline and the right main landing gear positioned 3.1 ft left of the launcher centerline.

Run A306 engaged at 33 knots (93.3 knots full scale) with a 12.5-in. right steering vector applied. On this run, a total of 12 vertical straps were broken. (See fig. A19.) The vehicle stopped with the nose landing gear positioned 11.2 ft left of the launcher centerline and the right main landing gear positioned 7.8 ft left of the launcher centerline.

The 12 straps broken on this run were not caught in the nose landing gear (i.e., no evidence was seen in the video). All American Engineering Company concluded that these straps were on the long side of the off-centerline net and that they resisted the loads imposed by the short side of the net and arresting gear as the loads came on well before the long side arresting system. These straps, numbering only 12, were unable to resist the forces of the short side of the net until the remainder of the long side of the net was tensioned all the way to the energy absorber.

Runs A303 to A306 were launched 10.9 in. left of the runway centerline. For these runs, the model came to a stop completely off the edge of the runway in spite of the fact that runs A305 and A306 had a fixed steer angle to try to make them go toward the runway centerline. This result tends to confirm the similar vehicle behavior that occurred on the 1/27.5-scale test reported in the main body of this paper.

Conclusions

1. The net enveloped the wing properly for all 1/8-scale model tests and brought the vehicle to a stop. This ability was attributed primarily to the upper horizontal bundle tearaways, net supports, and upstream location of the water twister energy absorbers.
2. The problem of net entanglement around the main landing gear wheels was solved primarily by installing lower horizontal bundle tearaways similar to the upper bundle tearaways. No entanglement occurred on any arrestment after the lower bundle tearaways were installed.
3. The number of vertical straps broken by the nose landing gear on a given arrestment never exceeded three. This number was determined to not cause failure of the nose landing gear.
4. For run A306, 12 vertical straps were broken not by the nose landing gear but by the asymmetrical loading of this off-centerline engagement at high speed.
5. For five of the six runs when net engagement occurred with the model at the runway edge, the model ran off the side of the runway during arrested rollout. Thus, it appears advisable to try to engage the net in the center portion.

Table AI. Scaling Factors for 1/8-Scale Model

$[\lambda = 1/8]$

Definition	Symbol	Scaling factor
Length	L	λL
Acceleration	a	$1a$
Mass	m	$\lambda^3 m$
Area	A	$\lambda^2 A$
Volume	V	$\lambda^3 V$
Force	F	$\lambda^3 F$
Weight	w	$\lambda^3 w$
Velocity	v	$\sqrt{\lambda}\, v$
Time	t	$\sqrt{\lambda}\, t$
Inertia	I	$\lambda^5 I$

Table AII. Pertinent Parameters for Model Scale, Full Scale, and Orbiter

Parameter	1/8-scale value	Full-scale value	Orbiter value
Mass, slugs	15.8	8 096	8 074
Mass, lbm	509.1	260 682	260 000
Center of gravity:			
Height, in. (from runway)	24.5	196	197
Distance from nose, in.	107.0	856	850
Moment of inertia:			
Yaw, slugs-ft^2	262.5	8 602 000	8 617 000
Roll, slugs-ft^2	57.3	1 879 000	1 055 000

Table AIII. Arresting System Parameters for Model Scale, Full Scale, and Orbiter

Parameter	1/8-scale value	Full-scale value	Orbiter value
Net configuration:			
Length, in.	52.96	423.66	423.7
Window size:			
Height, ft	4.10	32.83	32.8
Width, ft	1.89 to 3.35	15.13 to 26.77	15.14 to 26.78
Height of top bundle, ft	3.23	25.83	25.80
Bottom bundle offset, ft	0.88	7.00	7.00
Break strength of net element members:			
Verticals, lb	12	6 144	6 000
Top horizontals, lb	12	6 144	6 000
Bottom horizontals, lb	12	6 144	6 000
Top tearaway strap, lb	15.5	7 936	8 000
Bottom tearaway strap, lb	15.5	7 936	8 000
Kevlar suspension line, lb	180	92 160	22 900
Inner suspension line, lb	1	512	200
Auxiliary suspension line, lb	190	97 280	20 000
Bottom bundle tiedown, lb	0.5 (21 ea)	256 (21 ea)	100 (24 ea)
Top bundle ties to catenary, lb	1	512	200
Weight of net without inertia cords, lb	1.44	740	
Weight of net with inertia cords, lb	4	2 048	2 250
Suspended net weight, lb	2.28	1 167	1 075
Energy absorbers:			
Rotor drag coefficient	0.0005	16.4	0.33
Inertia of rotating parts	0.13	4 260	50
Tape length, ft	78	624	730
Tape thickness, in.	0.312	2.496	0.225
Tape width, in.	1.75	14	8.5
Tape strength, lb	26 000	13 312 000	210 000
Tape weight, lb/ft	0.156	79.9	1.4

Table AIV. Test Data for 1/8-Scale Model

Run	Aim point position on centerline	Net plane entry, deg	Engagement velocity, knots	Peak tension, lb		Maximum longitudinal deceleration, g	Runout, ft	Deviation from launch centerline, ft	Energy absorber payout, ft		Number of straps broken	Remarks
				Left	Right				Left	Right		
A101	On	90	11.0				39.8	1.5	19.2	18.8	0	Lower horizontal bundle on MLG
A102	On	90	10.9				38.3	1.2	18.6	17.3	0	Lower horizontal bundle on MLG
A103	On	90	11.1				40.3	0.1	19.3	19.4	0	Lower horizontal bundle on MLG
A104	On	90	14.1	66	70	0.32	59.5	0.7	38.5	38.3	2 vert., 2 horiz.	Added tearaways to lower bundle
A105	On	90	17.8	105	103	0.44	65.8	0.3	44.3	43.8	2 vert., 1 horiz.	
A106	On	90	24.2	182	166	0.72	71.2	0.8	48.5	48.6	0	Vertical straps tied back at centerline
A107	On	90	10.9	45	42	0.28	52.1	0.9	31.3	30.8	0	Vertical straps tied back at centerline
A108	On	90	33.8				74.5	1.1	51.5	51.8	0	Lost left NLG gear tire
A109	On	90	33.8	416	325	1.40	75.0	0.1	52.2	51.8	1 vert., 1 horiz.	NLG tire separated from hub
A110	On	85	14.8		57	0.32	65.0	10.6	42.2	40.3	3 vert., 1 horiz.	Vehicle tracking off centerline
A111	On	85	15.0	75	70	0.34	65.2	0.3	40.6	42.3	0	Vertical straps tied back at centerline
A112	On	85	25.2	161	172	0.72	75.3	1.8	49.8	51.3	0	
A113	On	90	25.2	158	160	0.68	87.0	1.9	63.9	63.9	0	
A114	On	85	11.3	33	37	0.24	62.4	2.2	37.3	40.0	0	
A115	On	85	33.8	250	237	1.00	92.6	4.4	66.4	66.8	0	Vehicle corrected toward 85° centerline
A201	5.44 ft off	85	12.0	40	38	0.18	58.0	2.3	36.9	33.0	0	Vehicle tracking off centerline
A202	5.44 ft off	85	19.7	127	93	0.48	69.7	4.8	48.4	44.4	0	Vehicle tracking off centerline
A203	5.44 ft off	90	12.2	56	28	0.16	56.3	0.8	39.8	32.8	1 horiz.	
A204	5.44 ft off	90	19.4	120	105	0.46	68.2	6.2	45.0	50.0	2 vert.	
A205	5.44 ft off	90	15.2	73	58	0.30	64.0	1.0	44.2	37.8	0	Appeared to catch vertical strap but did not break
A206	5.44 ft off	90	24.6	193	133	0.60	73.5	0.5	53.8	47.7	0	
A207	5.44 ft off	90	15.2	88	63	0.24	74.0	2.4	54.6	48.7	0	
A208	5.44 ft off	90	25.2	216	158	0.62	80.2	7.8	70.3	64.4	1 vert.	
A301	10.9 ft off	90	12.2	60	30	0.20	62.9	0.3	48.6	34.9	0	
A302	10.9 ft off	90	14.8	85	32	0.26	71.8	2.8	56.5	43.5	0	
A303	10.9 ft off	90	19.2	133	68	0.40	79.6	8.6	64.0	52.8	0	Vehicle drifted off runway
A304	10.9 ft off	90	24.5	173	135	0.64	83.2	12.1	67.6	56.6	1 horiz.	Vehicle drifted off runway
A305	10.9 ft off	90	24.6	166	141	0.76	84.5	6.2	68.2	56.8	3 vert.	
A306	10.9 ft off	90	33.0	303	230	1.34	88.6	11.2	71.4	60.7	12 vert.	Broke 12 adjacent vertical straps

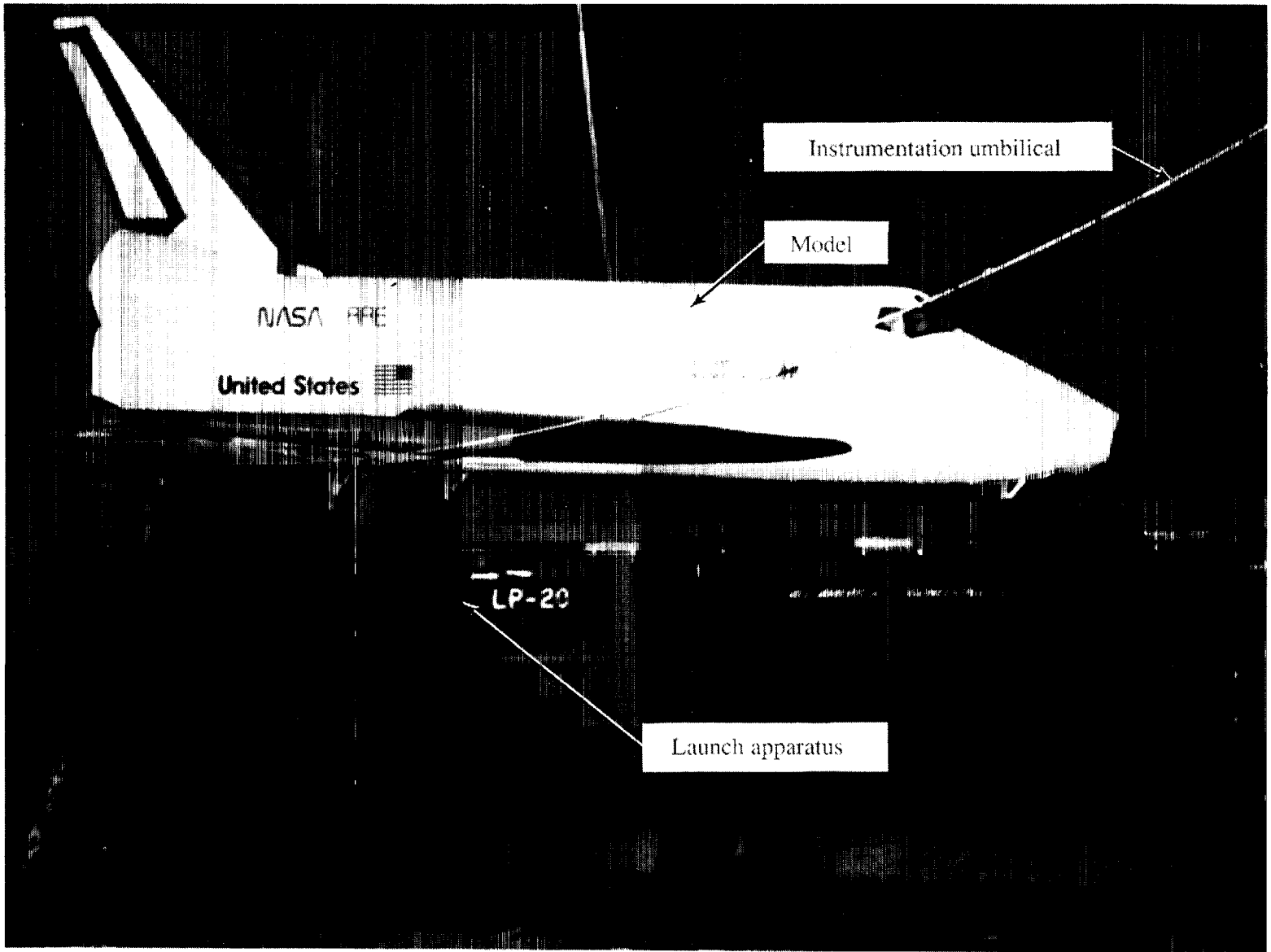

L-92-1129

Figure A1. 1/8-scale model on launch apparatus.

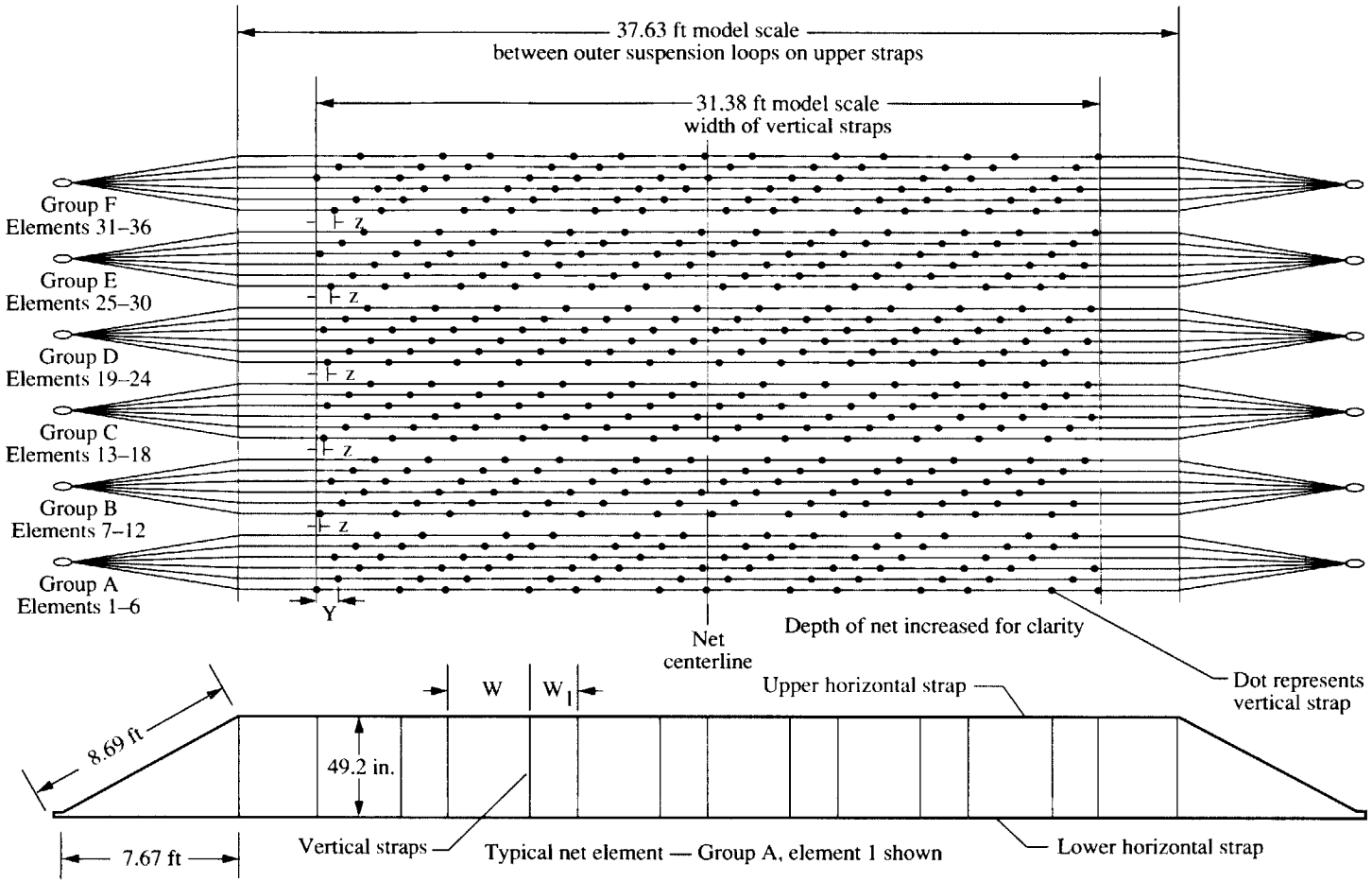

Group	Window width		Offset,	Spacing,
	W, in.	W_1, in.	Z, in.	Y, in.
A	40.17	22.71	0	10.47
B	36.69	26.21	1.74	10.47
C	33.20	29.70	3.48	10.47
D	29.70	33.20	5.24	10.47
E	26.21	36.69	6.98	10.47
F	22.71	40.17	8.73	10.47

Note: With net assembled, a single vertical strap should be located every 0.87 in. with no overlap.

Figure A2. 36-element net used for 1/8-scale model arrestment.

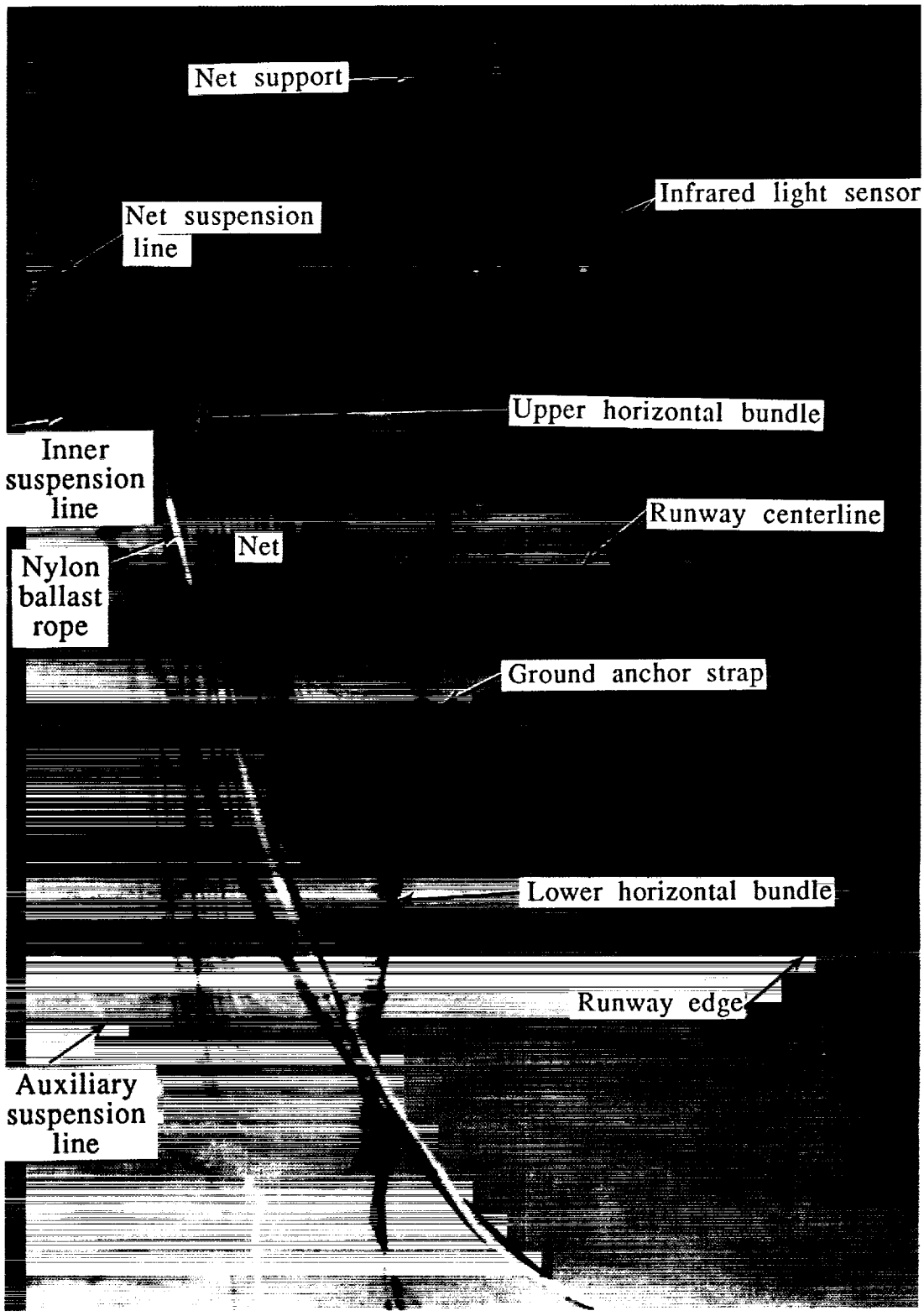

Figure A3. Side view of 1/8-scale model arresting net.

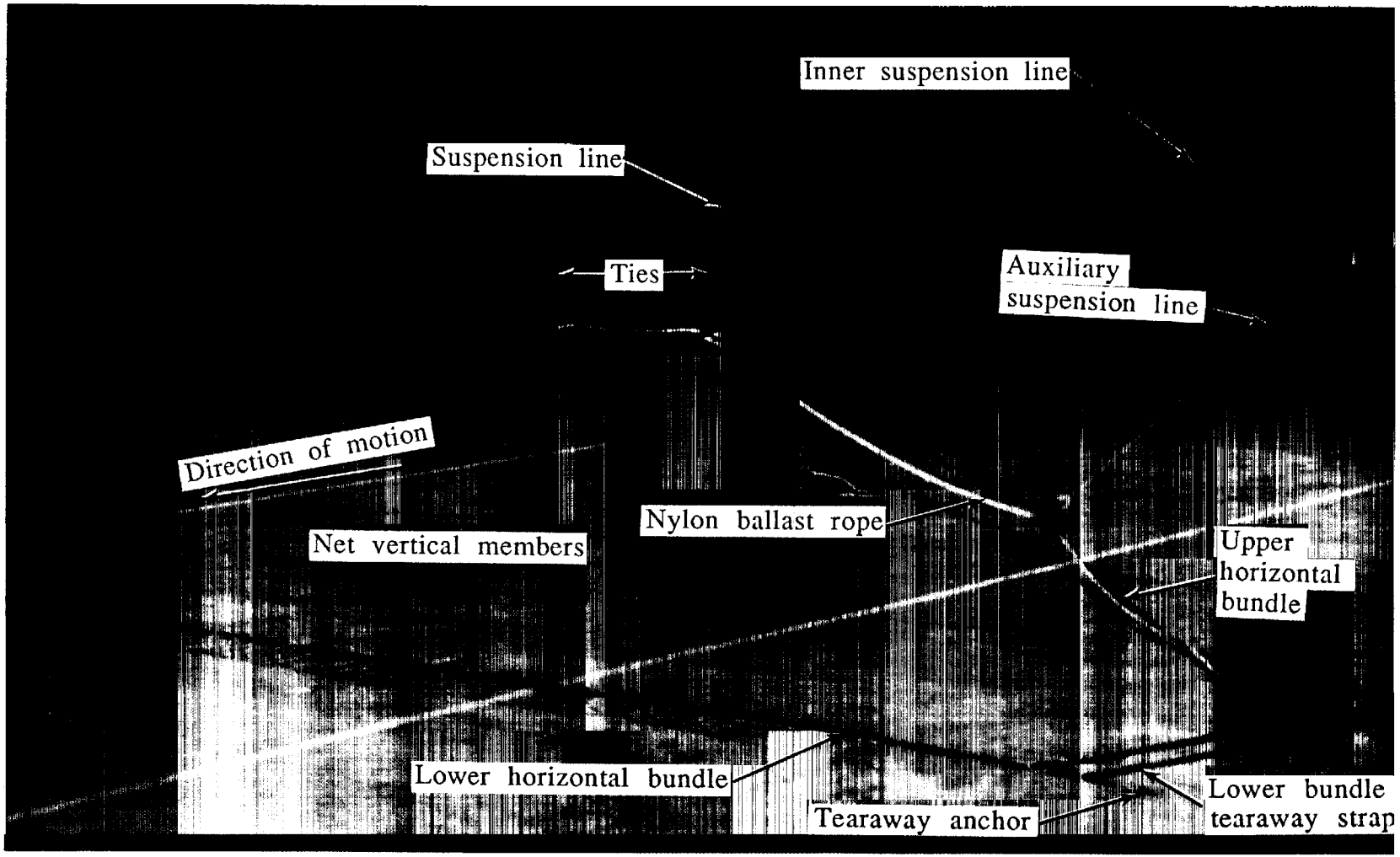

L-92-1122

Figure A4. End view of arrestment net.

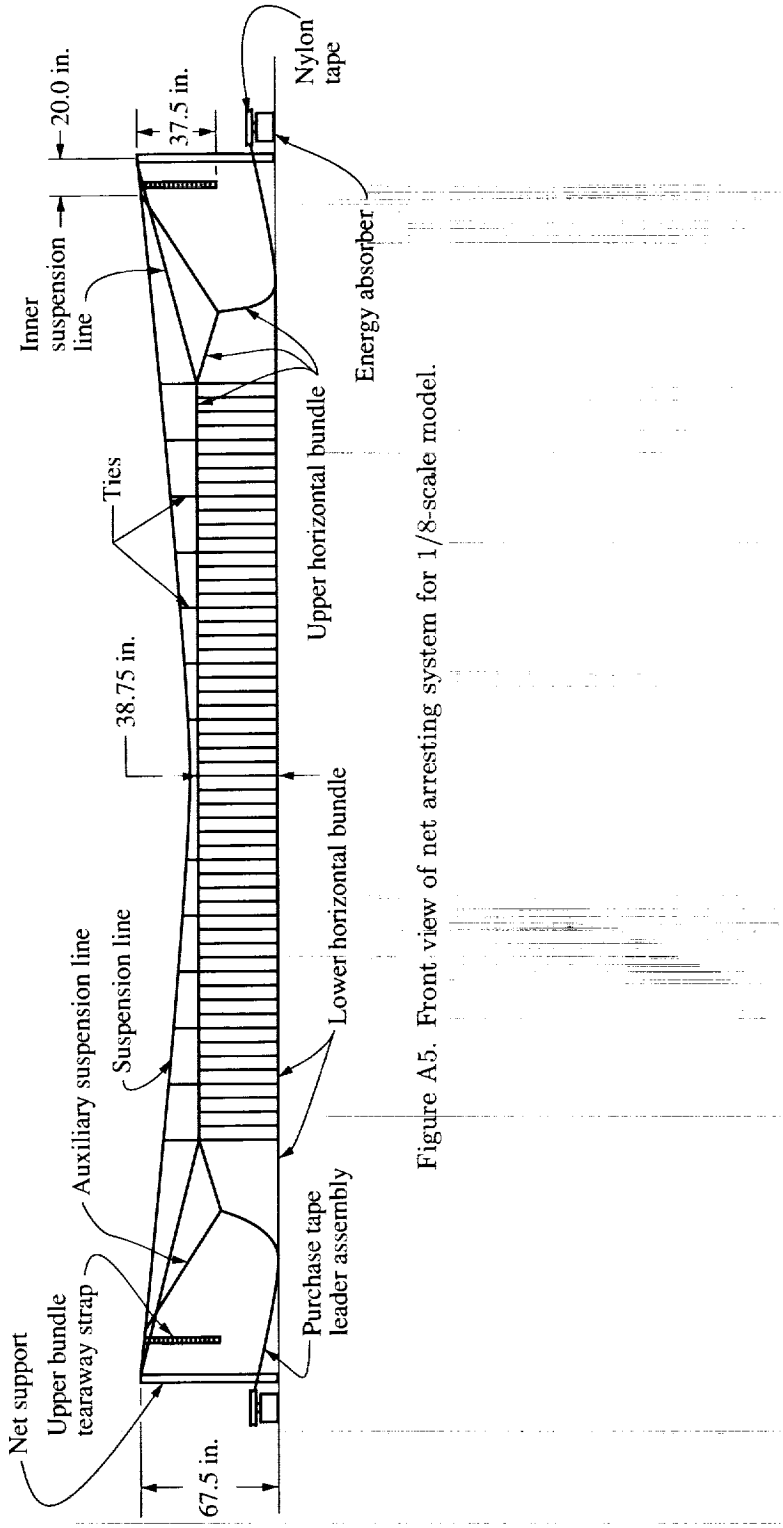

Figure A.5. Front view of net arresting system for 1/8-scale model.

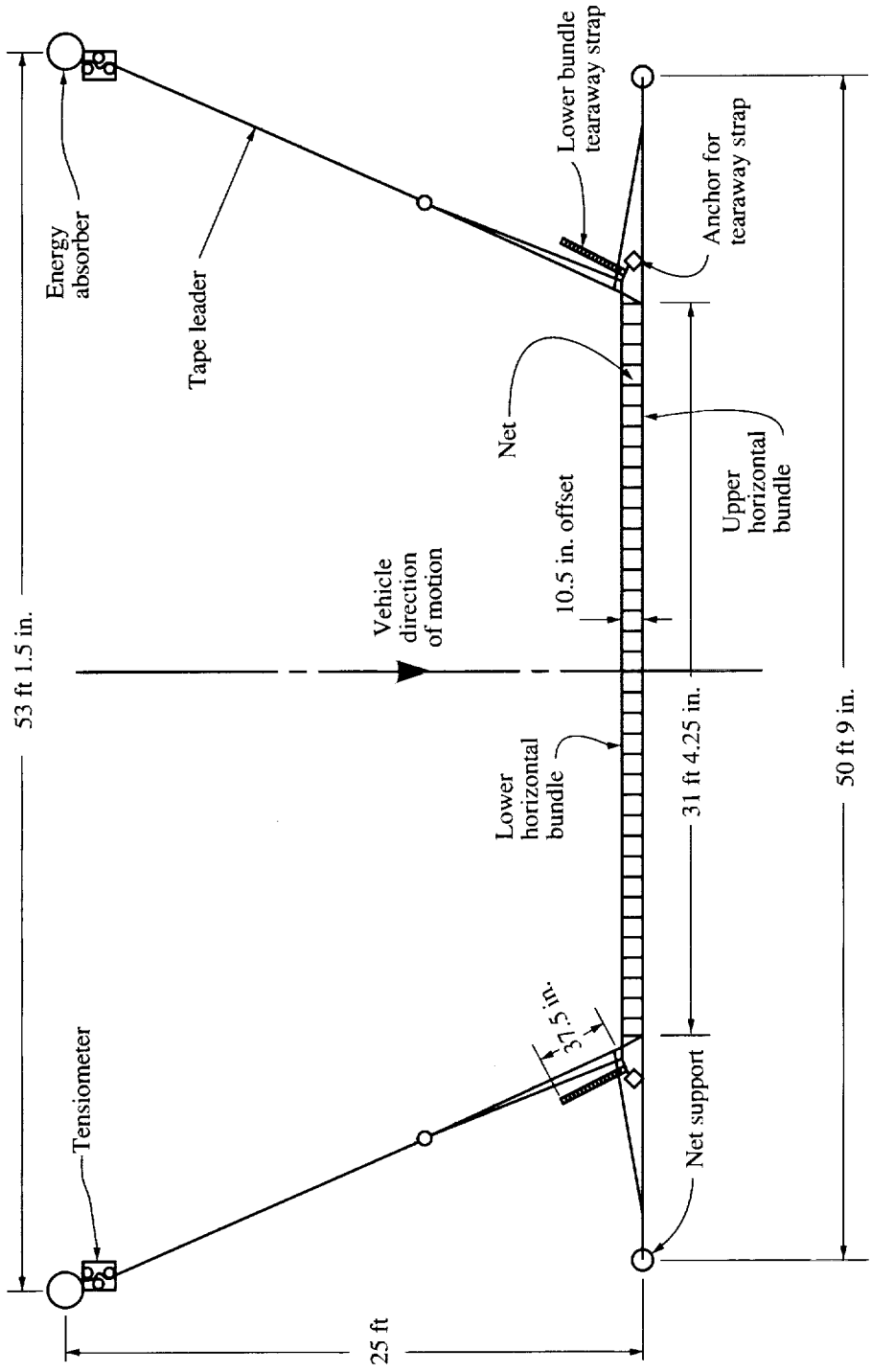

Figure A6. Top view of net arresting system for 1/8-scale model.

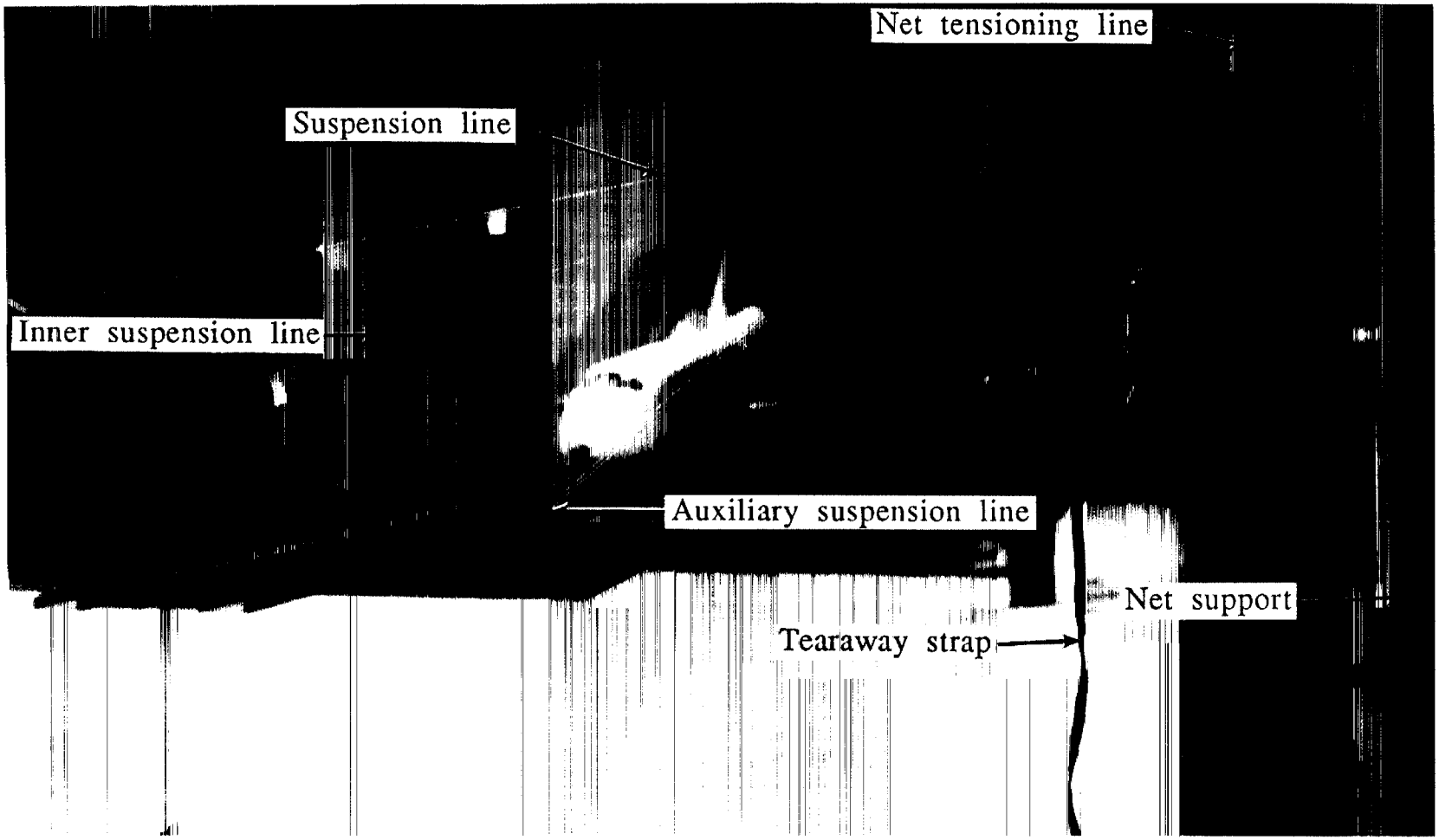

Figure A7. Net suspension lines.

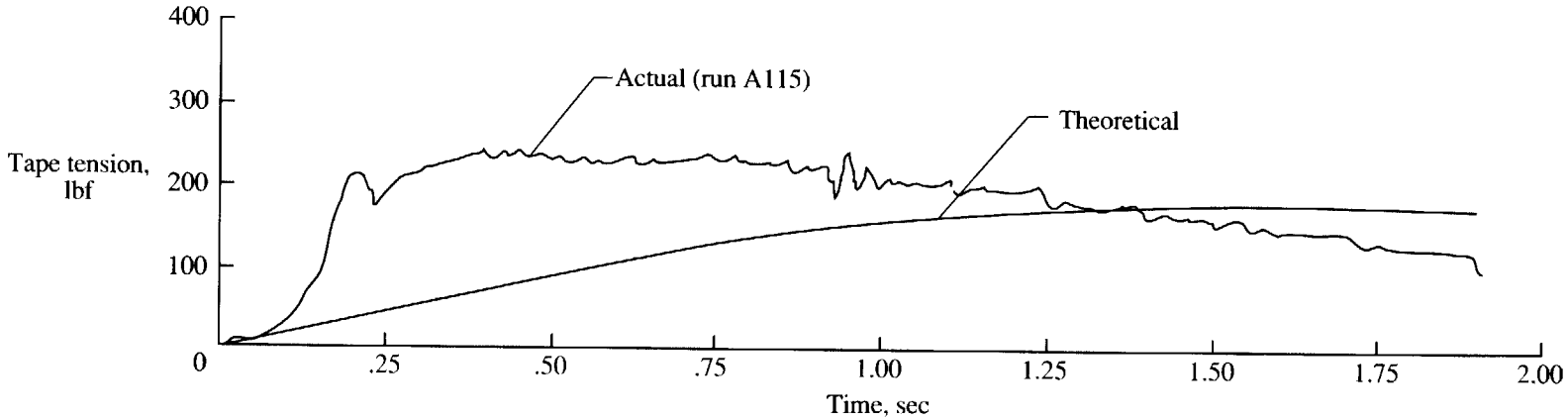

Figure A8. Arresting net tension loads time history for 1/8-scale model.

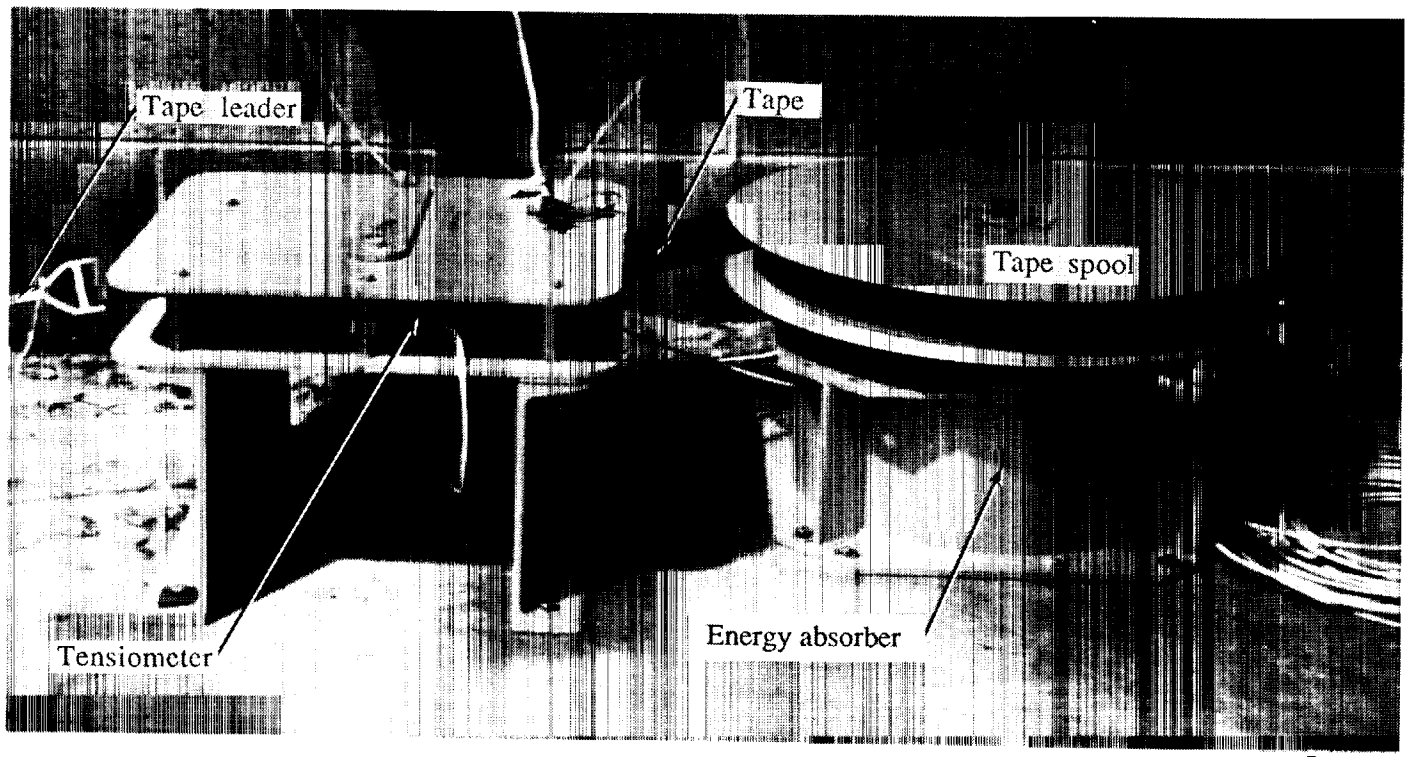

Figure A9. 14-in-diameter energy absorber used in 1/8-scale model test.

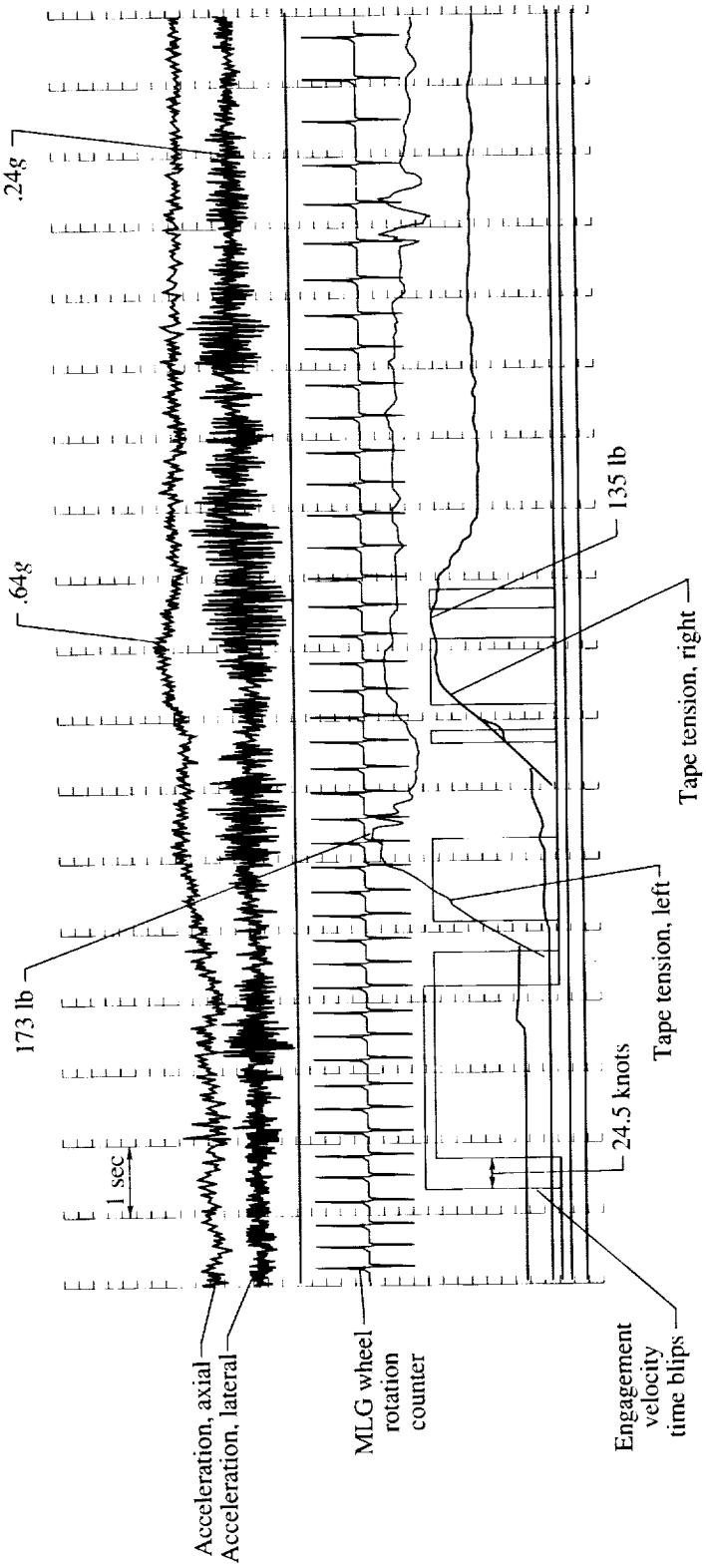

Figure A10. Typical time history during test (run A304).

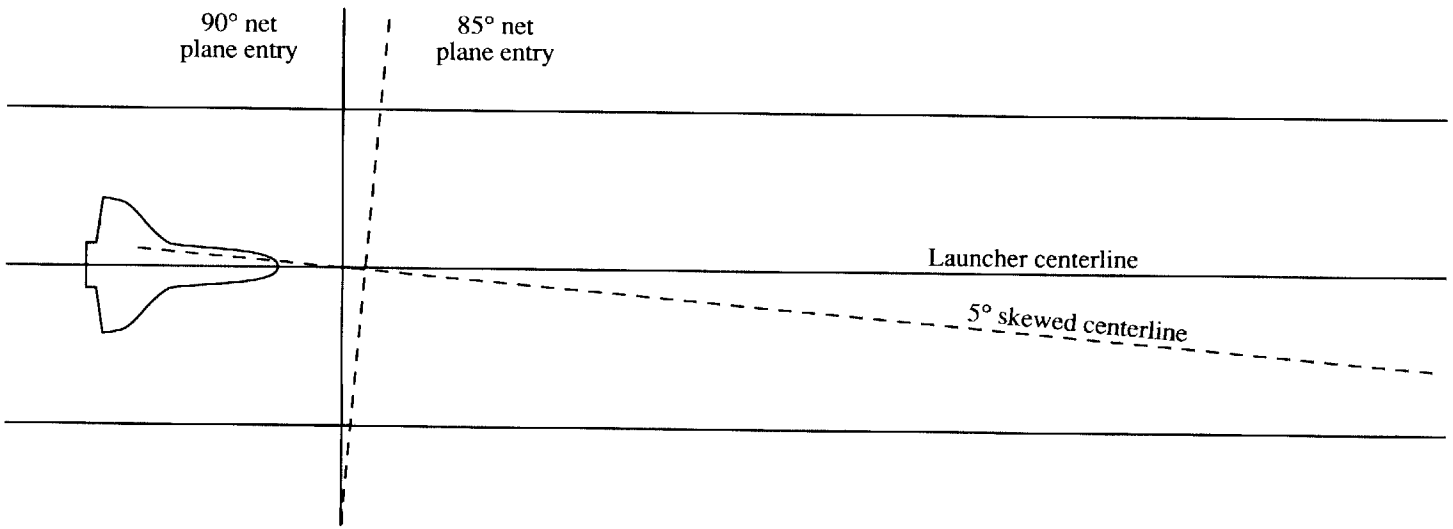

Figure A11. Layout for vehicle entering net at an 85° net entry plane.

L-93-59

Figure A12. Lower horizontal bundle entanglement of main landing gear.

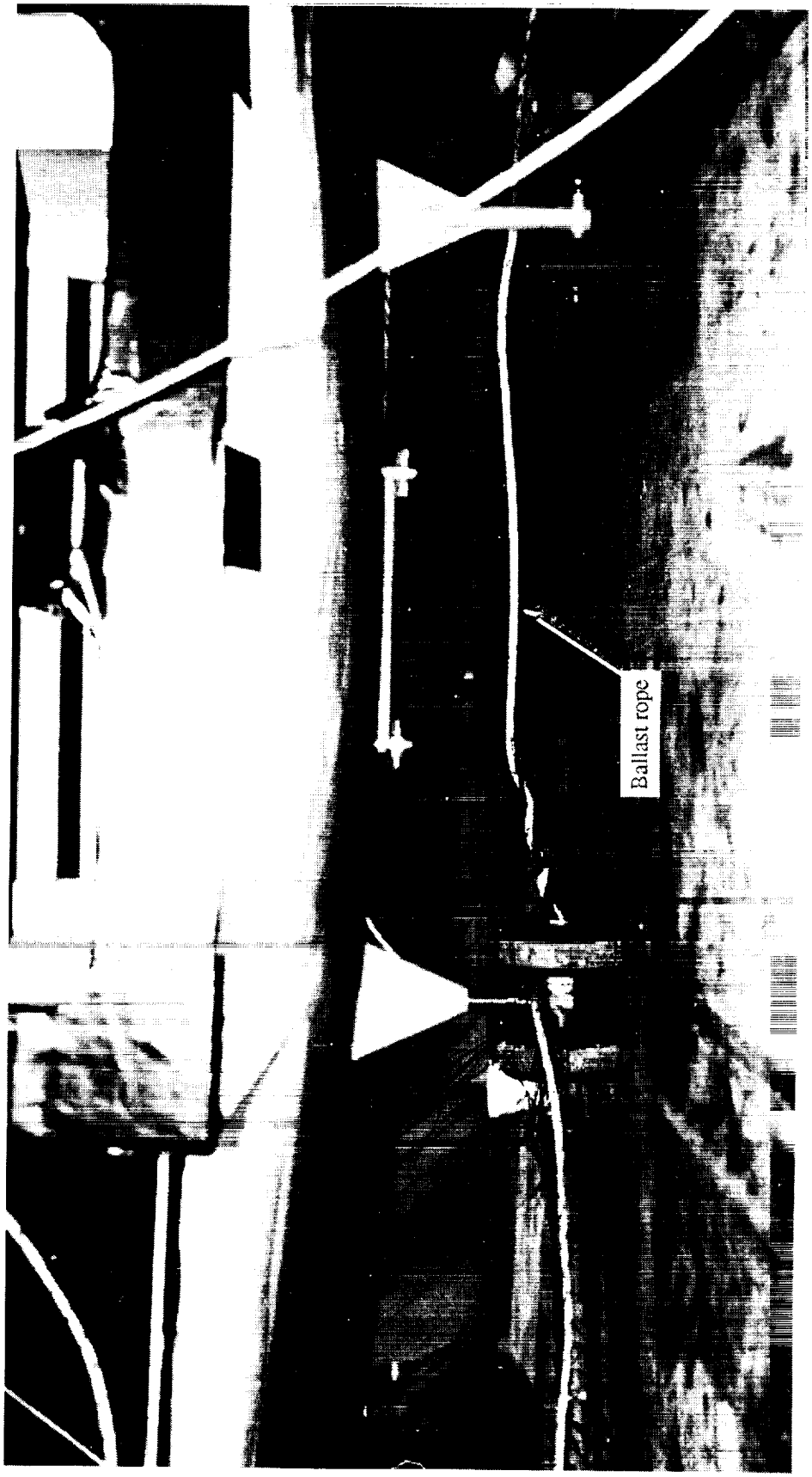

Figure A13. Lower horizontal bundle and lower ballast rope entanglement of main gear.

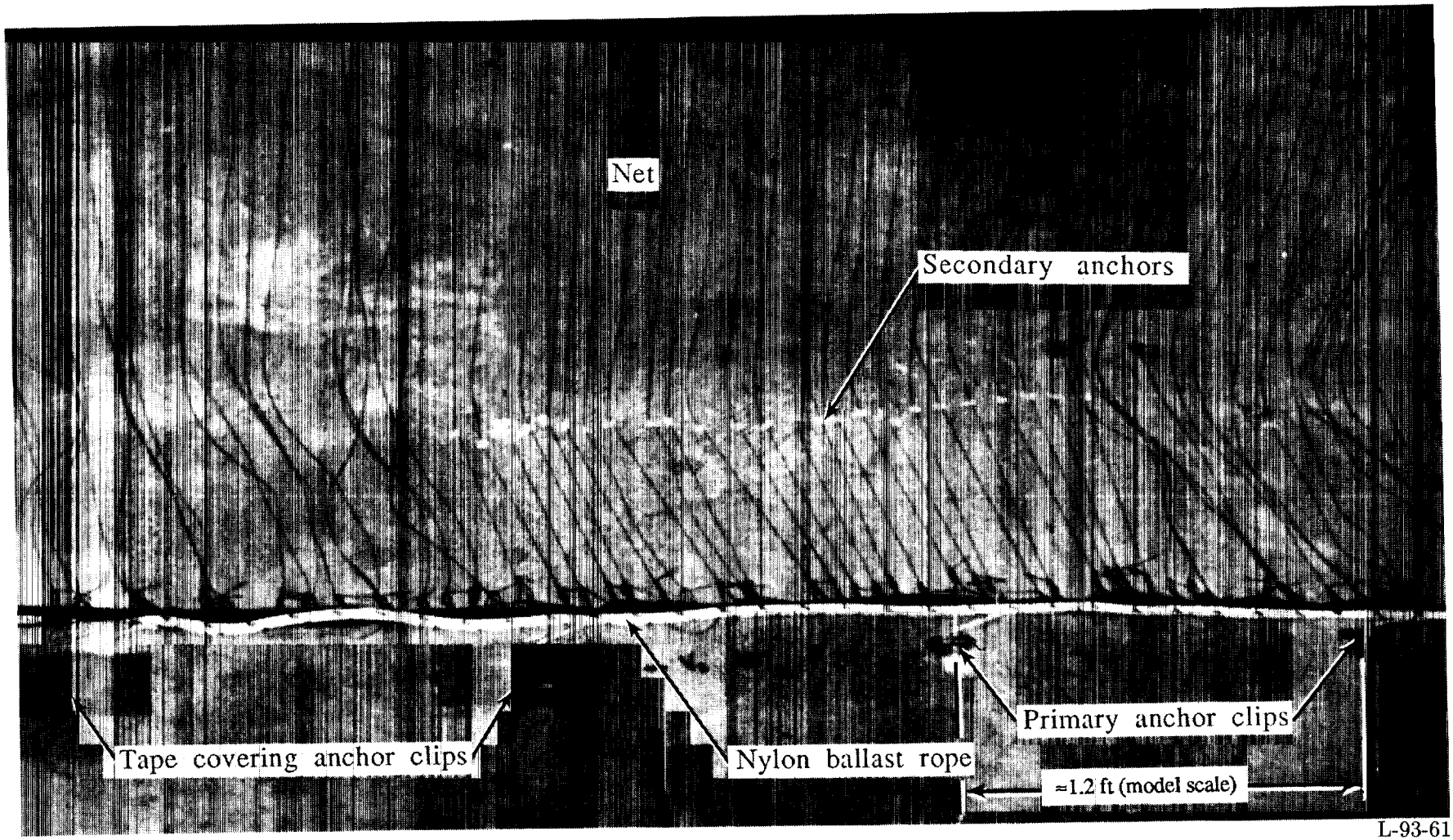

Figure A14. Covered anchor clips used to prevent net damage.

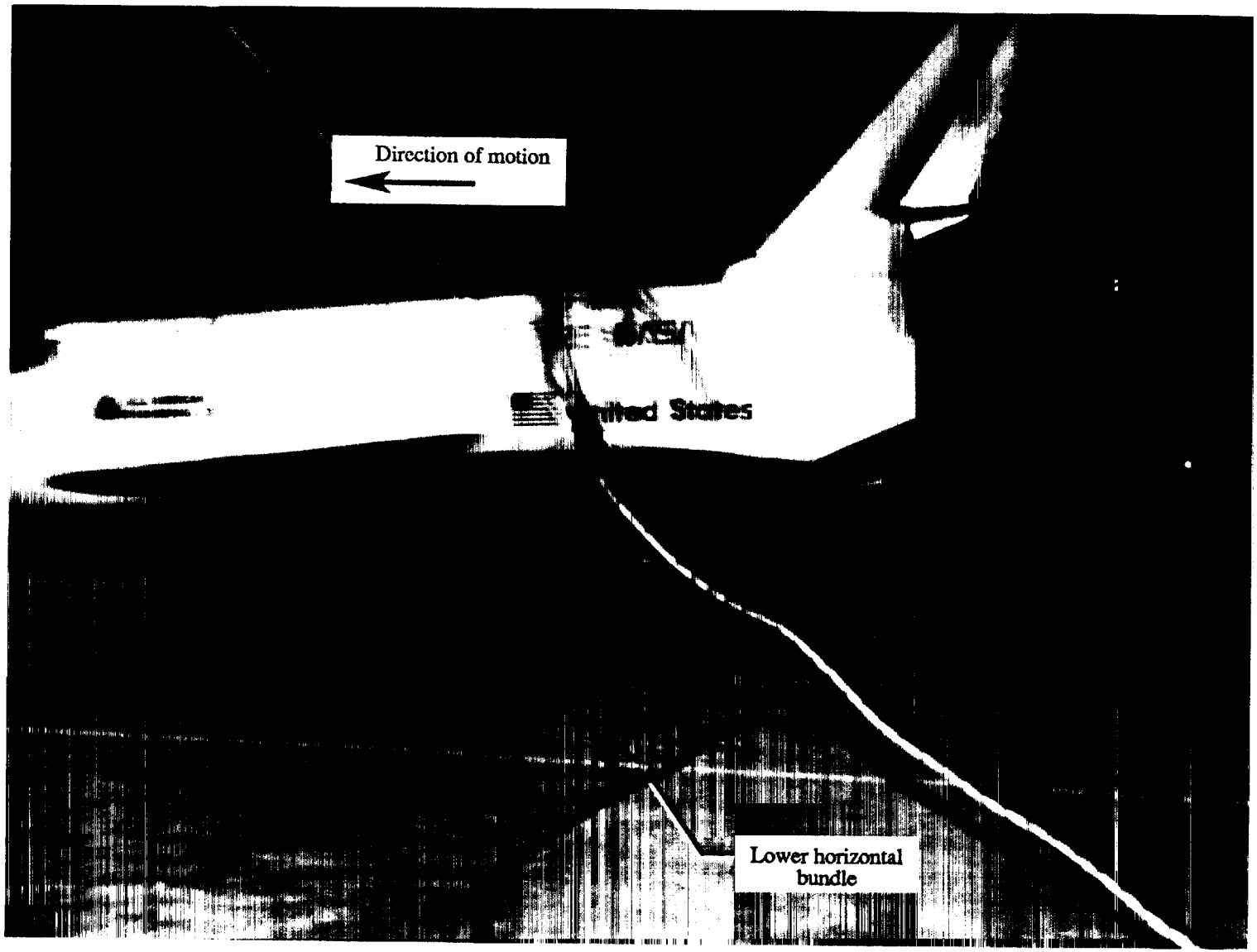

L-93-62

Figure A15. Slack in lower horizontal bundle resulting in main landing gear entanglement during initial net engagement.

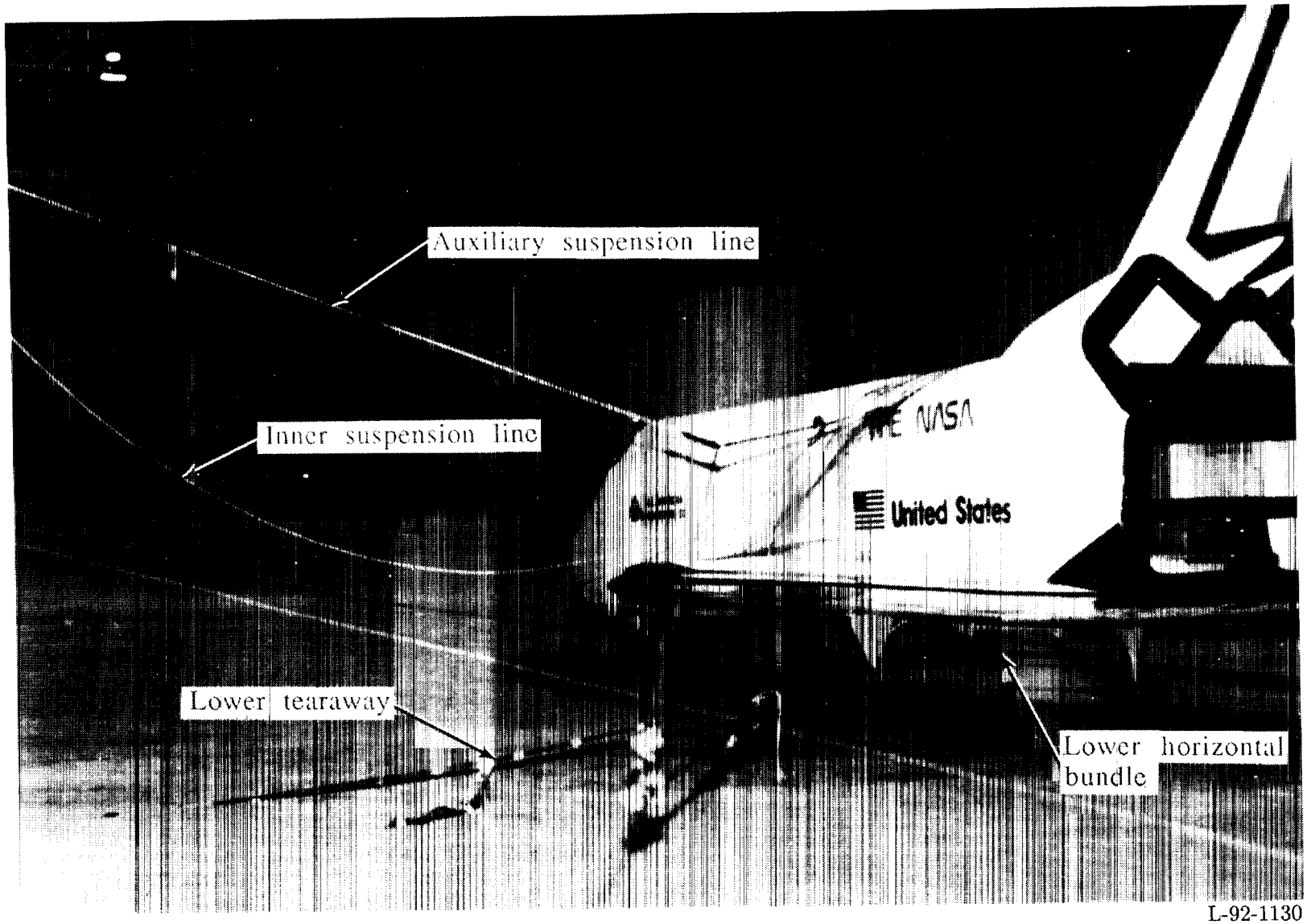

Figure A16. Lower tearaway maintaining sufficient tension of lower horizontal bundle until main gear strut is cleanly caught by lower bundle (during initial engagement before tearaway is broken).

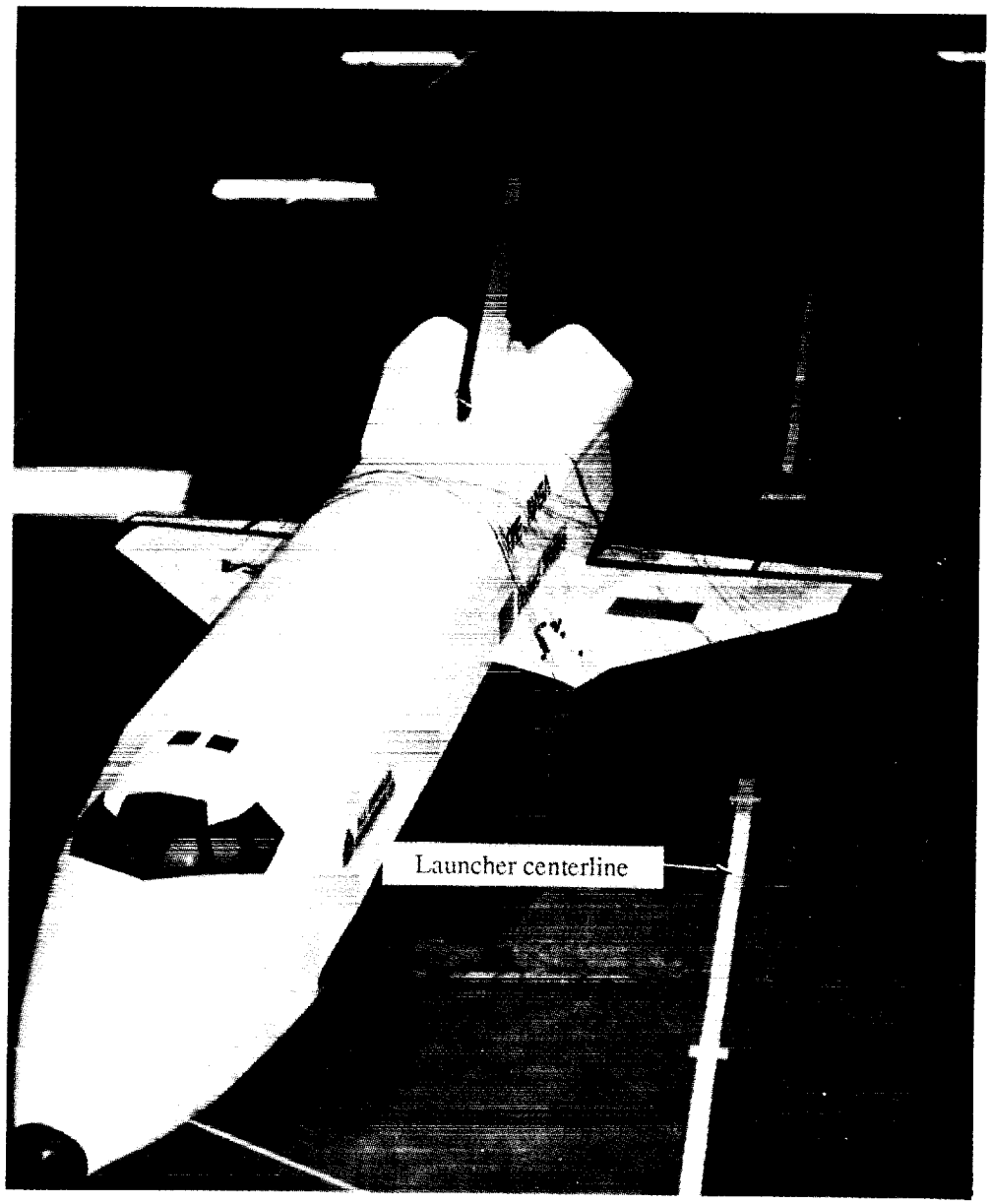

L-93-63

Figure A17. 5°-skewed net, model tracked toward 5°-skewed centerline during run A115.

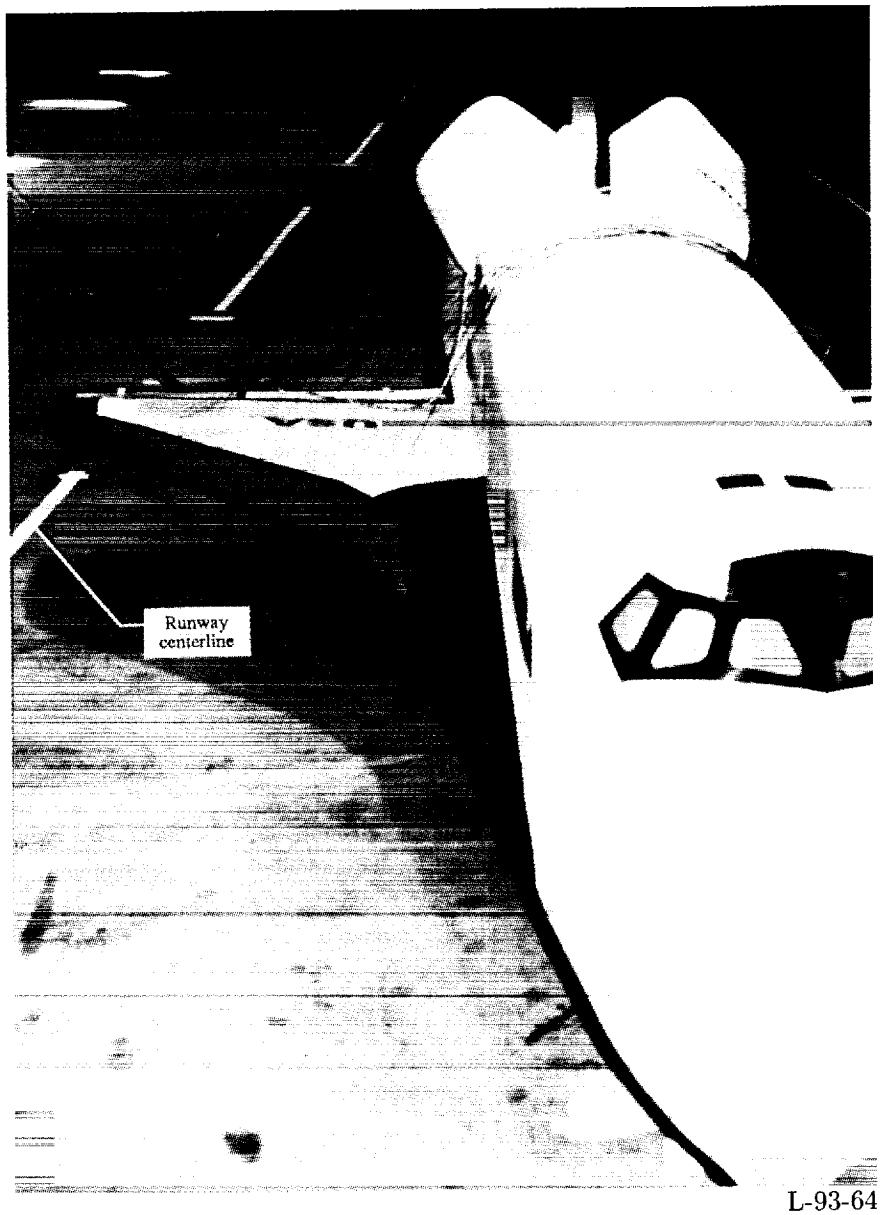

L-93-64

Figure A18. Engagement 5.44 ft off of runway centerline for run A203. Model moved slightly toward edge of runway.

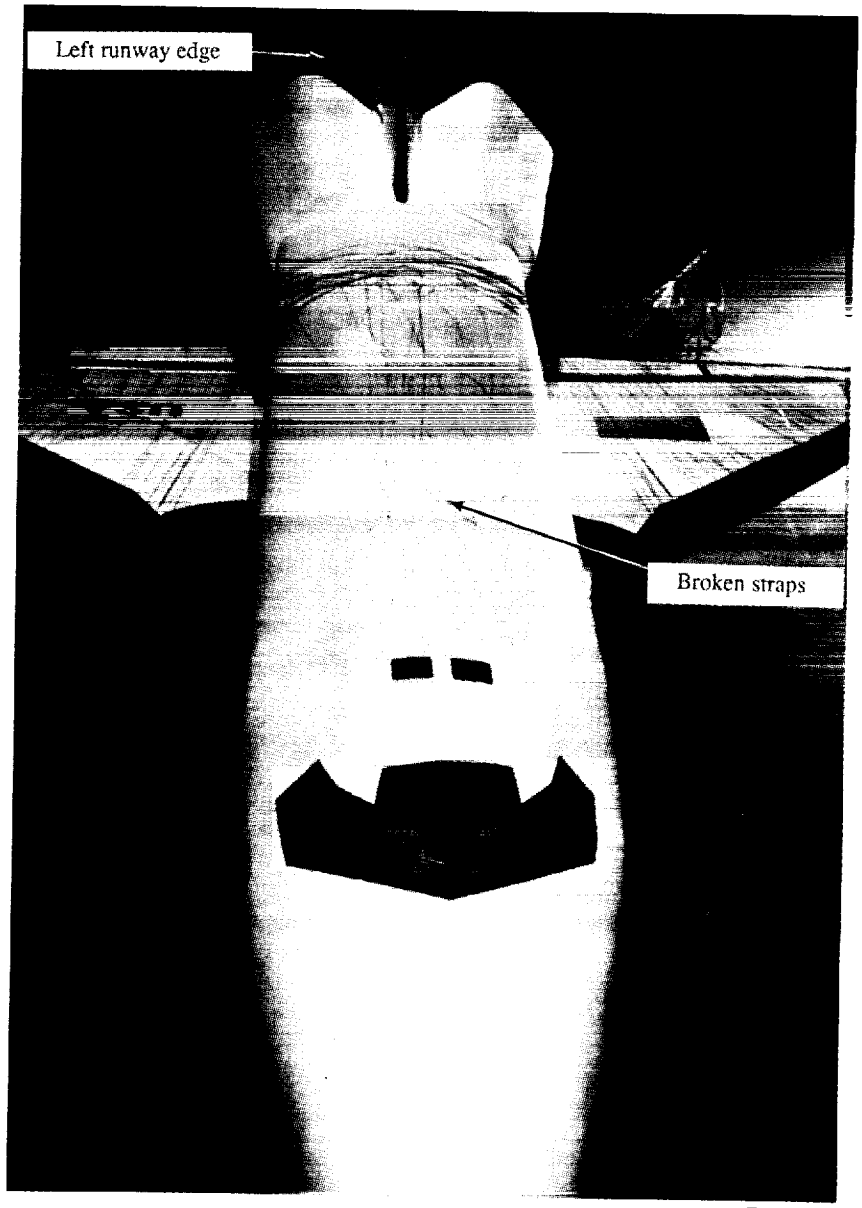

L-93-65

Figure A19. Net engagement was 10.88 ft off of runway centerline; vehicle ran off runway edge for run A306 (twelve broken straps).

References

1. Parker, Richard V.: Arrestment Considerations for the Space Shuttle. *Technology Today and Tomorrow – Eighth Space Congress Proceedings*, Volume II, Canaveral Council of Technical Societies, 1971, pp. 7-69–7-80.

2. Gwynne, G. M.: *Assessment of a Linear Hydraulic Energy Absorber/Barrier Net Combination for Airfield Arresting.* RAE TR-80136, British Royal Aircraft Establ., Oct. 1980.

3. Gaggiani, Salvatore: The Problem of Stopping Barriers. *Rivista Aeronaut.*, vol. 45, Mar. 1969, pp. 431–454.

4. Langhaar, Henry L.: *Dimensional Analysis and Theory of Models.* John Wiley & Sons, Inc., c.1951.

5. Schaible, John J.: Evaluation of the 44B-2E Aircraft Arresting System With Deadloads and the F-14 Aircraft. NATF-EN-1138, U.S. Navy, Apr. 30, 1976. (Available from DTIC as AD B011 019L.)

6. Davis, Pamela A.; Stubbs, Sandy M.; and Tanner, John A.: *Langley Aircraft Landing Dynamics Facility.* NASA RP-1189, 1987.

REPORT DOCUMENTATION PAGE

Form Approved
OMB No. 0704-0188

1. AGENCY USE ONLY *(Leave blank)*	2. REPORT DATE	3. REPORT TYPE AND DATES COVERED
	December 1993	Technical Paper

4. TITLE AND SUBTITLE
Studies of Shuttle Orbiter Arrestment System

5. FUNDING NUMBERS
WU 505-63-10-02

6. AUTHOR(S)
Pamela A. Davis and Sandy M. Stubbs

7. PERFORMING ORGANIZATION NAME(S) AND ADDRESS(ES)
NASA Langley Research Center
Hampton, VA 23681-0001

8. PERFORMING ORGANIZATION REPORT NUMBER
L-17186

9. SPONSORING/MONITORING AGENCY NAME(S) AND ADDRESS(ES)
National Aeronautics and Space Administration
Washington, DC 20546-0001

10. SPONSORING/MONITORING AGENCY REPORT NUMBER
NASA TP-3370

11. SUPPLEMENTARY NOTES
All American Engineering Co., now known as Engineered Systems, a Division of Daytron, Inc., conducted the 1/8-scale tests reported in the appendix.

12a. DISTRIBUTION/AVAILABILITY STATEMENT
Unclassified–Unlimited

Subject Category 05

12b. DISTRIBUTION CODE

13. ABSTRACT *(Maximum 200 words)*
Scale model studies of the Shuttle orbiter arrestment system (SOAS) were completed with a 1/27.5-scale model at the NASA Langley Research Center. The purpose of these studies was to determine the proper configuration for a net arrestment system to bring the orbiter to a safe stop with minimal damage in the event of a runway overrun. Tests were conducted for runway on-centerline and off-centerline engagements at simulated speeds up to ≈100 knots (full scale). The results of these tests defined the interaction of the net and the orbiter, the dynamics of off-centerline engagements, and the maximum number of vertical net straps that may become entangled with the nose gear. In addition to these tests, a test program with a 1/8-scale model was conducted by the arrestment system contractor, and the results are presented in the appendix.

14. SUBJECT TERMS	15. NUMBER OF PAGES
Arrestment; Net; Shuttle; Orbiter	87
	16. PRICE CODE A05

17. SECURITY CLASSIFICATION OF REPORT	18. SECURITY CLASSIFICATION OF THIS PAGE	19. SECURITY CLASSIFICATION OF ABSTRACT	20. LIMITATION OF ABSTRACT
Unclassified	Unclassified		